

Institute for Clinical and Experimental Surgery
Saarland University, Homburg/Saar
(Director: Prof. Dr. med. M. D. Menger)

**In vivo analysis of menstrual and non-menstrual tissue in
murine endometriosis models**

A dissertation for the doctoral degree
Doctor of Medicine (Dr. med.)
at the Medical Faculty of Saarland University

2024

by Krista Teodorova Yordanova
born on 07.07.1991 in Dobrich, Bulgaria

to Kevin, Natalia, Teodor und Tedi

Content

1. Summary	1
2. Zusammenfassung	3
3. Introduction	5
3.1 Human endometriosis	5
3.1.1 Definition and prevalence of endometriosis	5
3.1.2 Morphology and classification of human endometriosis	5
3.1.3 Pathogenesis of human endometriosis	6
3.1.4 Symptoms, diagnosis and therapy of human endometriosis	7
3.2 Cycles	9
3.2.1 The female menstrual cycle	9
3.2.2 The estrus cycle of mice	11
3.2.3 Differences between the cycles	13
3.3 The menstruating mouse model	13
3.4 Animal models in endometriosis research	14
3.4.1 Primate models	14
3.4.2 Rodent models	15
4. Aim of the study	17
5. Materials and methods	18
5.1 Animals	18
5.2 Menstruating mouse model	18
5.3 Identification of the estrous cycle phase	20
5.4 Experimental protocol	21
5.5 Intraperitoneal endometriosis model	23
5.5.1 Induction of intraperitoneal endometriosis	23

5.5.2	High-resolution ultrasound imaging.....	25
5.6	Dorsal skinfold chamber model	26
5.6.1	Preparation of the dorsal skinfold chamber	26
5.6.2	Transplantation of endometrial fragments into the dorsal skinfold chamber	27
5.6.3	Intravital fluorescence microscopy	28
5.7	Histology and immunohistochemistry.....	30
5.8	Statistical analyses	31
6.	Results	32
6.1	Evaluation of the intraperitoneal endometriosis model	32
6.1.1	Macroscopic and microscopic characteristics of non-menstrual and menstrual donor tissue	32
6.1.2	Growth of intraperitoneal endometriotic lesions	33
6.1.3	Macroscopic assessment of intraperitoneal endometriotic lesions	34
6.1.4	Engraftment of non-menstrual and menstrual uterine tissue fragments	35
6.1.5	Immunohistochemical analyses of intraperitoneal endometriotic lesions	36
6.2	Evaluation of the dorsal skinfold chamber model	38
6.2.1	Evaluation of non-menstrual and menstrual endometrial fragments	38
6.2.2	Early vascularization of endometriotic lesions	39
6.2.3	Histomorphology of endometriotic lesions	43
6.3	Summary of the results.....	44
7.	Discussion	46
7.1	Discussion of materials and methods	46
7.1.1	Menstruating mouse model.....	46
7.1.2	Intraperitoneal model of endometriosis	47
7.1.3	Dorsal skinfold chamber model.....	48
7.1.4	Experimental protocol of the study.....	49
7.2	Discussion of the results.....	49
7.3	Conclusion.....	51
8.	References.....	53

9. Acknowledgements.....	65
10. Curriculum vitae.....	66
11. Publications.....	67

1. Summary

Endometriosis is a common gynecological condition, defined by the presence of ectopic endometrial tissue outside the uterine cavity, also known as endometriotic lesions. Endometriosis spontaneously occurs in humans and menstruating primates. It is characterized by a broad spectrum of unspecific pain symptoms, including dysmenorrhea, dysuria and dyspareunia and is often associated with infertility. Main treatment options are symptomatic pain-oriented treatment with diverse pain and anti-inflammatory medications, long-term ovarian suppression by means of pharmacological inhibition of the ovarian estrogen production as well as surgical removal of endometriotic lesions. However, the pain recurrence rates as well as re-operation rates are high. Furthermore, long-term ovarian suppression is associated with considerable side effects and is sometimes ineffective. Therefore, effective therapeutic strategies with a low risk of side effects are urgently needed. For the purpose of developing and testing such strategies under highly standardized conditions, suitable animal models are important.

Due to the fact that mouse models are relatively low-cost and offer the significant advantage that mice can be genetically modified to express fluorescent marker proteins or to delete disease-relevant target genes, they are of increasing interest in endometriosis research. Since mice do not menstruate, they do not spontaneously develop endometriosis. As a result, endometriotic lesions must be experimentally induced by surgically transplanting or injecting uterine tissue fragments into the abdominal cavity of the mice. The induced endometriotic lesions were found to be similar to human lesions regarding estrogen receptor expression, macrophage infiltration and inflammation. However, as the grafts do not recapitulate the tissue characteristics at the time of retrograde menstruation, experimentally induced endometriotic lesions may markedly differ in growth, hormone reactivity and vascularization. To overcome this problem, a novel mouse model of endometriosis has previously been developed by transplanting syngeneic endometrial tissue from menstrual mice into the abdominal cavity of recipient mice. It was observed that the induced endometriotic lesions resembled human lesions in terms of estrogen receptor expression, inflammation and macrophage infiltration. However, it has not yet been examined under identical experimental conditions whether these lesions significantly differ from those derived from conventionally used non-menstrual mouse endometrial tissue.

To analyze this in the present thesis, non-menstrual and menstrual tissue fragments from syngeneic donor mice were simultaneously transplanted into the peritoneal cavity and dorsal skinfold chambers of non-ovariectomized (non-ovx), ovariectomized (ovx) and ovariectomized, estrogen-substituted (ovx+E2) recipient animals. This provided the possibility to directly compare the two different tissue types under the same experimental conditions. The implantation, growth and vascularization of newly forming endometriotic lesions were assessed through high-resolution ultrasound imaging, intravital fluorescence microscopy, histological analyses and immunohistochemistry. In the intraperitoneal endometriosis mouse model, a similar growth of non-menstrual and menstrual tissue was observed in non-ovx animals. Furthermore, hormonal deprivation in the ovx mice led to a comparable significant overall suppression of lesion growth. This could be completely reversed by estrogen substitution. Of interest, a significant difference between the lesion volumes of endometriotic lesions developing from non-menstrual and menstrual tissue fragments was observed in the ovx+E2 mice. By means of immunohistochemistry it was shown that lesions from menstrual tissue fragments exhibit a

significantly lower microvessel density. In the second part of the thesis, the vascularization of non-menstrual and menstrual endometrial fragments inside the dorsal skinfold chamber was analyzed using intravital fluorescence microscopy. These experiments demonstrated a significantly lower functional microvessel density in menstrual fragments compared to non-menstrual ones, indicating delayed vascularization and reduced blood perfusion of menstrual tissue grafts.

In conclusion, this is the first study to compare the development of endometriotic lesions from murine menstrual and non-menstrual tissue fragments under identical experimental conditions. It was found that growth and vascularization of the two tissue types are similar in the normal cycling mouse. However, there were distinct differences in growth and vascularization of lesions in ovx mice under exogenous estrogen stimulation. These findings indicate that in principle, non-menstrual and menstrual murine endometrium is suitable for the experimental induction of endometriosis in mice. Nonetheless, the choice of the experimental approach should be carefully adapted to the study's definite purpose and it may be suggested to combine different approaches to gain the best reproducible and valid results.

2. Zusammenfassung

Die Endometriose ist eine weit verbreitete gynäkologische Erkrankung, die durch das Vorhandensein von ektopem Endometriumgewebe außerhalb der Gebärmutterhöhle, sogenannte Endometrioseherde, definiert ist. Die Endometriose tritt bei Menschen und bei menstruierenden Primaten spontan auf. Sie ist durch ein breites Spektrum unspezifischer Schmerzsymptome gekennzeichnet, zu denen Dysmenorrhoe, Dysurie und Dyspareunie zählen, und geht häufig mit Unfruchtbarkeit einher. Hauptbehandlungsoptionen umfassen die symptomatische, schmerzorientierte Behandlung mit verschiedenen schmerz- und entzündungshemmenden Medikamenten, eine langfristige ovarielle Suppression durch pharmakologische Hemmung der ovariellen Östrogenproduktion sowie die operative Entfernung von Endometrioseherden. Allerdings sind die Schmerzrezidiv- und Re-Operationsraten hoch. Außerdem ist eine langfristige ovarielle Suppression mit erheblichen Nebenwirkungen verbunden und erweist sich manchmal als unwirksam. Es werden daher dringend effiziente und nebenwirkungsarme Therapiestrategien benötigt. Für die Entwicklung und Erprobung solcher Strategien unter standardisierten Bedingungen sind geeignete Tiermodelle von größter Bedeutung.

Da Mausmodelle relativ kostengünstig sind und den großen Vorteil bieten, dass Mäuse gentechnisch so verändert werden können, dass sie fluoreszierende Markerproteine exprimieren oder ihnen krankheitsrelevante Zielgene fehlen, sind sie für die Endometrioseforschung von zunehmenden Interesse. Da Mäuse nicht menstruieren, entwickeln sie keine spontane Endometriose. Daher müssen Endometrioseherde experimentell durch chirurgische Transplantation oder Injektion von Gebärmuttergewebefragmenten in die Bauchhöhle der Mäuse induziert. Endometrioseherde, die sich aus solchen Gewebetransplantaten entwickeln, weisen nachweislich ähnliche makro- und mikroskopische Merkmale auf wie humane Endometrioseherde. Da die Transplantate jedoch nicht die Gewebecharakteristika zum Zeitpunkt der retrograden Menstruation aufweisen, können sich die experimentell induzierten Endometrioseherde in Bezug auf Wachstum, Hormonreaktivität und Vaskularisierung deutlich unterscheiden. Um dieses Problem zu lösen, wurde in der Vergangenheit ein neuartiges Mausmodell für die Endometriose entwickelt, bei dem syngenes Endometriumgewebe menstruierender Mäuse in das Peritoneum von Empfängermäusen transplantiert wird. Dabei wurde beobachtet, dass die induzierten Endometrioseherde humanen Herden in Bezug auf Östrogenrezeptorexpression, Entzündung und Makrophageninfiltration ähnlich sind. Bislang wurde jedoch noch nie unter identischen Versuchsbedingungen untersucht, ob sich diese Herde deutlich von Herden, die aus herkömmlich verwendetem, nicht menstruellem Endometriumgewebe stammen, unterscheiden.

Um dies in der vorliegenden Arbeit zu untersuchen, wurden nicht-menstruelle und menstruelle Gewebefragmente von syngenem Spendermäusen simultan in die Peritonealhöhle und in Rückenhautkammern von nicht-ovariotomierten (non-ovx), ovariotomierten (ovx) und ovariotomierten, östrogensubstituierten (ovx+E2) Empfängertieren transplantiert. Dies ermöglichte einen direkten Vergleich der beiden unterschiedlichen Gewebetypen unter denselben Versuchsbedingungen. Das Anwachsen, das Wachstum und die Vaskularisierung der neu entstehenden Endometrioseherde wurden mittels hochauflösender Ultraschallbildgebung, intravitaler Fluoreszenzmikroskopie, Histologie und Immunhistochemie analysiert. Im intraperitonealen

Endometriose-Mausmodell zeigte sich in non-ovx Tieren ein vergleichbares Wachstum von Herden, die aus nicht-menstruellem und menstruellem Gewebe stammten. Darüber hinaus führte der Hormonentzug in der ovx Gruppe zu einer vergleichbar signifikanten Hemmung des Herdwachstums. Dies konnte durch eine Östrogensubstitution vollständig rückgängig gemacht werden. Interessanterweise wurde ein signifikanter Unterschied zwischen den Herdvolumina der nicht-menstruellen und menstruellen Gewebefragmente in der ovx+E2 Gruppe beobachtet. Mittels Immunhistochemie wurde gezeigt, dass die menstruellen Gewebefragmente eine deutlich geringere Mikrogefäßdichte aufweisen. Im zweiten Teil der Arbeit wurde die Vaskularisierung von nicht-menstruellen und menstruellen Transplantaten in der Rückenhautkammer mittels intravitale Fluoreszenzmikroskopie analysiert. Diese Experimente zeigten eine signifikant geringere funktionelle Mikrogefäßdichte in menstruellen Fragmenten im Vergleich zu nicht-menstruellen Fragmenten, was auf eine verzögerte Vaskularisierung und verminderte Durchblutung der menstruellen Gewebefragmente hinweist.

Zusammenfassend lässt sich sagen, dass dies die erste Arbeit ist, welche die Entwicklung von menstruellen und nicht-menstruellen Gewebefragmenten der Maus zu Endometrioseherden unter identischen experimentellen Bedingungen vergleicht. Es wurde gezeigt, dass das Wachstum und die Vaskularisierung der beiden Gewebetypen in der normalen zyklischen Maus ähnlich sind. Allerdings zeigten sich bei ovx Mäusen unter exogener Östrogensubstitution deutliche Unterschiede im Wachstum und der Vaskularisierung der Herde. Diese Ergebnisse belegen, dass prinzipiell sowohl nicht-menstruelles als auch menstruelles Endometrium der Maus für die experimentelle Induktion von Endometrioseherden geeignet ist. Nichtsdestotrotz sollte die Wahl des experimentellen Ansatzes sorgfältig auf den konkreten Zweck einer Studie ausgerichtet sein und es wird empfohlen, verschiedene Ansätze miteinander zu kombinieren, um die bestmöglichen reproduzierbaren und validen Ergebnisse zu erhalten.

3. Introduction

3.1 Human endometriosis

3.1.1 Definition and prevalence of endometriosis

Endometriosis is a common inflammatory, estrogen-dependent disease (Giudice, 2010). It is defined by the presence of endometrial tissue outside the uterine cavity, referred to as endometriotic lesions and is associated with chronic pelvic pain, dysmenorrhea and infertility (Galle, 1989; Culley *et al.*, 2013; Smolarz *et al.*, 2021). The prevalence of endometriosis lies between 6% and 10% in women of reproductive age (Eskenazi and Warner, 1997) and can reach 50% in women experiencing chronic pelvic pain or suffering from infertility (Giudice and Kao, 2004; Giudice, 2010). Endometriotic lesions are most commonly found in the small pelvic region and develop on the pelvic organs, such as the ovaries and the fallopian tubes, on the peritoneum or in the Douglas pouch (Harada *et al.*, 2014). Endometriosis can also develop outside the small pelvic region on the intestine, ureter or even inside the thorax (Alwadhi *et al.*, 2016). The different forms of endometriosis can vary in symptoms and require different therapeutic approaches based on location, severity and individual progress of the disease (Kennedy *et al.*, 2005; Debus and Schuhmacher, 2013).

3.1.2 Morphology and classification of human endometriosis

Endometriosis is classically characterized by the presence of endometrial glands and stromal tissue outside the uterine cavity. Endometriotic lesions exhibit a diverse morphology. Commonly, they are small, dark brown lesions grouped at the surface of organs or the peritoneal wall (Kennedy *et al.*, 2005). Occasionally, the ectopic endometrial tissue can exhibit a red or bluish pigmentation, white discoloration or the same color as the surrounding tissue. Some endometriotic lesions appear as plaques or scar tissue. Others form polyps, small cysts or cysts containing thick brown fluid, referred to as endometriomas. Endometriotic lesions can also grow infiltratively and develop subperitoneally by invading the surrounding tissue. This type of endometriosis is called deep-infiltrating endometriosis (Kennedy *et al.*, 2005; Debus and Schuhmacher, 2013). The histological appearance of endometriotic lesions can also be diverse. Most common are lesions consisting of highly differentiated endometrial glands and stromal tissue, whereas endometriotic lesions with low epithelial differentiation and hypertrophic glands are rare (Giudice, 2010; Debus and Schuhmacher, 2013; Bulun *et al.*, 2019).

There are different classification systems used for the categorization of endometriosis. The revised American Society for Reproductive Medicine (r-ASRM) classification is the most widely known and represents an established method for describing surgical findings in the field of endometriosis diagnostics (Valle and Sciarra, 2003). The Enzian classification is an addition to the r-ASRM, which also considers cases of deep-infiltrating endometriosis (Johnson *et al.*, 2017). The r-ASRM and the Enzian classification allow the systematical documentation of the disease and enable its categorization in different stages dependent on the lesion size, location and growth behavior (Johnson *et al.*, 2017). In addition, the fertility index (EFI) provides a prediction of the fertility outcome of endometriosis patients and can considerably influence the treatment strategies (Revised American Society for Reproductive Medicine classification of endometriosis: 1996, 1997; Johnson *et al.*, 2016; Lee *et al.*, 2021).

3.1.3 Pathogenesis of human endometriosis

The pathogenesis of endometriosis has not been ultimately clarified. Various theories provide a possible explanation for the development of this disease, but until now none of them has been able to completely explain the progress of the disease. Some theories describe the development of endometriosis out of the existing uterine endometrium, whereas others postulate the development of ectopic endometrium from non-endometrial cells. The most widely accepted theory is Sampson's implantation theory. This theory describes the development of endometriosis in the peritoneal cavity due to the growth of vital endometrial cells derived from menstrual blood. The menstrual blood reaches the peritoneal cavity through retrograde menstruation (D'Hooghe and Debrock, 2002), i.e. reflux of shed endometrial debris through the fallopian tubes into the peritoneal cavity. It is a physiological, commonly found process in many women. According to the implantation theory, the development of endometriosis is menstrual cycle-dependent, which explains its occurrence in species experiencing menstrual bleeding, like humans and some non-human primates (Merrill, 1968; Emera *et al.*, 2012).

The metaplasia theory describes the in-situ development of endometriosis from other cell types, such as embryonic cell rests (Russell, 1899; Longo, 1979) or peritoneal mesothelium (Suginami, 1991; Matsuura *et al.*, 1999). Metaplasia can be influenced by factors like active inflammation or hormone levels (Petruškevičiūtė and Bužinskienė, 2021). The theory of metaplasia can explain the rare occurrence of endometriosis in patients, who do not physiologically possess endometrium (Giannarini *et al.*, 2006; Mok-Lin *et al.*, 2010) as well as the development of endometriotic lesions outside the pelvic region (Acar *et al.*, 2015; Alwadhi *et al.*, 2016).

The different theories of the pathogenesis of endometriosis do not explain why this condition occurs in some women but not in others. The limited manifestation of endometriosis suggests the existence of additional factors that influence its development. In this context, the immune system plays an important role. In fact, it is assumed that women suffering from endometriosis exhibit a limited immunological response to ectopic endometrium, which facilitates the implantation and development of endometriotic lesions (Lebovic *et al.*, 2001). Another factor is genetic predisposition. It has been proven that women with first-line relatives, who suffer from endometriosis, have a higher risk of developing the condition than women with no affected family members (Simpson *et al.*, 1980; Kennedy *et al.*, 1995). The fact that endometriosis is a chronic disease that is typically found in women of reproductive age can be explained by the sensibility of endometriotic lesions against estrogen. Endometriotic lesions express estrogen receptors and aromatases, i.e. enzymes that facilitate the transformation of androgens to estrogens (Giudice, 2010). Therefore, the elevated levels of estrogen, which are physiologically present in women in their fertile years, contribute to the growth of the ectopic endometrium (Kitawaki *et al.*, 2002; Burney and Giudice, 2012).

Although the pathogenesis of human endometriosis has not completely been clarified, it is known that the vascularization of endometriotic lesions is a crucial step in its development. Similar to growing tumors, endometriotic lesions develop a functional vascular network in order to ensure a continuous blood flow, oxygenation and nutrient supply (Groothuis *et al.*, 2005). Consequently, clinical studies detected elevated levels of pro-angiogenic factors in the peritoneal fluid of patients with endometriosis when compared to women without the disease (Nap *et al.*, 2004). Due to the vascularization characteristics of endometriotic lesions, the early form of active endometriosis typically presents as red

lesions containing a high density of blood vessels (Nisolle *et al.*, 1993). Because of its dependence on blood vessel formation, endometriosis has been classified as an angiogenic disease similar to cancer (Healy *et al.*, 1998). Moreover, anti-angiogenic agents have already been tested as a promising therapeutic approach for its treatment (Soares *et al.*, 2012; Laschke and Menger, 2018).

Different mechanisms, which contribute to the vascularization of endometriotic lesions, have been identified. These mechanisms include angiogenesis, vasculogenesis and inosculation. Angiogenesis is the development of new blood vessels from pre-existing ones. This is a physiological process required for wound healing, but it is also important for the development of cancer and endometriosis (Chang *et al.*, 2004). Angiogenesis undergoes the regulation of different pro-angiogenic factors, such as vascular endothelial growth factor (VEGF) and matrix metalloproteinases (MMPs) (Potente *et al.*, 2011). In contrast, vasculogenesis is defined as the *de novo* formation of blood vessels from endothelial progenitor cells (EPCs). Previous studies suggest that this process may be hormonally regulated. In fact, Rudzitis-Auth *et al.* (2016) demonstrated that treating mice with β -estradiol 17-valerate facilitates the incorporation of EPCs into the newly forming microvessels of surgically induced endometriotic lesions. Finally, inosculation describes the interconnection of individual blood vessels or entire microvascular networks with each other (Laschke and Menger, 2018). Previous research has highlighted the importance of tissue integrity in the development of ectopic endometriotic lesions. The tissue integrity requires the presence of a functional vascular network, which can readily connect with other vascular networks, facilitating faster and more effective lesion development. Consistent with this view, Nap *et al.* (2003) demonstrated that transplanting endometrial fragments, rather than dispersed endometrial cells from menstrual effluent, leads to the formation of endometriotic lesions.

The importance of vascularization for human endometriosis provides a broad research field for the development of novel diagnostic and therapeutic strategies. Biochemical markers that indicate the vascularization of lesions have been previously identified. Of particular interest is VEGF (McLaren *et al.*, 1996). Additional significant pro-angiogenic factors include inflammatory cytokines, such as interleukin (IL)-8 and tumor necrosis factor (TNF)- α . These cytokines stimulate the growth and local formation of new blood vessels and hold a vital role in processes, such as angiogenesis, vasculogenesis and inosculation of endometriotic lesions (McLaren, 2000; Kyama *et al.*, 2006; Laschke and Menger, 2018). Based on these findings, one aim of this thesis was to investigate the early vascularization of endometriotic lesions under the influence of different hormonal conditions. For this purpose, endometriotic lesions were induced in the dorsal skinfold chamber model and analyzed through repeated intravital fluorescence microscopy (Laschke and Menger, 2007).

3.1.4 Symptoms, diagnosis and therapy of human endometriosis

Typical symptoms of endometriosis patients are chronic pelvic pain, abdominal pain, dysmenorrhea, dyspareunia and infertility (Pellicer *et al.*, 2001; Momoeda *et al.*, 2002; Berkley *et al.*, 2005; Giudice, 2010). Endometriotic lesions are often found in the pelvic area, which explains chronic pelvic pain as the most common symptom (Giudice, 2010; Nnoaham *et al.*, 2011). The complaints can be related to the menstrual cycle or can occur unpredictably (Giudice, 2010; Debus and Schuhmacher, 2013). They often do not correlate with the histopathological findings and can vary in quality and intensity, becoming a considerable physical and mental burden for the affected patients (Evans *et al.*, 2007). Endometriosis-

associated infertility is still an object of active research (Bergqvist and D'Hooghe, 2002; Tanbo and Fedorcsak, 2017). One of the factors regarded as relevant for its occurrence is the mechanical obstruction of the tubes, which is caused by the growth of endometriotic lesions inside them or invasion of their wall (Valle and Sciarra, 2003; Tanbo and Fedorcsak, 2017). Furthermore, it is considered that alterations in the consistency of the peritoneal fluid in women with endometriosis can disturb sperm motility (Oral *et al.*, 1996). Other possible factors relevant for developing endometriosis-associated infertility are ovulatory dysfunction (Dmowski and Radwanska, 1984) and an altered endometrial environment (Pellicer *et al.*, 2001).

The diagnosis of endometriosis can be prolonged and difficult. This is due to the fact that patients with endometriosis can experience a variety of pain symptoms that often mimic other conditions, such as inflammatory pelvic diseases, psychological diseases or even urological disorders, including interstitial cystitis (Debus and Schuhmacher, 2013). Part of the diagnostic process is a thorough gynecological examination and anamnesis. Nevertheless, visualization of endometriotic lesions through laparoscopic surgery or laparotomy is still the golden standard in diagnosing the disease. This method has a high sensitivity and provides the opportunity to define the exact type, stage and location of endometriosis (Kennedy *et al.*, 2005; Schleedoorn *et al.*, 2016; Rolla, 2019). Non-invasive methods, such as transvaginal ultrasound and magnetic resonance tomography (MRT), may be also used in the diagnosis or as an additional visualization method for the planning of surgical interventions (Valle and Sciarra, 2003; Kennedy *et al.*, 2005; Giudice, 2010).

The treatment of endometriosis aims to relieve disease-associated pain, to improve the patient's quality of life and to enhance fertility (Momoeda *et al.*, 2002; c *et al.*, 2021). It can be differentiated between medicinal and surgical therapy (Rolla, 2019). Endometriosis is an estrogen-dependent disease that develops mainly in women with an active hormonal cycle. Based on this fact, medicinal therapy is likely associated with a considerable recurrence rate of endometriosis as long as ovarian hormonal production is present (Valle and Sciarra, 2003). Drug treatment can be either pain-oriented or aiming at disturbing the growth of endometriotic lesions by influencing the hormonal cycle or by combining both strategies (Giudice and Kao, 2004). Various therapeutic approaches are employed to manage symptoms and impact the progression of endometriotic lesions. These include nonsteroidal anti-inflammatory drugs (NSAIDs), oral contraceptives, gestagens, gonadotropin-releasing hormone (GnRH) agonists and antagonists as well as surgical therapy (Kalaitzopoulos *et al.*, 2021).

NSAIDs are used in the pain-oriented treatment of endometriosis. These drugs can be applied as a single treatment in patients with milder pain complaints or combined with other therapeutic methods (Kalaitzopoulos *et al.*, 2021). The application of NSAIDs does not influence the growth of endometriotic lesions, because it does not intervene with the hormonal cycle. Moreover, there is no conclusive evidence for the efficiency of NSAIDs in relieving endometriosis-associated pain (Allen *et al.*, 2005; Brown *et al.*, 2017).

Widely used oral contraceptives are estrogen-progesterone-combined agents (Bedaiwy *et al.*, 2016). Long-term application of a high dosage of these drugs inhibits the GnRH production of the hypothalamus. Consequently, the synthesis of luteinizing hormone (LH) and follicle-stimulating hormone (FSH) in the pituitary gland is suppressed, resulting in a reduced ovarian activity with amenorrhea (Valle and Sciarra, 2003; Debus and Schuhmacher, 2013). Monophasic oral contraceptives containing a

constant dose of estrogen and progesterone have become the preferable representative of this group because of their better tolerance. Furthermore, oral contraceptives can sustain therapeutic results after surgical intervention (Debus and Schuhmacher, 2013).

Another possible treatment is the substitution of gestagens. Gestagen supplementation suppresses the hypothalamic hormone secretion and is proven to be effective in the pain management of endometriosis (Valle and Sciarra, 2003). Considerable side effects of this therapeutic approach are breakthrough bleedings, fluid retention, depression, breast tenderness and nausea (Debus and Schuhmacher, 2013).

The continuous substitution of GnRH agonists results in the downregulation of GnRH receptors in the pituitary glands. This leads to their desensitization against GnRH and inhibits the production of LH and FSH, which suppresses the ovarian hormone production and induces a hypogonadotropic, hypogonadal state (Magon, 2011). Hence, this group of medications is an excellent choice for the preoperative reduction of endometriotic lesions or postoperative treatment. During the application of GnRH agonists, endometriotic lesions cease their growth and start regressing. Unfortunately, this method cannot replace surgical therapy since a rapid redevelopment of the lesions after 9 to 12 months is expected after discontinuing GnRH agonist treatment (Valle and Sciarra, 2003). Moreover, the hypogonadotropic state is associated with considerable side effects, such as temperature sensitivity, regression of the vaginal epithelium and loss of bone mass (Magon, 2011). For these reasons, GnRH agonists are not suitable for long-term use and have a limited application time of up to 6 months (Giudice, 2010). However, there is the possibility of a so-called add-back therapy. This means the continuous substitution of low doses of estrogen and progesterone combined with GnRH agonists to reduce bone loss without promoting the growth of endometriotic lesions (Surrey, 1999; Rolla, 2019).

A novel therapeutic option is the use of GnRH antagonists. This medication also leads to the suppression of the hypothalamic-pituitary axis and reduces estrogen and progesterone levels, but provides a dose-dependent hormonal suppression and rapid normalization of the cycle after discontinuation (Kalaitzopoulos *et al.*, 2021; Osuga *et al.*, 2021).

Surgical therapy, performed primarily through minimally invasive surgery, is strongly indicated in all women with severe complaints, like those suffering from decreased fertility, long-term pain symptoms or obstruction of organs through the excessive growth of endometriotic lesions (Kennedy *et al.*, 2005; Rolla, 2019). The surgical intervention can be performed as a primary or secondary method after unsuccessful conservative therapy. It is aimed at lysing adhesions and removing endometriotic lesions, improving fertility and decreasing pain. However, recurrence of endometriosis can be expected even after a surgical intervention as long as the woman possesses an active cycle (Kennedy *et al.*, 2005; Practice Committee of the American Society for Reproductive Medicine, 2014). Therefore, drug therapy often accompanies surgical therapy (Giudice, 2010).

3.2 Cycles

3.2.1 The female menstrual cycle

The woman's menstrual cycle plays a vital role in developing and maintaining endometriosis. Hence,

the knowledge of its underlying mechanisms can provide a better understanding of the pathogenic factors determining the development and growth of endometriotic lesions. Mice do not exhibit a menstrual cycle but a hormonal cycle called the estrous cycle. Furthermore, they do not develop endometriosis spontaneously. Nonetheless, rodents represent essential subjects for endometriosis research.

The female menstrual cycle is a complex cycle of hormonal changes and the physiological answer of the body. It begins with puberty, is a sign of the sexual maturity of the woman and her reproductive ability and ends with the menopause. The menstrual cycle starts on the first day of the bleeding and ends the day before the subsequent bleeding. The cycle of the woman commonly has a duration of approximately 28 days. However, this period can vary depending on the time needed for the development of a mature follicle. The hormonal changes during this period influence the woman's uterus, breasts and vagina with the endometrial layer of the uterus going through the most drastic changes. Therefore, the woman's cycle is commonly divided into a hormonal cycle representing the hormonal fluctuations and the cycle of the endometrium (Fig. 1A) (Teschner and Hinrichsen, 2013).

The female menstrual cycle underlies the regulation of GnRH and, in consequence, the gonadotropic hormones LH and FSH. These hormones are released in pulses into the bloodstream to reach their target - the ovaries (Teschner and Hinrichsen, 2013; Ver, 2013). The function of FSH is to stimulate the growth of the ovarian follicles. FSH together with LH promotes androgen synthesis in the ovaries and the evolution of the follicles from primary to tertiary follicles. Furthermore, LH is an activating signal for ovulation and causes a preovulatory increase in gestagen production in the follicles. The hypothalamic functions can be stimulated or inhibited through a feedback mechanism based on the physiological concentration of the produced ovarian hormones (Teschner and Hinrichsen, 2013).

The growth of the ovarian follicles begins with the secretion of GnRH and subsequent production of FSH. In the first phase of the ovarian (hormonal) cycle, a dominant follicle is selected and continues developing as the other follicles cease their growth. With the follicle's growth, the production of estrogen increases and the FSH production ceases as an answer to the negative feedback. In addition, under the influence of estrogen, a new functional layer of endometrium starts developing in the uterus. This process can be attributed to the proliferative phase of the endometrial cycle (Fig. 1A) (Jabbour *et al.*, 2006). The fast elevation of estrogen in the late follicular phase stimulates the synthesis and release of LH. LH urges a preovulatory progesterone boost (Fig. 2A). The preovulatory concentration of LH can reach ten times of its basic concentration. If a tertiary follicle has been developed at this point, ovulation can take place. The ovulation process is described as LH and progesterone-dependent activation of proteolytic enzymes and prostaglandins, which initiates the rupture of the follicle wall and the release of the egg from the ovary. The period after the ovulation is called the luteal phase (Fig. 1A). After the ovulation, the rest of the ruptured follicle is vascularized and builds the corpus luteum that takes on the production of progesterone for the preparation of pregnancy. As a result, the progesterone levels increase and, thus, lead to a decreasing LH and FSH production via a negative feedback mechanism.

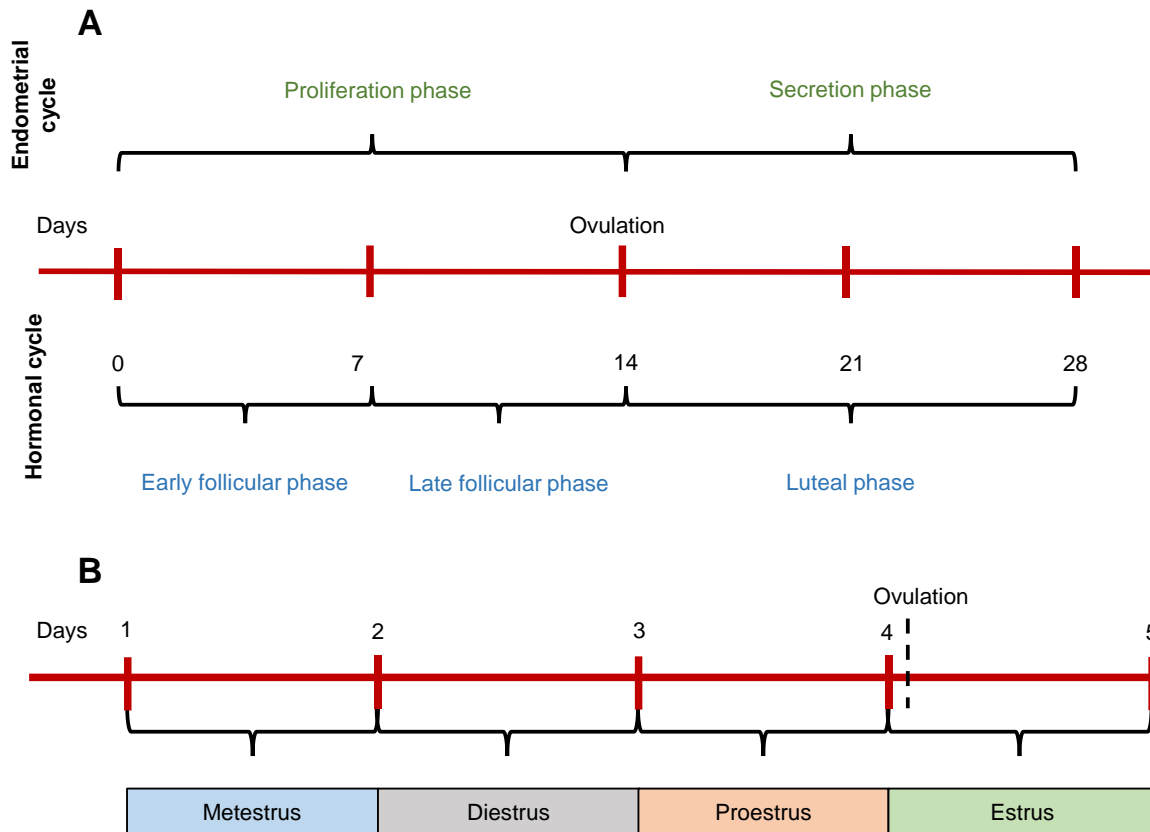


Figure 1: Graphic representation of the phases and duration of the female menstrual cycle and the mouse estrous cycle. **A:** The female menstrual cycle is divided into a hormonal and endometrial cycle and lasts for approximately 28 days (modified from “Gynäkologische Endokrinologie“, Teschner and Hinrichsen, 2013). **B:** The estrous cycle of the mouse is divided into 4 phases and lasts for approximately 4-5 days (modified from “Central circadian control of female reproductive function“, Miller and Takahashi, 2014).

If a pregnancy does not occur, the corpus luteum starts regressing, causing the progesterone levels to fall rapidly and activating menstrual bleeding (Fig. 2A). In this phase of the cycle, the inhibition of FSH decreases and a new cycle can begin (Teschner and Hinrichsen, 2013).

During the late secretion phase of the endometrial cycle (Fig. 1A), the progesterone withdrawal causes a contraction of the arteries in the endometrial layer of the uterus, the endometrium shrinks and the superficial layer gets damaged through a complete absence of blood circulation. In the following proliferation phase, the endometrial arteries regain their function through proteolytic enzymes. The blood flows to the necrotic tissue, resulting in the shedding of the damaged endometrial layer by menstrual bleeding. The woman loses 50 to 100 mL of blood during this process. In the course of the proliferation phase, the wound developing during the desquamation of the endometrium starts regenerating from the underlying layers (Fig. 1A) (Teschner and Hinrichsen, 2013).

3.2.2 The estrus cycle of mice

The mouse does not menstruate like humans and some non-human primates. Its reproductive cycle is called the estrous cycle (Allen, 1922). The estrous cycle lasts 4 to 5 days and can be divided into 4 phases: metestrus, diestrus, proestrus and estrus (Fig. 1B) (Allen, 1922; Byers *et al.*, 2012). Similar to

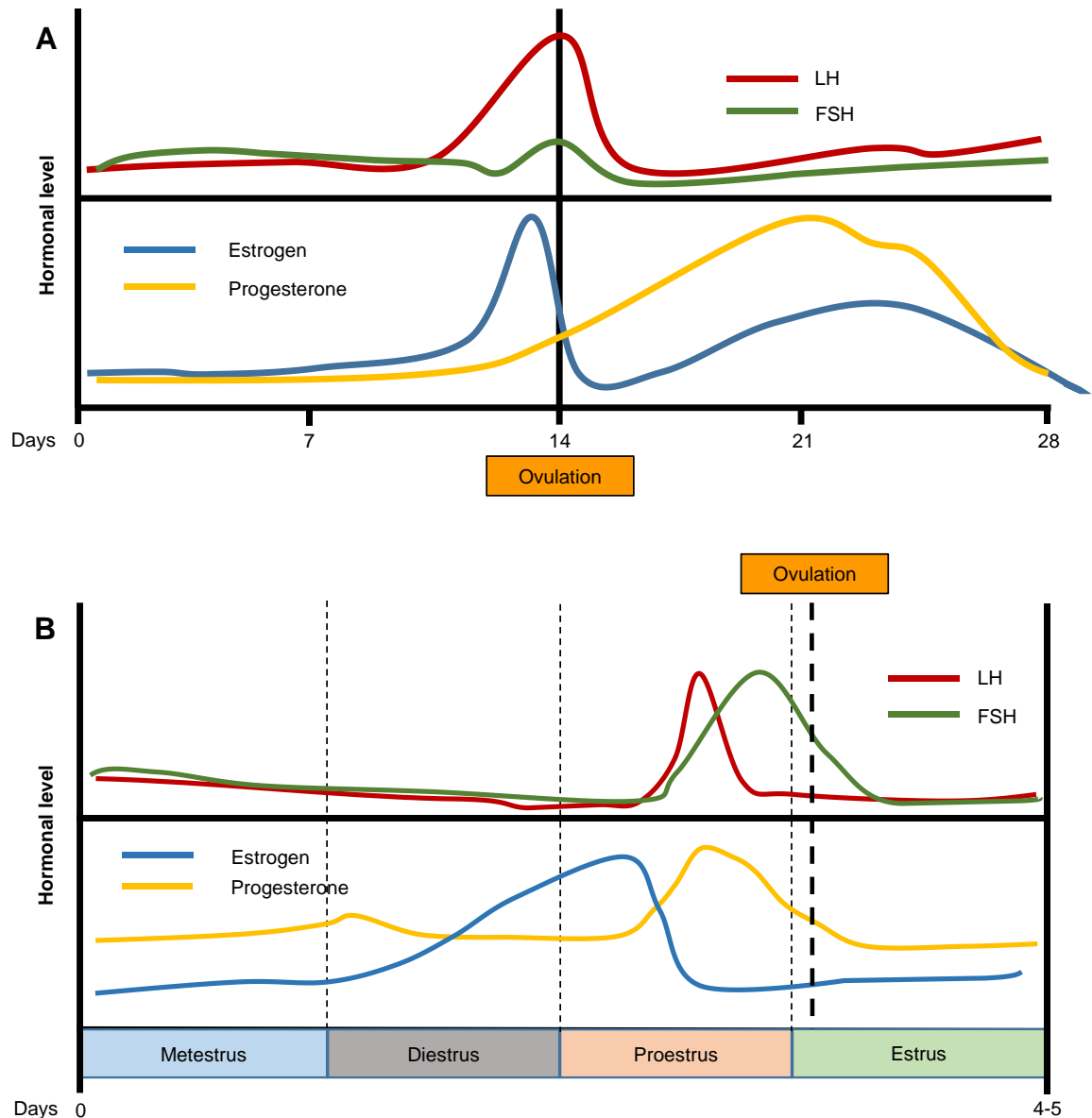


Figure 2: Graphic representation of the hormonal levels during the female menstrual cycle and the estrous cycle of the mouse. **A:** The hormonal levels of LH and FSH in women undergo cyclic changes. Accordingly, estrogen and progesterone levels fluctuate through the 28 days of the female menstrual cycle (modified from “Gynäkologische Endokrinologie”, Teschner and Hinrichsen, 2013). **B:** The hormonal levels of LH and FSH in the mouse undergo cyclic changes. Accordingly, estrogen and progesterone levels fluctuate through the 4-5 days of the estrous cycle (modified from “Central circadian control of female reproductive function,” Miller and Takahashi, 2014).

the human menstrual cycle, all estrous cycle phases are regulated by the hormone production of the hypothalamus and the gonadotropic hormones (LH and FSH) of the pituitary gland (Parkening *et al.*, 1982a, 1982b). GnRH produced by the hypothalamus stimulates the synthesis of LH and FSH in the pituitary gland, which, after releasing into the bloodstream, reach the ovaries. There, they control the production of sex steroids and the development of the follicles. FSH stimulates the growth of the primary follicles and, together with LH, is responsible for the induction of androgen production. Additionally, LH serves as an ovulation stimulus (Plant, 2012).

During the cycle, metestrus and diestrus are characterized by low hormonal levels. The estrogen

production of the granulosa cells of the maturing follicles reaches its peak during proestrus, causing GnRH pulsatile release to be more frequent (Fig. 2B). The peak in the estrogen level serves the primary purpose of stimulating the production of LH (Fig. 2B) (Bronson *et al.*, 1966). Furthermore, a progesterone increase during proestrus contributes to a spike in LH concentrations. As LH is the hormone responsible for the final progress of the maturing follicle, its spontaneous peak represents the required stimulus for ovulation. Ovulation occurs shortly after the LH spike (14 to 16 h), usually in the estrus phase (Chaffin and Vandevort, 2016).

The mouse is a spontaneous ovulatory, which can ovulate without stimulation by a male animal (Allen, 1922). After ovulation, a corpus luteum develops and takes over the progesterone production, which is required to sustain pregnancy (Tomac *et al.*, 2011). The continued existence of the corpus luteum depends on the release of the luteotropic hormone prolactin of the pituitary gland. The production of this hormone is also dependent on a mating process. If no copulation or sterile mating occurs, the corpus luteum degenerates and a new cycle begins (Bronson *et al.*, 1966).

3.2.3 Differences between the cycles

A major difference between the human and the murine cycle is their lengths. This is due to the different time needed to develop a functional follicle ready for ovulation. The human menstrual cycle is approximately 28 days long. The mouse estrous cycle lasts for 4-5 days (Figs. 1A, B). The estrous cycle length can strongly vary because of its susceptibility to the caging conditions and the light-dark rhythm (Bronson *et al.*, 1966; Plant, 2012). Female mice caged together can have a longer cycle or even stop cycling, a condition, which is called anestrus (Whitten, 1959; Bronson *et al.*, 1966). Women experience two hormonal peaks of estrogen and progesterone during the menstrual cycle. These peaks occur in the two parts of the cycle and are separated by the ovulation (Fig. 2A) (Teschner and Hinrichsen, 2013). In contrast, the estrogen and progesterone peaks of the mouse estrous cycle almost overlap (Fig. 2B). During the estrous cycle, the vagina and uterus of the mice change their morphology, but these changes are mild compared to those in humans (Allen, 1922). In contrast to the shedding of a woman's endometrium in the absence of pregnancy (Teschner and Hinrichsen, 2013), the mouse endometrium starts degenerating and gets reabsorbed (Rudolph *et al.*, 2012).

3.3 The menstruating mouse model

Because mice do not physiologically menstruate, different methods for the experimental induction of menstruation in these rodents have been established for research purposes. The induction of menstruation in the mouse was first described in 1984 by Finn and Pope, who successfully decidualized mouse endometrium. This was achieved by estrogen and progesterone substitution and stimulation of the decidualization by injecting arachidonic oil into the uterine horns. After withdrawal of the hormonal substitution, destruction of the endometrial vessels and degeneration of endometrial tissue occurred. The model was later improved by using implants for hormonal substitution (Brasted *et al.*, 2003). Finn and Pope describe a time-dependent increase in decidualization after injection of oil into the uterine lumen, which serves as a decidualization stimulus. According to this finding, later models have been adapted to allow a full decidualization of the endometrium. These models integrate a break of up to 4

days between the non-invasive decidualization stimulus and the removal of the progesterone implant, after which the harvesting of the menstrual endometrium occurs (Menning *et al.*, 2012; Cousins *et al.*, 2014; Greaves *et al.*, 2014). In other studies, decidualization of the endometrium was sustained using mifepristone, a progesterone receptor antagonist that causes pharmacological progesterone withdrawal (Xu *et al.*, 2007). In the field of endometriosis research, the decidualized uteri of mice can serve as a source for uterine tissue fragments that are grafted into recipient animals in order to experimentally induce endometriosis (Kaitu'u-Lino *et al.*, 2007; Evans *et al.*, 2011; Greaves *et al.*, 2014; Ferrero *et al.*, 2017). The engrafted endometrial tissue develops into endometriotic lesions with proven similarities to human endometriotic lesions (Cousins *et al.*, 2014). Both lesion types highly express estrogen receptor (ER)- β and are better vascularized when compared to the physiological peritoneum (Greaves *et al.*, 2014).

3.4 Animal models in endometriosis research

Endometriosis is a common gynecological disease and, thus, has been the subject of many experimental studies. Nonetheless, the exact pathogenesis of this disease is still an open question. Moreover, the failure of drugs to achieve healing and treatment free of side effects for endometriosis patients indicates the necessity for further research in this field (Rice, 2002). Diagnostics and monitoring of endometriosis often include invasive methods. Another difficulty is the prolonged diagnostic period, often resulting in the diagnosis of the disease in an advanced stage (Hadfield *et al.*, 1996). This complicated and prolonged process makes it impossible to observe the early development of the disease in women. For this purpose, animal models have been developed. These models allow for studying the mechanisms of endometriotic lesion development and permit the testing of novel medications and different treatment options (Story and Kennedy, 2004; Einspanier *et al.*, 2006; Grümmer, 2006; Burns *et al.*, 2022). As already mentioned, endometriosis develops spontaneously only in humans and non-human primates. This has led to the development of experimental methods for the induction of endometriosis in laboratory animals that do not exhibit a menstrual cycle.

3.4.1 Primate models

One of the most suitable species for endometriosis studies are non-human primates. They share multiple similarities with humans, like a menstrual cycle, an identical reproductive anatomy and endocrinology. Moreover, they are big enough to perform laparoscopic surgery with instruments fitted for humans (Marks, 1982; Fazleabas *et al.*, 2002). Other than humans, they are the only species that spontaneously develop endometriosis (Merrill, 1968; MacKenzie and Casey, 1975; Bertens *et al.*, 1982; D'Hooghe *et al.*, 1996). This can be explained by Sampson's theory of retrograde menstruation (Sampson, 1927), which connects the onset of the disease to an active menstrual cycle. In the case of some non-human primates, endometriosis is thought to be the result of often repeated menstrual cycles that have not been interrupted by pregnancy (D'Hooghe *et al.*, 1996; Tirado-González *et al.*, 2010). Such conditions are present in animals in captivity. The high number of cycles associated with retrograde menstruation causes a higher exposure rate of the peritoneum to the refluxed blood and leads to the development of endometriosis (Sampson, 1927). The long period needed for the natural onset of this

condition makes the experimental induction of the disease an advantageous method. There is an enormous diversity in the approaches used for this purpose (Story and Kennedy, 2004; Grümmer, 2006; Burns *et al.*, 2022). Experimental induction of endometriosis is possible by obstructing the animal's cervix, so that menstrual flow can be directed to the peritoneal cavity (Te Linde and Scott, 1950). Other techniques involve the mechanical sealing of the cervix (D'Hooghe *et al.*, 1994) or the surgical transplantation of ectopic endometrial tissue into the peritoneal cavity (D'Hooghe *et al.*, 1995; Fazleabas *et al.*, 2002). However, the high maintenance and preparation costs of primate models as well as major ethical concerns restrict their use to a minimum.

3.4.2 Rodent models

Rodents are favored in endometriosis research due to their low costs, easy accessibility and keeping. Furthermore, they offer the possibility of genetic engineering in order to express fluorescent marker proteins (Becker *et al.*, 2006) or to delete disease-relevant target genes (Rakhila *et al.*, 2014; Mattos *et al.*, 2019). However, rodents, except the spiny mouse (Bellofiore *et al.*, 2018), do not menstruate and, thus, do not develop endometriosis spontaneously. Nonetheless, the condition can be induced for experimental purposes by means of surgical transplantation or inoculation of endometrial fragments.

Rodent animal models can be divided into homologous and heterologous models (Somigliana *et al.*, 1999; Grümmer, 2006). The homologous model has not only been developed in mice (Cummings and Metcalf, 1995; Dogan *et al.*, 2004; Hirata *et al.*, 2005) but also in rats (Vernon and Wilson, 1985; Sotnikova *et al.*, 2010), hamsters (Steinleitner *et al.*, 1991) and rabbits (Rock *et al.*, 1993). It is further divided into autologous and syngeneic models. For the induction of endometriosis in the autologous model, the donor of endometrial fragments and the recipient animal in which endometriosis is surgically induced, are identical (Cummings and Metcalf, 1995). In the syngeneic model, a genetically identical animal to the recipient animal is used as a donor (Bacci *et al.*, 2009). For induction of endometriosis, the donor uterus is removed and cut into small fragments. These tissue samples can then be inoculated by injection into the peritoneal cavity of the recipient or surgically transplanted with or without suturing (Grümmer, 2006; Körbel *et al.*, 2010; Wilkosz *et al.*, 2011; Nenicu *et al.*, 2014). For intraperitoneal transplantation, the uterine tissue fragments can obtain all the layers of the uterus or contain only the endometrial layer after separating the endometrium from the myometrium and the perimetrium (Somigliana *et al.*, 1999; Hirata *et al.*, 2005). Both approaches lead to the development of viable intraperitoneal endometriotic lesions.

The endometrial tissue of rodents does not exactly match the human endometrium, which has led to the development of the heterologous model (Zamah *et al.*, 1984). In this model, endometrial or endometriotic tissue samples obtained from patients with endometriosis are transplanted into immunodeficient rodents to prevent their immunological rejection. The most frequently used animals for this purpose are severe combined immune deficiency (SCID) mice and athymic nude mice (Bruner *et al.*, 1997; Grümmer *et al.*, 2001; Hull *et al.*, 2005).

A dense vascular network is a characteristic feature of endometriotic lesions. Consequently, researchers are actively investigating the vascularization of endometriotic lesions in order to develop novel treatment approaches that disrupt their blood supply. The dorsal skinfold chamber model is a rodent animal model that enables the *in vivo* visualization of vascular network formation and the

quantitative assessment of distinct microhemodynamic parameters. The use of the dorsal skinfold chamber in endometriosis research has already provided valuable results. It has been shown that endometrial fragments transplanted in the dorsal skinfold chamber of ovariectomized hamsters experience a delay in vascularization, proving the importance of the ovarian function for the development of the disease (Laschke *et al.*, 2005). Moreover, it has been shown that different compounds, such as telmisartan (Nenicu *et al.*, 2014) and rapamycin (Laschke *et al.*, 2006), effectively induce the regression of endometriotic lesions due to the inhibition of vascularization.

The homologous mouse model of endometriosis is a common animal model in endometriosis research. This model still undergoes innovations and changes. The menstruating mouse is a promising step in the evolution of this model, as it closer mimics the tissue characteristics required for the development of the disease when compared to models using non-menstrual endometrium. However, so far, there has not been any direct comparison of the two approaches under identical experimental conditions. Therefore, in this thesis endometriosis was surgically induced by transplantation of both menstrual and non-menstrual uterine tissue fragments from syngeneic donor mice into the peritoneal cavity or dorsal skinfold chambers of non-ovariectomized (non-ovx), ovariectomized (ovx) and ovariectomized, estrogen-substituted (ovx+E2) recipient mice. The transplantation of the two different types of tissue in the same animals provided for the first time the opportunity to directly compare the development and vascularization of the grafts over time.

4. Aim of the study

In the present thesis, endometriotic lesions originating from murine non-menstrual and murine menstrual tissue were induced under identical experimental conditions in the mouse intraperitoneal model of endometriosis as well as the mouse dorsal skinfold chamber model. The development of endometriotic lesions was analyzed by means of repeated in vivo ultrasound imaging and intravital fluorescence microscopy. By this, the following hypotheses were tested:

- (1) Non-menstrual and menstrual uterine donor tissues exhibit comparable macroscopic and histological characteristics.
- (2) Both non-menstrual and menstrual uterine tissue grafts can develop into endometriotic lesions consisting of stromal tissue and cyst-like dilated endometrial glands.
- (3) Estrogen deprivation suppresses the growth of both non-menstrual and menstrual endometriotic lesions within the intraperitoneal mouse model of endometriosis.
- (4) Estrogen supplementation stimulates the growth of both non-menstrual and menstrual endometriotic lesions within the intraperitoneal mouse model of endometriosis.
- (5) Non-menstrual and menstrual endometriotic lesions exhibit a similar vascularization pattern as well as similar cellular proliferation under identical hormonal conditions within the intraperitoneal mouse model of endometriosis.
- (6) Non-menstrual and menstrual endometriotic lesions do not differ in their early vascularization within the dorsal skinfold chamber model.

5. Materials and methods

5.1 Animals

All animals for the experiments of this thesis were bred and analyzed at the Institute for Clinical and Experimental Surgery, Medical Faculty of Saarland University. The animal experiments were approved by the governmental animal welfare committee of Saarland, Germany (permit number: 36/2015) and were conducted according to the NIH Guidelines for the Care and Use of Laboratory Animals (NIH Publication #85-23 Rev. 1985). All donor animals, which provided menstrual and non-menstrual tissue for the induction of endometriotic lesions, were female, transgenic C57BL/6-TgN (ACTB-eGFP) 1Osb/J mice. These animals were 10 to 14 weeks old and had a body weight between 20 to 25 g. They expressed green fluorescent protein (GFP) in all their body cells except erythrocytes and hair. Accordingly, the GFP⁺ donor tissue, including GFP⁺ microvessels, could be differentiated from the GFP⁻ recipient tissue at any time point. Female C57BL/6 wildtype mice (reproductive age of 12 to 16 weeks, body weight between 22 to 28 g) served as recipient animals.

All animals were accommodated at a constant temperature of 22-24°C on a 12h/12h day/night cycle and a relative humidity of 50-60%. They received standard pellet food (Altromin, Lage, Germany) and tap water *ad libitum*.

5.2 Menstruating mouse model

For the induction of menstruation in the donor mice, an adapted, modified version of the protocol of Cousins *et al.* (2014) was used as the basis. A graphic overview of the menstruation protocol is depicted in Fig. 3.

On day 0, the donor animals underwent an ovariectomy. At the beginning of the procedure, the animals were anesthetized with a mixture of ketamine (100 mg/kg body weight Ursotamin®, Serumwerke Bernburg, Bernburg, Germany) and xylazine (12 mg/kg body weight, Rompun®, Bayer, Leverkusen, Germany) that was injected intraperitoneally (i.p.). Their backs were shaved and exposed to medical disinfectant spray (Softasept N, B Braun, Melsungen, Germany). An approximately 2 cm incision, was made in the middle of the back of the anesthetized animals, which provided easy access to the ovaries. The right ovary was pulled out, fixated with a small clamp and the blood supply through the arteria and vena ovaria and other connected small vessels was interrupted by means of electrical coagulation (High temperature cautery loop tip 2" extended shaft, Bovie, Medical corporation, Clearwater, Florida, USA). The left ovary was removed accordingly. After verifying that there was no internal bleeding, the wound was closed by a continuous 5.0 Prolene suture (Ethicon, Norderstedt, Germany). The animals received 5 mg/kg carprofen (Zoetis GmbH, Berlin, Germany) subcutaneously (s.c.) as pain medication. The operation lasted approximately 15 minutes and the animals underwent a recovery period until day 5 post ovariectomy (Fig. 3).

Thereafter, the mice received a repeated estrogen substitution (Fig. 3). The substitution was performed as a daily morning (every day at 06:30 a.m.) s.c. injection of 100 ng 17β-estradiol (E2, Sigma-

Aldrich, Taufkirchen, Germany) dissolved in 100 μ L sesame oil between days 5-7 followed by s.c. injection of 5 ng E2 between days 10-12.

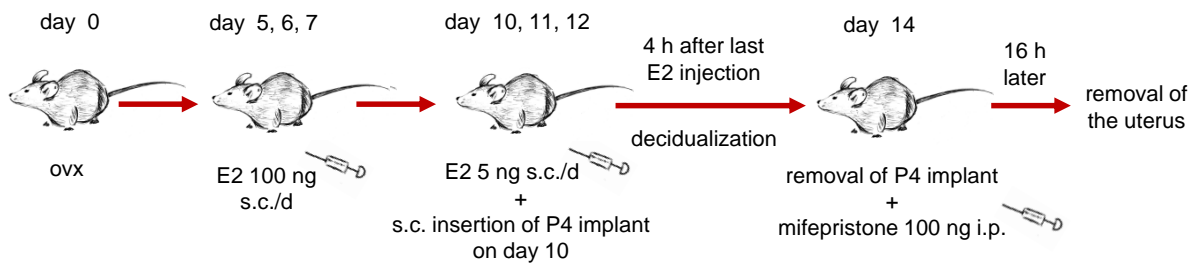


Figure 3: Schematic overview of the applied experimental protocol for the induction of menstruation in mice. The animals were first ovariectomized (ovx) to deplete endogenous steroid production. From day 5, the mice repeatedly received a daily s.c. injection of 100 ng E2 between days 5-7 followed by a s.c. injection of 5 ng E2 between days 10-12. On day 10, a Silastic tube was inserted s.c. on the back of the mice for continuous delivery of P4 between days 10-14. On day 12, approximately 4 h after the last E2 injection, the deciduation of the endometrium was induced by injecting 20 μ L of sesame oil into the lumen of the uterine horns. On day 14, the Silastic tube implant was removed, followed by a s.c. injection of 100 ng mifepristone. After additional 16 h the menstrual uterine horns were removed (modified from Nenicu A *et al.*, 2021).

On the 10th day, the mice received a progesterone implant (Cohen and Milligan, 1993). The implant consisted of a Silastic tube (inside diameter / outside diameter: 1.5 / 3.1 mm, length 15 mm, Dow Corning Corp., Midland, MI, USA) filled with progesterone (P4, 0.5 mg per day, Calbiochem, EMD Millipore, Billerica, MA, USA) and was inserted s.c. for the purpose of continuous delivery of the hormone between the days 10 to 14. For the preparation of the implant, a 15-mm part of a Silastic tube was cut off and disinfected. The Silastic tube was then closed on one end with a wooden plug and filled with progesterone (~2.0 mg) from the other end until the entire length of the tube was filled. After the tube was filled, the opened end was closed with another wooden plug (Fig. 4A). The implant was disinfected with 70% alcohol, cleaned with sterile phosphate-buffered saline (PBS) solution and put into a sterile petri dish filled with PBS and left in an incubator at 37°C for 48 h. Shortly before implantation into the animal, the P4 implant was removed from the incubator and the wooden plugs were pulled out of the tubing (Fig. 4B). The open implant was then inserted s.c. through a small incision into the skinfold of the mouse and the cut was then closed with two 5.0 Prolene sutures (Ethicon) (Fig. 4C).

The last E2 application occurred on the 12th day, followed by deciduation approximately 4 h later. For the induction of deciduation, the mice were anesthetized, the hair of the abdomen was shaved and the operating field was exposed to medical disinfectant spray (Softasept N, B Braun). The animals underwent a laparotomy. After identification of the uterus, the abdominal wall was stabilized by means of small clamps for easier access to the uterine horns. One of the horns was fixated and sesame oil was carefully injected into its lumen. After a small amount of the oil (~20 μ L) was visible through the wall of the enlarged horn, the injection was stopped. Subsequently, a small ligature was placed on the puncture site of the needle to prevent a backflow of the oil (Peterse *et al.*, 2018). This procedure was repeated with the second uterine horn. The animals were then left to recover for 1 day. Early in the morning on the 14th day, the P4 implant was removed through a small intracutaneous incision on the back of the animals. The cut was then closed with 5.0 Prolene sutures (Ethicon). Following this procedure, the animals were injected s.c. with 100 ng mifepristone (Bayer, Leverkusen, Germany)

dissolved in 5% v/v ethanol and 95% sesame oil (Rudolph *et al.*, 2012). The menstruating uterus was removed approximately 16 h after the mifepristone injection and the donor animals received a pentobarbital overdose (200 mg/kg body weight, Narcoren®, Merial GmbH, Halbermoos, Germany) for sacrifice.

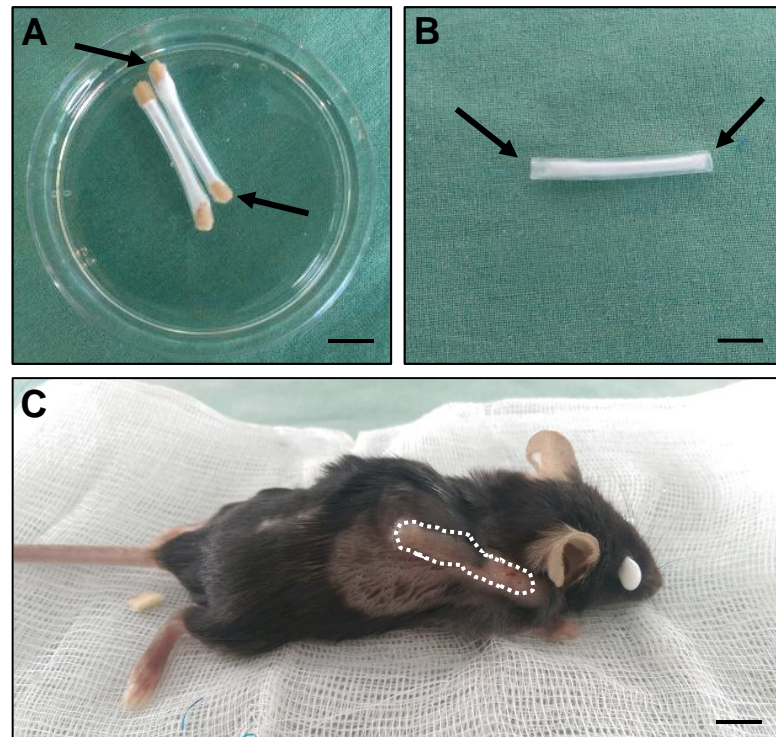


Figure 4: Preparation of a P4 implant used for continuous progesterone substitution during the induction of menstruation in mice. **A:** After the Silastic tubes were filled with P4 (~2.0 mg), they were closed on both ends with wooden plugs (arrows). **B:** Before implantation into the mice, both ends of the Silastic tubes were opened (arrows). **C:** One P4 implant was placed *s.c* in the dorsal skinfold of the mice (borders marked by dotted lines). Scale bars: A: 4.5 mm; B: 3.9 mm; C: 4.7 mm.

5.3 Identification of the estrous cycle phase

To minimize the differences between individual animals related to different hormonal levels, a vaginal lavage was performed in order to identify animals in the estrus phase. Only animals in this phase were used as donor animals for the generation of non-menstrual tissue fragments, as recipient animals for the induction of intraperitoneal endometriosis and for the preparation of the dorsal skinfold chamber. For this purpose, the mice were restrained, 20 μ L of 0.9% saline (B Braun) were carefully pipetted into the vagina and subsequently transferred to a glass slide for examination under a phase contrast microscope (CH-2, Olympus, Hamburg, Germany). The vaginal lavage method is based on the knowledge of the morphological changes of the vagina during the estrous cycle. At the end of the cycle's diestrus phase, the mitosis index in the vaginal walls starts increasing, new cell layers develop and the epithelium is thickening (Allen, 1922). The proliferation of the vaginal epithelium reaches its climax in proestrus. During the following estrus phase, the epithelium begins to cornify, which results in the shedding of the cells in the vaginal lumen. The alterations in the vaginal epithelium cause an active leukocytosis in the metestrus phase. Leukocytes remain the predominant cell type within the vaginal fluid throughout the

diestrus phase. The changes described in the cycle's different phases are reflected in the vaginal milieu and the cell spectrum it beholds. Determination of the phases of the estrous cycle was possible through the identification of the cells present in the lavage fluid (Fig. 5).

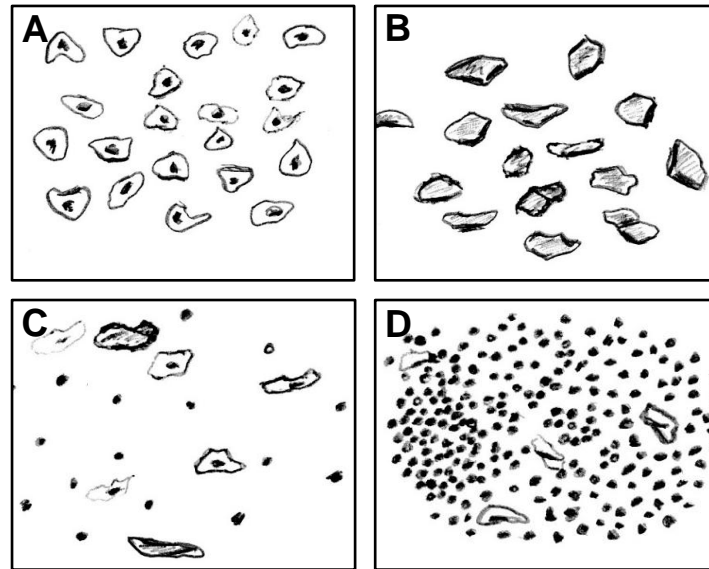


Figure 5: Graphic representation of cell populations in the vaginal fluid of mice obtained through a vaginal lavage (modified from “Mouse estrous cycle identification tool and images”, Byers et al., 2012). **A:** The proestrus phase is characterized by nucleated cells. **B:** The estrus phase is characterized by non-nucleated cornified cells. **C:** The metestrus phase is characterized by a mixed cell population containing cornified cells, nucleated cells and leukocytes. **D:** The diestrus phase is characterized by leukocytes.

5.4 Experimental protocol

The current thesis was separated in two parts. The first part included the surgical induction of intraperitoneal endometriosis in mice, applying the principles of the syngeneic homologous mouse model (Fig. 6A) to analyze the development of non-menstrual and menstrual grafts into typical endometriotic lesions under identical experimental conditions. The second part comprised the transplantation and analyses of non-menstrual and menstrual endometrial grafts in the dorsal skinfold chamber model (Fig. 6B).

For the induction of intraperitoneal endometriosis, menstrual and non-menstrual uterine tissue fragments were harvested from 18 donor animals and transplanted i.p. in 30 recipient animals (Fig. 6A). Two tissue fragments were harvested from non-menstrual uteri of 12 donor animals in the phase of estrus (non-menstrual lesions) and two other fragments were harvested from menstrual uteri of 6 donors (menstrual lesions). Both non-menstrual and menstrual uterine tissue fragments were transplanted in the same recipient animal. The recipients were randomly assigned into three hormonal states (recipient groups) consisting of 10 animals each (Fig. 6A). The animals of the first recipient group received no treatment and were in the estrus phase of the cycle on the day of transplantation. These mice exhibited an active estrous cycle throughout the entire experiment (non-ovx mice). The second recipient group underwent an ovariectomy five days prior to the induction of endometriosis. These animals received weekly s.c. injections of 100 μ L corn oil (ovx mice). The recipients of the third group underwent ovariectomy under the same conditions as described above and received a s.c. injection of 30 μ g/mL

E2 valerate dissolved in 100 μ L corn oil (estradiol-valerate, Santa Cruz Biotechnology, Heidelberg, Germany) on the day of ovariectomy (ovx+E2 mice). The s.c. E2 injections were repeated weekly. On the 28th observation day, the endometriotic lesions, which developed inside the recipients, were harvested for histological and immunohistochemical analyses.

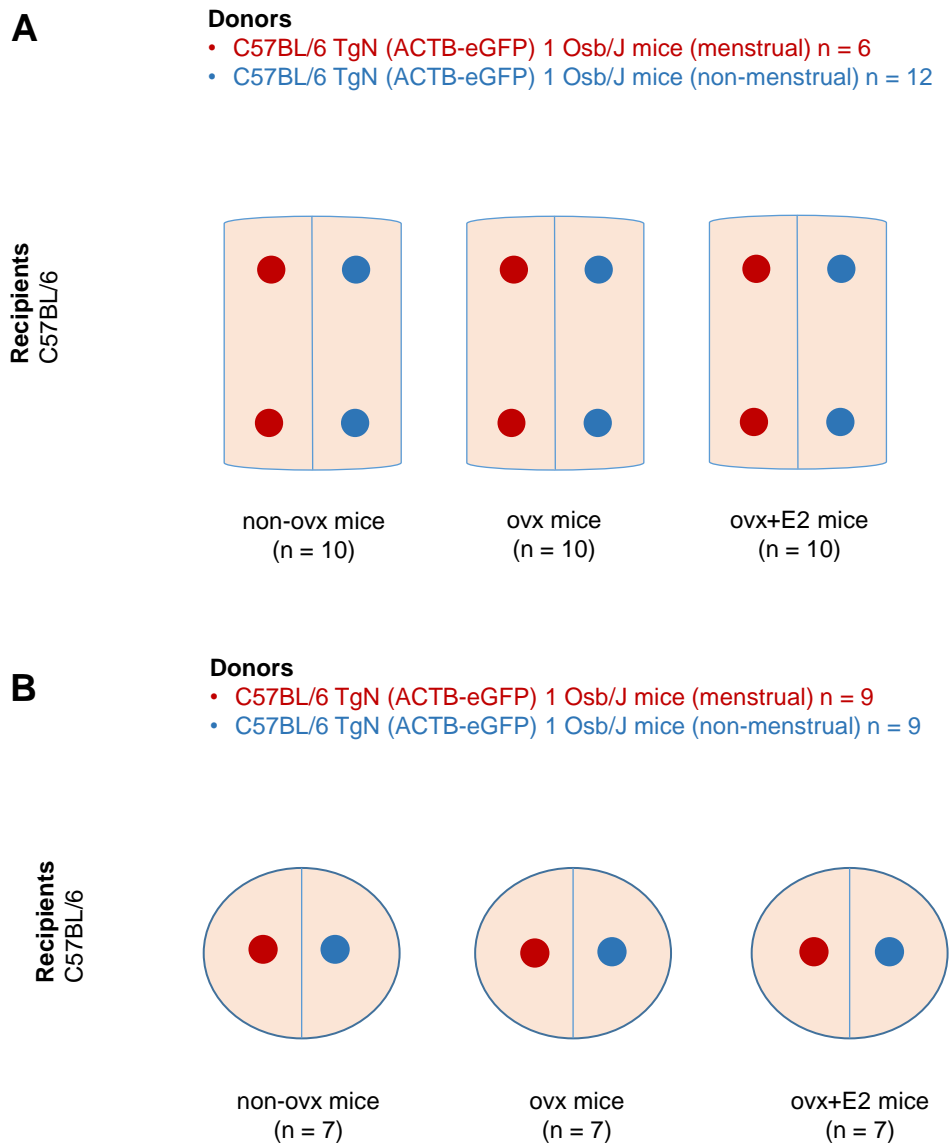


Figure 6: Graphic representation of the study protocol. **A:** Two donor (menstrual and non-menstrual) and three recipient animal groups (non-ovx, ovx and ovx+E2) were used for the intraperitoneal model of endometriosis in the first part of the thesis. Two menstrual (red) and two non-menstrual (blue) uterine tissue fragments were transplanted in each recipient animal. The non-ovx group consisted of animals, which received no treatment and were in the estrus phase of the cycle on the day of induction of endometriosis. The ovx group consisted of ovariectomized animals injected s.c. with corn oil (vehicle). The ovx+E2 group consisted of ovariectomized animals injected s.c. with E2. **B:** Two donor (menstrual and non-menstrual) and three recipient animal groups (non-ovx, ovx and ovx+E2) were used for the dorsal skinfold chamber model of endometriosis in the second part of the thesis. The animal groups were identical to the groups in (A) with the exception that only two endometrial fragments (one menstrual (red) and one non-menstrual (blue) fragments) were transplanted into the observation window of each chamber.

For the dorsal skinfold chamber model, which was used in the second part of the thesis menstrual and non-menstrual endometrial fragments were harvested from 18 donor animals and transplanted in 21 recipient animals (Fig. 6B). One tissue fragment was harvested from non-menstrual uteri of 9 donor animals in the phase of estrus (non-menstrual lesions) and one other fragment was harvested from the menstrual uteri of 9 donors (menstrual lesions). Both the non-menstrual and menstrual grafts were transplanted in the same recipient animal. The recipient animals were randomly assigned to three hormonal states (recipient groups), non-ovx, ovx and ovx+E2 mice, analog to the first part of the thesis (Fig. 6B). Each of the groups contained 7 animals. Each animal received a dorsal skinfold chamber in which two endometrial fragments, one non-menstrual and one menstrual, were transplanted. The non-ovx mice received no further treatment. All animals of the non-ovx group were in the estrus phase of the estrous cycle on the day of chamber implantation. The recipients of the ovx and ovx+E2 groups were ovariectomized a week before the implantation of the skinfold chamber to have enough time for recovery. The ovariectomy was performed by means of median laparotomy so as not to damage the back's skin, facilitating successful implantation of the dorsal skinfold chamber. The animals of the ovx and ovx+E2 groups received weekly s.c. injections of corn oil (vehicle of E2) and E2, respectively. Upon concluding the experiments, the endometriotic lesions that had developed within the recipients were collected on the 14th day for histological and immunohistochemical analyses.

5.5 Intraperitoneal endometriosis model

5.5.1 Induction of intraperitoneal endometriosis

In the first part of the thesis the intraperitoneal mouse model of endometriosis was used (Fig. 7A).

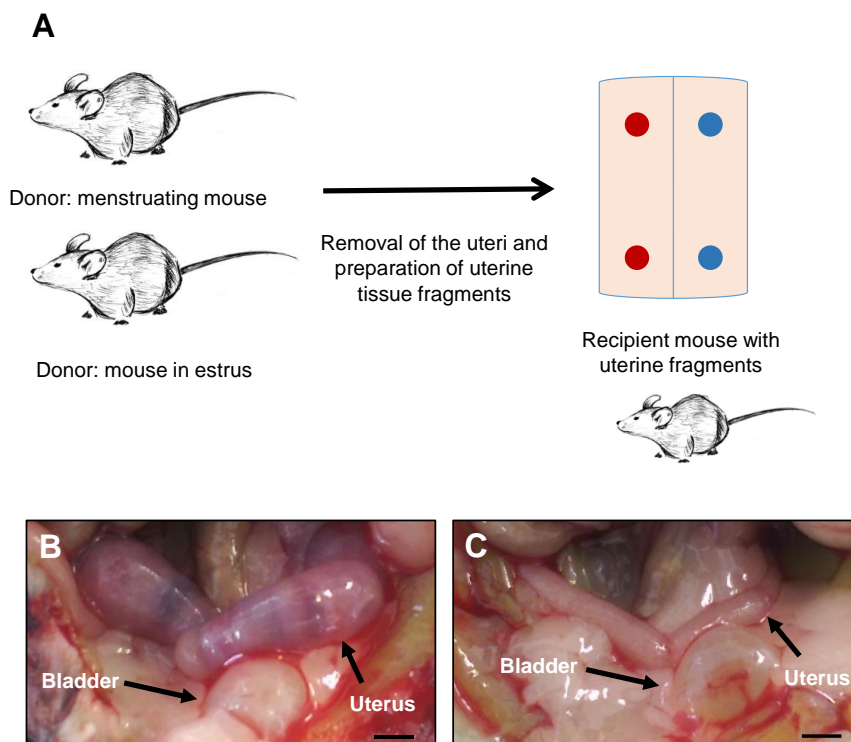


Figure 7: Graphic representation of the homologous intraperitoneal mouse model of endometriosis. **A:** The recipient animals received two menstrual (red) and two non-menstrual (blue) uterine tissue fragments. **B, C:** Donor menstrual uterus (B) in comparison to the donor non-menstrual uterus (C) in situ. Scale bars: 7 mm.

All donor animals were anesthetized with a ketamine (100 mg/kg body weight Ursotamin®, Serumwerke Bernburg) and xylazine (12 mg/kg body weight Rompun®, Bayer) mixture injected i.p. at the beginning of the procedure. Before the median laparotomy, the animal's abdomen was treated with a medical disinfectant spray (Softasept N, B Braun). All instruments for the procedure were cleaned and disinfected with 70% alcohol. After localizing the uterus (Figs. 7B, C), both uterine horns were separated from the uterine ligament and removed from the animal's abdomen. The uterus, deprived of any connective tissue, was placed in a petri dish containing 37°C warm Dulbecco's modified Eagle medium (DMEM, 10% fetal calf serum (FCS), 100 U/mL penicillin, 0.1 mg/mL streptomycin, PAA Laboratories GmbH, Cölbe, Germany) and a cork plate placed on the bottom. The uterus was pinned down onto the cork plate. Both horns were cut open longitudinally following the line, where the ligament of the uterus inserted to the uterine wall.

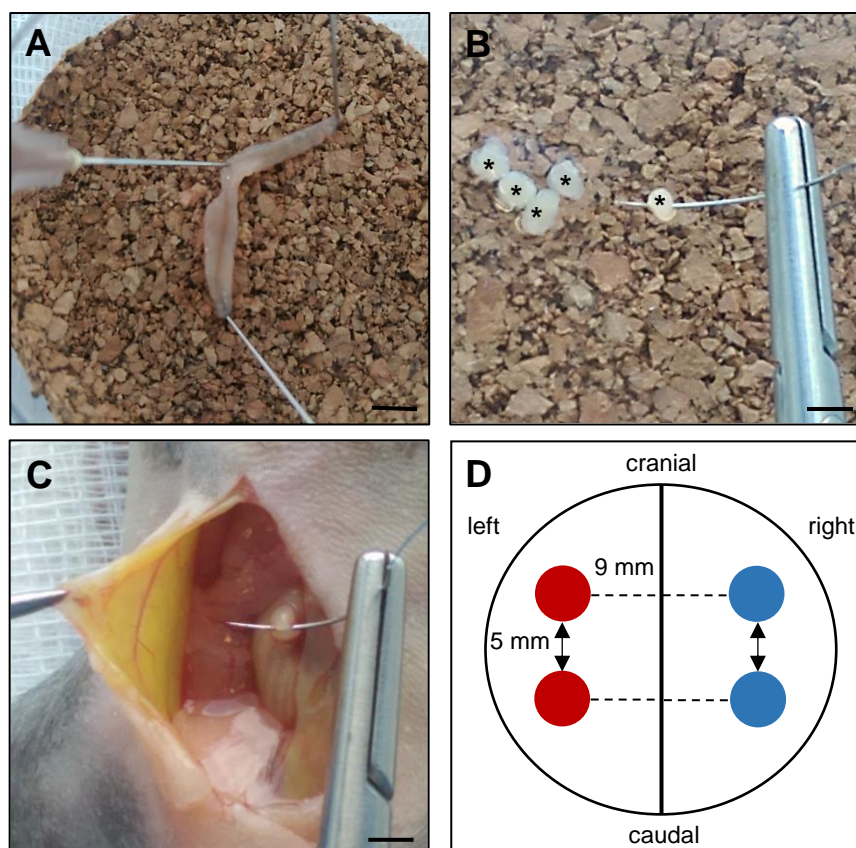


Figure 8: Preparation and transplantation of donor uterine tissue fragments for the induction of intraperitoneal endometriosis. **A:** After removing the uterus from the donor animals, it was placed in a petri dish and pinned to a cork with the myometrial and perimetrial layers facing the cork. **B:** Uterine tissue fragments ready for transplantation (asterisks) after being prepared by means of a biopsy punch. **C:** The uterine tissue fragments were sutured onto the peritoneal wall of the recipient animal. **D:** The non-menstrual (blue) and menstrual (red) uterine tissue fragments were positioned approximately 9 mm (dotted line) from the laparotomy cut (continuous line) in two quadrants on the left and right sides. The fragments were placed with a distance of 5 mm (arrows) to each other. Scale bars: A: 5 mm; B, C: 2 mm.

The procedure was performed under a stereomicroscope (M651, Leica Microsystems, Wetzlar, Germany) with microsurgical instruments. The divided horns were placed with the myometrial and perimetrial layer facing the cork (Fig. 8A) and round tissue samples were cut off using a 2-mm diameter

biopsy punch (Stiefel Laboratorium GmbH, Offenbach am Main, Germany). The uterine tissue fragments contained all uterine layers. The fragments were placed in a separate sterile petri dish with warm DMEM. This procedure was used for the preparation of non-menstrual uterine tissue fragments originating from mice in the estrus and for menstrual fragments, which were obtained from a menstruating uterus. Two non-menstrual uterine tissue fragments and two menstrual uterine tissue fragments were transplanted in each recipient animal. At the end of the procedure, the donor animals were sacrificed with an overdose of pentobarbital (200 mg/kg, Narcoren®, Merial GmbH).

For the transplantation of the uterine tissue fragments, the recipient animals (mature wildtype C57BL/6 mice) were anesthetized i.p. with a ketamine (100 mg/kg body weight Ursotamin®, Serumwerke Bernburg) and xylazine (12 mg/kg body weight Rompun®, Bayer) mixture. Before the laparotomy, the abdomen was shaved and chemically depilated (Asid-med Cream, ASID BONZ GmbH, Herrenberg, Germany). The area was cleaned with warm water and treated with a medical disinfectant (Softasept N, B Braun). The linea alba served as a reference for the median laparotomy and the incision was made along this line. The donor uterine tissue fragments were then fixed intraperitoneally on both sides of the laparotomy incision onto the peritoneal wall using a 6.0 Prolene suture (Ethicon) (Fig. 8B, C). The uterine tissue fragments were positioned with a distance of approximately 9 mm from the laparotomy cut in 2 quadrants on the left and two quadrants on the right side. They were placed with a distance of 5 mm to each other so they could be easily differentiated during later evaluations (Fig. 8D). The non-menstrual fragments were transplanted on the right side and the menstrual fragments were transplanted on the left side of the abdominal wall.

5.5.2 High-resolution ultrasound imaging

The newly developing endometriotic lesions inside the peritoneal cavity of the recipient mice were repeatedly analyzed using a Vevo 770™ high-resolution ultrasound imaging system (Visual Sonics, Toronto, Canada) (Laschke *et al.*, 2011; Nenicu *et al.*, 2014). Imaging was performed on the day of the transplantation of the uterine tissue fragments (day 0) as well as on days 7, 14, 21 and 28 and lasted approximately 15 minutes. For this purpose, the animals were placed in a Plexiglas box and anesthetized with isoflurane 5% (Baxter Deutschland GmbH, Unterschleißheim, Germany). Subsequently, 2% isoflurane (Baxter Deutschland GmbH) in 100% oxygen was used for the maintenance of anesthesia. The hair from the abdomen of the animals was chemically depilated (Asid-med Cream, ASID BONZ GmbH) to enable optimal contact with the ultrasound head. The mice were fixed in supine position. A water gel (Aquasonic 100, Parker, Fairfield, NJ, USA) was applied to the abdomen. A real-time micro-visualization (VisualSonics)-ultrasound head with a frequency of 40 MHz and 6 mm focus depth was used for the generation of two-dimensional images. A linear monitor captured images at an interval of 50 µm. The ultrasound images were analyzed with a three-dimensional reconstruction analyses software (VisualSonics) distributed with the ultrasound imaging system. The boundaries of the endometriotic lesions and their anechoic cyst-like dilated glands were manually outlined in parallel slides of the three-dimensional ultrasound images. The used images were separated by means of manual image segmentation. The overall volume of the endometriotic lesions and the volume of their cysts and stromal tissue (overall lesion volume and cyst volume in mm³) were determined based on the outlined areas (VisualSonics software). On day 28, the animals were sacrificed with an

overdose of pentobarbital i.p. (200 mg/kg, Narcoren®, Merial GmbH) and the endometriotic lesions were harvested for histological and immunohistochemical analyses.

5.6 Dorsal skinfold chamber model

5.6.1 Preparation of the dorsal skinfold chamber

The dorsal skinfold chamber model was used to analyze the vascularization of newly developing non-menstrual and menstrual endometriotic lesions. The dorsal skinfold chamber consists of two symmetrical titanium frames (weight: ~2 g) with a small observation window, which were implanted on the extended dorsal skinfold of the animals (Laschke *et al.*, 2011).

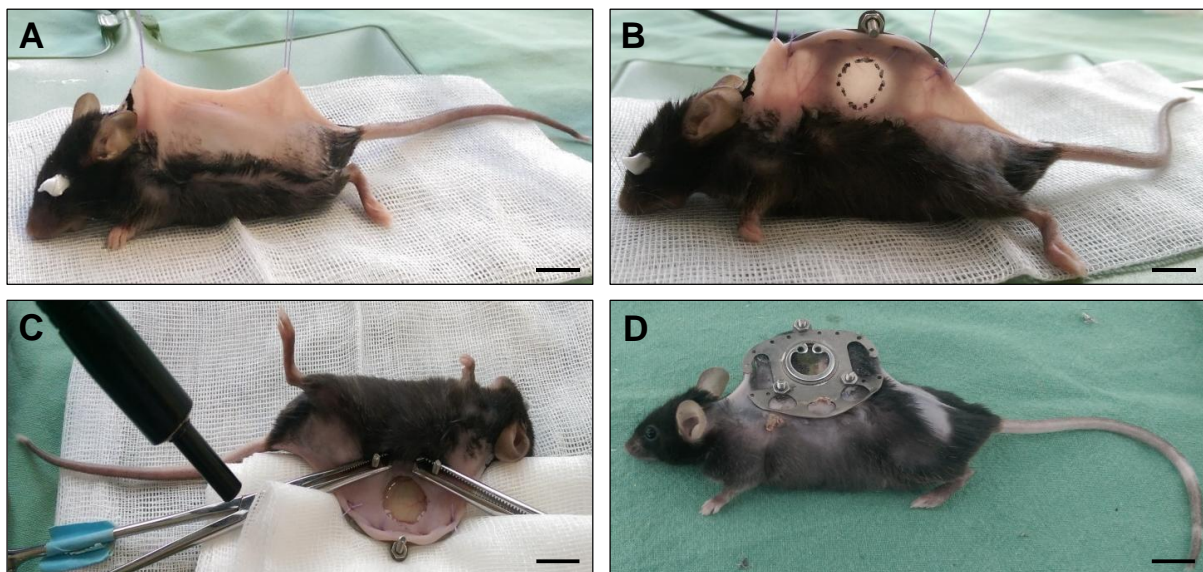


Figure 9: Preparation of the dorsal skinfold chamber. **A:** A recipient animal with stretched dorsal skinfold. **B:** The first frame of the chamber is stitched to the back side of the skinfold between the two visible major vessels and the location of the chamber's window is encircled. **C:** Preparation of the observation window under a stereomicroscope. **D:** A recipient animal after implantation of the second frame of the chamber: The observation window is covered with a cover glass and a snap ring. Scale bars: A, D: 11 mm; B: 9 mm; C: 13 mm.

For the preparation of the chamber, the animal was placed in deep anesthesia (ketamine 100 mg/kg body weight, Ursotamin®, Serumwerke Bernburg and xylazine 12 mg/kg body weight, Rompun®, Bayer), the hair from the back was carefully shaved and chemically depilated (Asid-med Cream, ASID BONZ GmbH), the skin was cleaned with water and disinfected with medical disinfectant spray (Softasept N, B Braun). The dorsal skinfold was stretched and trans-illumination was used for the visualization of the main underlying vessels on both sides of the skinfold. The vessels were positioned in an overlapping position and the skinfold was fixated with two 5-0 silk sutures. These sutures were used to secure the stretched skinfold, one near the head and the other one near the tail of the mouse (Fig. 9A). The first frame of the chamber was stitched to the back side of the skinfold between the two visible major vessels (Fig. 9B). The two screws of the frame were then passed through small openings made in the area of the proximal back of the mouse and caudal from this point in the pelvic region. The location of the

observation window was marked in a circular area (Fig. 9B). Subsequently, the mouse was placed in lateral position under a stereomicroscope (M651, Leica Microsystems). The cutis, subcutis, panniculus carnosus muscle and the two layers of retractor muscle were removed in the marked area of the observation window using microsurgical instruments (Fig. 9C). Accordingly, the striated panniculus carnosus muscle, located on the back side of the skinfold, was exposed. This procedure was performed carefully to avoid unnecessary contamination and damage of the underlying tissue, which served as the observation field for later microscopic analyses. The second frame of the chamber was inserted and the observation field was flushed with 0.9% NaCl before covering it with a cover glass. The glass was then secured with a snap ring (Fig. 9D). The skinfold chamber was not burdening for the animals. They showed normal cleaning, feeding and sleeping habits. After the preparation of the chamber, the animals were left to recover for 48 h prior to the transplantation of endometrial fragments into the observation window.

5.6.2 Transplantation of endometrial fragments into the dorsal skinfold chamber

In the second part of this thesis, the donor animals used for the dorsal chamber model were divided into two groups. The first donor group consisted of transgenic C57BL/6-TgN (ACTb-eGFP) mice in the phase of estrus and the second group of menstruating transgenic C57BL/6-TgN (ACTb-eGFP) mice. The induction of endometriotic lesions in the dorsal skinfold chamber was performed according to Feng *et al.* (2012). The donor animals were anesthetized by i.p. injection of a mixture of ketamine (100 mg/kg body weight Ursotamin®, Serumwerke Bernburg) and xylazine (12 mg/kg body weight Rompun®, Bayer). After a median laparotomy, both horns of the uterus were localized, removed and placed in a petri dish containing 37°C warm DMEM (PAA Laboratories GmbH) and a cork plate. The petri dish was then positioned under a stereomicroscope (M651, Leica Microsystems). The uterine horns were fixated on the cork plate with needles and cut open longitudinally following the line, where the ligament of the uterus inserted to the uterine wall. The horns were then fixed with the endometrial epithelium facing the cork. The myometrial and perimetrial layers were carefully removed, ensuring that the epithelial layer of the endometrium remained intact. The obtained endometrial tissue was placed in another petri dish containing DMEM (PAA Laboratories GmbH) and cut into fragments with a size of ~0.9 mm² using a template (Figs. 10A-D). The fragments were then transferred into a petri dish containing bisbenzimidazole (200 µg/mL, Sigma-Aldrich), left there for 2 minutes and were subsequently transferred to a petri dish containing 37°C warm DMEM (PAA Laboratories GmbH). After transplantation into the dorsal skinfold chamber, the bisbenzimidazole-stained endometrial fragments exhibited a bright fluorescence upon ultraviolet light epi-illumination and, thus, could be easily localized and differentiated from the non-stained host tissue.

For the transplantation of the endometrial fragments, the mice with dorsal skinfold chambers were anesthetized by means of an i.p. injection of ketamine (100 mg/kg body weight Ursotamin®, Serumwerke Bernburg) and xylazine (12 mg/kg body weight Rompun®, Bayer) and fixed in right lateral position on a plexiglas stage. The snap ring with the cover glass were removed from the observation window. The chamber was flushed with 0.9% NaCl and one endometrial tissue fragment from non-menstrual endometrium and one from menstrual endometrium were placed in the chamber ~4 mm apart

from each other. The non-menstrual fragment was always positioned caudally, while the menstrual

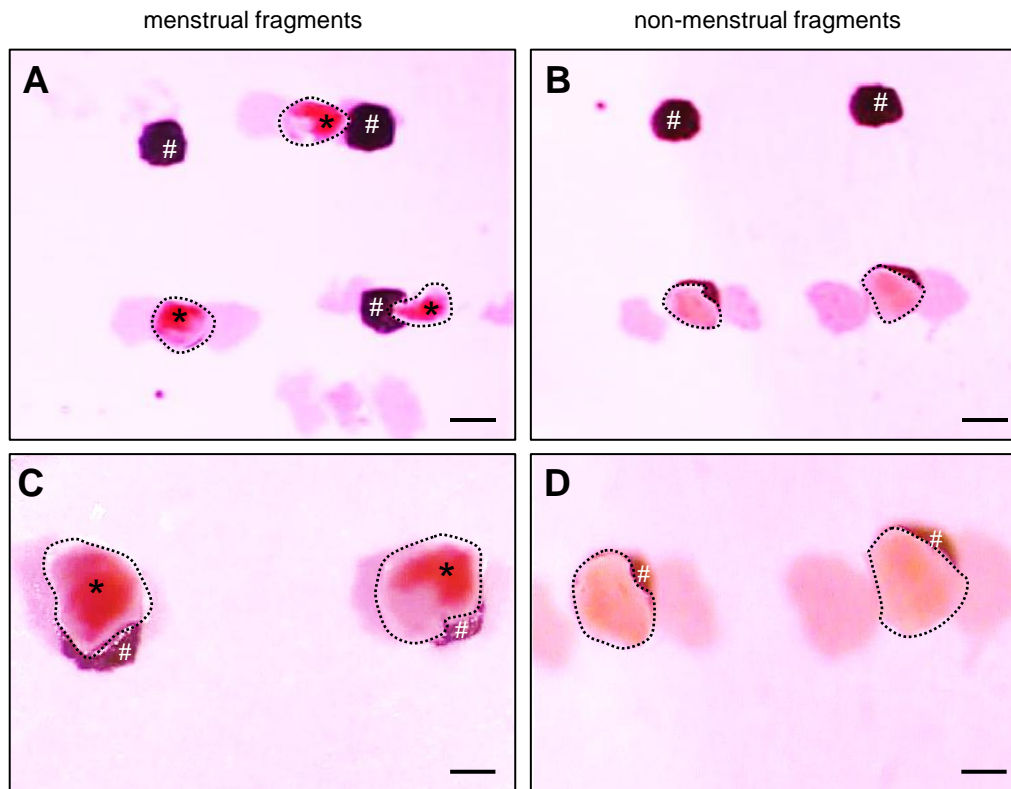


Figure 10: Preparation of endometrial fragments for transplantation in the dorsal skinfold chamber. **A-D:** The menstrual endometrial fragments ((A, C) dotted line = fragments border; asterisks = hemorrhages) and the non-menstrual fragments ((B, D) dotted line = fragments border) were placed in a petri dish containing DMEM. The fragments were cut using a template (white hashtag) and had a size of $\sim 0.9 \text{ mm}^2$. Scale bars A, B: 1 mm; C, D: 0.4 mm.

fragment was placed cranially within the observation window of the skinfold chamber. Finally, a new cover glass was put in the chamber's observation window and secured with a snap ring.

5.6.3 Intravital fluorescence microscopy

The vascularization of newly developing endometriotic lesions within the dorsal skinfold chamber was examined using intravital fluorescence microscopy. The animals were anesthetized by i.p. injection of ketamine (100 mg/kg body weight Ursotamin®, Serumwerke Bernburg) and xylazine (12 mg/kg body weight Rompun®, Bayer) and then secured in right lateral position on a plexiglas stage. The visualization of microvessels was enabled through contrast enhancement of blood plasma. For this purpose, 0.05 mL 5% fluorescein-isothiocyanate (FITC)-labeled dextran (molecular weight: 150,000 Da, Sigma-Aldrich) was injected intravenously via the retrobulbar space. Next, the dorsal skinfold chamber was positioned under a Zeiss Axiotech microscope (Zeiss, Oberkochen, Germany) equipped with 5x, 10x and 20x long-distance objectives (Zeiss) and a 100 W mercury lamp connected to an epi-illumination filter block for blue, green and ultraviolet light. The microscopic images were transferred to a 14-inch video screen (KV-14 CT1E, Sony, Tokyo, Japan) via a charge-coupled device video camera (FK6990, Pieper, Schwerte, Germany) and recorded on DVD for subsequent evaluation.

After the *in vivo* experiments, a quantitative offline analysis of the DVDs was conducted using the computer-assisted image analysis system CapImage (version 8.5, Zeintl, Heidelberg, Germany). The purpose of the image analyses was the evaluation of the functional microvessel density as well as diameter and centerline red blood cell (RBC) velocity of individual microvessels (Feng *et al.*, 2012; Nenicu *et al.*, 2014), as described in the following.

In order to determine the size of the endometrial tissue fragments, the fluorescent dye bisbenzimidazole was applied before the endometrial grafts were transplanted in the observation window of the dorsal skinfold chamber. Bisbenzimidazole emits a strong fluorescence when exposed to ultraviolet light. This ensured a clear distinction between the stained endometrial grafts and the neighboring unstained recipient tissue in the dorsal skinfold chamber.

To calculate the functional microvessel density for each graft, the total length of all blood-perfused microvessels within a defined area was assessed and then divided by the defined area. Consequently, the unit for the functional microvessel density was cm/cm^2 . For each graft, three areas were selected and analyzed to calculate the arithmetic mean value. This enabled the determination of the functional microvessel density for each graft on each evaluation day. The evaluated areas were chosen in a standardized manner on an imaginary horizontal line through the center of the transplants.

On each evaluation day, the diameters of ten microvessels per endometrial graft were measured and the arithmetic mean was calculated from these microvessels. These microvessels were also selected in a standardized manner: An imaginary horizontal and vertical line was drawn through the center of the graft and only microvessels crossing these lines were chosen. To determine the individual diameters of the selected microvessels, two endpoints on the borders of each chosen microvessel were connected by a line perpendicular to the microvessel's orientation in the video image. The length of this line was measured in micrometers (μm). The video recording was paused at an optimal point for these measurements, allowing a precise measurement of the diameter.

In the microvessels from which the diameters were determined, the centerline RBC velocity was additionally measured. Similarly as described for the vessel diameters the identical ten vessels per graft and per measurement day were selected and the arithmetic mean was calculated from all individual microvessels. To determine the centerline RBC velocity, the computer-assisted line-shift diagram method was used (Intaglietta *et al.*, 1970). For this purpose, a line was traced along the flow direction of the microvessel being measured on the processing screen. This line was positioned centrally within the vessel lumen. Subsequently, the video recording was played in real-time for approximately 10 seconds. During this time, the computer continuously generated grayscale profiles for each half-frame along the measurement line and stored them in an image buffer. Using these successive grayscale profiles, the computer generated a line-shift diagram consisting of bright and dark diagonal lines. These lines were formed due to the movement of plasma gaps (bright) and erythrocytes (dark) along the measurement line during the recording. The analyses of the slope of these generated lines enabled the determination of the centerline RBC velocity in micrometers per second ($\mu\text{m}/\text{s}$).

5.7 Histology and immunohistochemistry

5.7.1 Hematoxylin and eosin staining

The endometriotic lesions from the intraperitoneal mouse model and the dorsal skinfold chamber model were fixated for 24 h in 4% formalin and then embedded in paraffin. Subsequently, 3- μ m-thick sections were cut and stained with hematoxylin and eosin (HE) according to standard procedures. Hematoxylin is a dark blue stain that binds to basophilic structures, staining the cell nuclei, endoplasmic reticulum and ribosomes. Eosin is a pink stain and binds to acidophilic components like cellular proteins. The sections were examined with a light microscope (BX60, Olympus) to confirm the histomorphological characteristics of endometriotic lesions and, by this, to determine the take rate (%), i.e. the fraction of transplanted uterine tissue fragments that finally developed into endometriotic lesions containing endometrial stroma and glands. Only these lesions were included in the further quantitative analyses.

5.7.2 Ki67 staining

Ki67 staining was performed to analyze cell proliferation in the endometriotic lesions. This marker is expressed in all active phases of the cell cycle. For detecting Ki67⁺ cells, a polyclonal rabbit-Ki67 antibody (1:2000, ab66155, Abcam, Cambridge, UK) was used as primary antibody. This was followed by a biotin-labeled goat-anti-rabbit antibody (ready to use, Abcam), which served as secondary antibody. 3,3'-Diaminobenzidine was used as chromogen. The sections were counterstained with Mayer's hemalum solution (HX948000, Merck, Darmstadt, Germany). The stained sections were analyzed by means of light microscopy (BX60, Olympus). Quantitative analyses included the determination of the fraction of Ki67⁺ proliferating glandular and stromal cells (%) within the lesions.

5.7.3 CD31/GFP staining

In order to determine the microvessel density within the endometriotic lesions, a CD31/GFP immunofluorescence staining was performed. This staining method allowed for the differentiation between GFP⁺ and GFP⁻ microvessels within the lesions. For this purpose, paraffin-embedded 3- μ m-thick sections were stained with a monoclonal rat-anti-mouse antibody against CD31 (1:100, Dianova GmbH, Hamburg, Germany) to detect endothelial cells and with a goat-anti-GFP antibody (1:200, Biomol, Hamburg, Germany) for enhancement of the GFP fluorescence. A goat anti-rat IgG Alexa555 antibody (1:200, LifeTechnologies, Darmstadt, Hessen Germany) and a biotin-labeled donkey-anti-goat IgG antibody (1:15, Jackson ImmunoResearch, Baltimore, MD, USA), followed by Alexa488-labeled-streptavidin (1:50, LifeTechnologies), were used as secondary antibodies. For this staining, the sections were placed in Coplin jars with 0.05% citraconic anhydride solution (pH 7.4) for 1 h at 98°C and then incubated overnight at 4°C with the first antibody, followed by the incubation with the appropriate secondary antibody at 37°C for 2 h. Cell nuclei were stained with Hoechst 33342 (2 μ g/mL, Sigma-Aldrich) for all immunofluorescent microscopic analyses. The immunofluorescent sections were examined using a BZ-8000 fluorescence microscopic system (Keyence, Japan) to determine the microvessel density (in mm⁻²). To assess the tissue areas in the sections, a Biozero analysis software was used (Version 3.60, Keyence, Japan). For the calculation of the microvessel density, the overall number of CD31⁺ microvessels of a lesion section was divided by the stromal lesion area.

5.8 Statistical analyses

All experiments were designed to generate groups of equal size using randomization. The group sizes were chosen according to previous studies using the herein described endometriosis models (Feng *et al.*, 2012; Rudzitis-Auth *et al.*, 2012, 2013). Microsoft Excel 2016 (Microsoft Deutschland GmbH, Unterschleißheim, Deutschland) was used for the calculation of the different parameters. All graphs were designed by means of SigmaPlot 2013 (Jandel Corporation, San Rafael, CA, USA).

The data were first analyzed for normal distribution by means of the Shapiro-Wilk test and the Brown-Forsythe test. In case of parametric data, differences between two groups were assessed by the unpaired Student's t-test. In case of non-parametric data, the differences between the groups were assessed by the Mann-Whitney U test. Differences between multiple experimental groups were analyzed by one-way ANOVA followed by the Dunnett's test, including the correction of the α -error according to Bonferroni probabilities (parametric data). In case of non-parametric data, differences were assessed by ANOVA on Ranks followed by the Dunn's test (SigmaStat, Jandel Corporation, San Rafael, CA, USA). For better clarity of data presentation, both parametric and non-parametric data are given as mean \pm standard error of the mean (SEM). Statistical significance was accepted for a value of $P < 0.05$.

6. Results

6.1 Evaluation of the intraperitoneal endometriosis model

6.1.1 Macroscopic and microscopic characteristics of non-menstrual and menstrual donor tissue

In the first part of this thesis, non-menstrual and menstrual uterine tissue fragments originating from GFP⁺ donor mice were fixed onto the peritoneal wall of GFP⁻ recipient mice in order to analyze their development into endometriotic lesions over an observation period of 28 days.

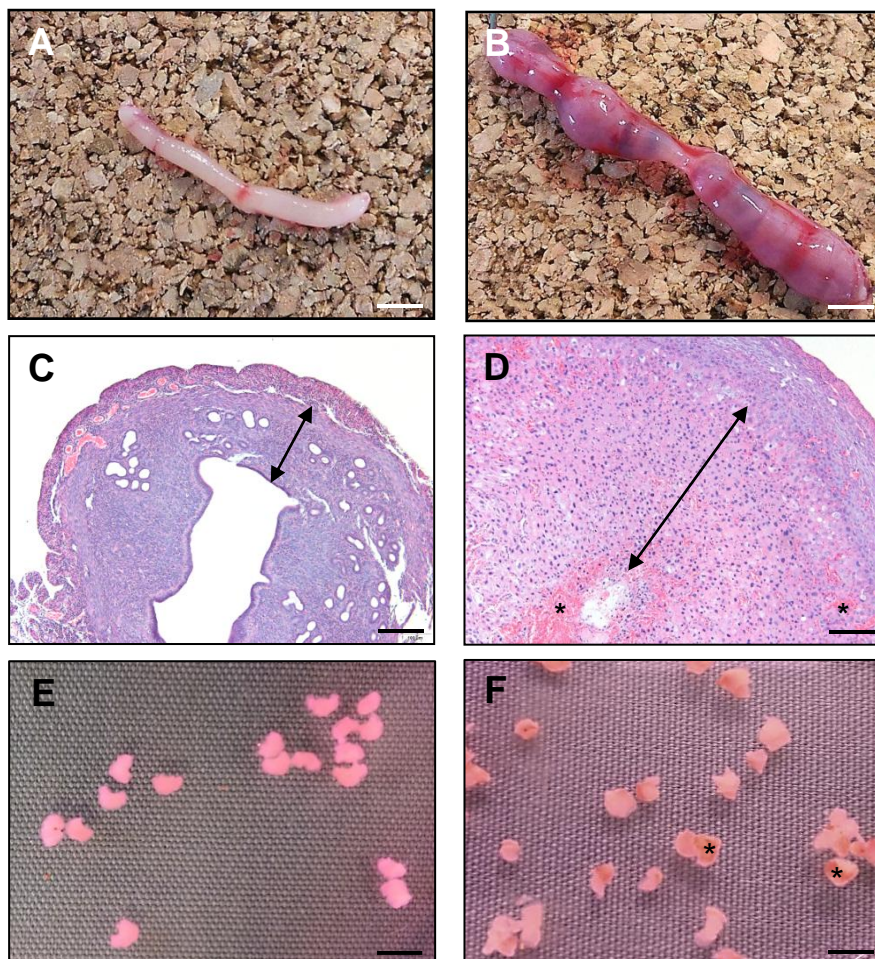


Figure 11: Comparison of non-menstrual and menstrual uterine donor tissue. **A, B:** Macroscopic appearance of a non-menstrual uterus (A) and a menstrual uterus (B) used to prepare uterine tissue fragments for the induction of endometriotic lesions. **C, D:** HE-stained histological sections of a non-menstrual (C, double arrow = endometrial layer) and a menstrual uterus (D, double arrow = endometrial layer; asterisks = hemorrhages). **E, F:** Uterine tissue fragments from a non-menstrual (E) and a menstrual (F, asterisks = hemorrhages) uterus. Scale bars: A, B = 9 mm; C, D = 270 μ m; E, F = 4 mm (modified from Nenicu A et al., 2021).

Firstly, the uteri were macroscopically evaluated after their removal from the donor animals. The non-menstrual uteri exhibited a normal size and light pink color (Fig. 11A). In comparison, the horns of the menstrual uteri were enlarged, dark pink and purple (Fig. 11B). Upon opening the horns of the menstrual

uteri, hemorrhages were observed inside the lumen. This confirmed the successful induction of menstruation. HE stainings were performed for a better understanding of the histomorphology of the donor uteri. These stainings showed that the non-menstrual uteri exhibit a compact endometrial layer with clearly defined glandular and stromal tissue (Fig. 11C). In contrast, the differentiation of the uterine layers was not possible inside the menstrual endometrium, as it was hyperplastic with visible hemorrhages (Fig. 11D). Uterine tissue samples were obtained using a punch biopsy. Macroscopically, the non-menstrual uterine tissue fragments were compact and round (Fig. 11E). In contrast, the menstrual uterine tissue fragments were looser, more fragile and porous with visible dark red hemorrhages (Fig. 11F).

6.1.2 Growth of intraperitoneal endometriotic lesions

The developing endometriotic lesions were repeatedly analyzed throughout an observation period of 28 days by means of high-resolution ultrasound (Figs. 12A-O). On the day of induction of intraperitoneal endometriosis (day 0), the uterine tissue fragments of all groups had a comparable initial volume of ~1.0-1.3 mm³ (Figs. 12G, H, I). In the non-ovx mice, both non-menstrual and menstrual endometriotic lesions comparably increased in their overall lesion volume over the 28-day observation period with no statistically significant differences (Figs. 12A, D, G). The growth of these endometriotic lesions was driven by an increase in the volume of stromal tissue (Fig. 12J) and the formation of fluid-filled cyst-like dilated endometrial glands (Figs. 12A, D, M). In the ovx mice, the growth of both menstrual and non-menstrual endometriotic lesions was inhibited, resulting in significantly smaller lesion volumes and stromal tissue volumes when compared to endometriotic lesions in the non-ovx animals over the observation period (Figs. 12B, E, H, K). The endometrial glands of the endometriotic lesions in ovx mice contained minimal fluid, preventing their visualization by ultrasound imaging (Fig. 12N). However, they were observable in histological sections. The non-menstrual endometriotic lesions that developed in the ovx+E2 mice exhibited a higher overall lesion volume as well as increased stromal tissue and cyst volume when compared to those of the non-ovx animals (Figs. 12C, I, L, O). For instance, on the final day of the 28-day experiment, the non-menstrual endometriotic lesions had grown to a volume of 3.4 ± 0.5 mm³, which was a threefold increase from the initial volume of 1.2 ± 0.0 mm³. In contrast, the menstrual endometriotic lesions within the ovx+E2 mice had a significantly smaller overall lesion volume, stromal tissue and cyst volume in comparison to both the non-menstrual endometriotic lesions of the ovx+E2 mice and the endometriotic lesions observed in the non-ovx mice (Figs. 12F, I, L, O).

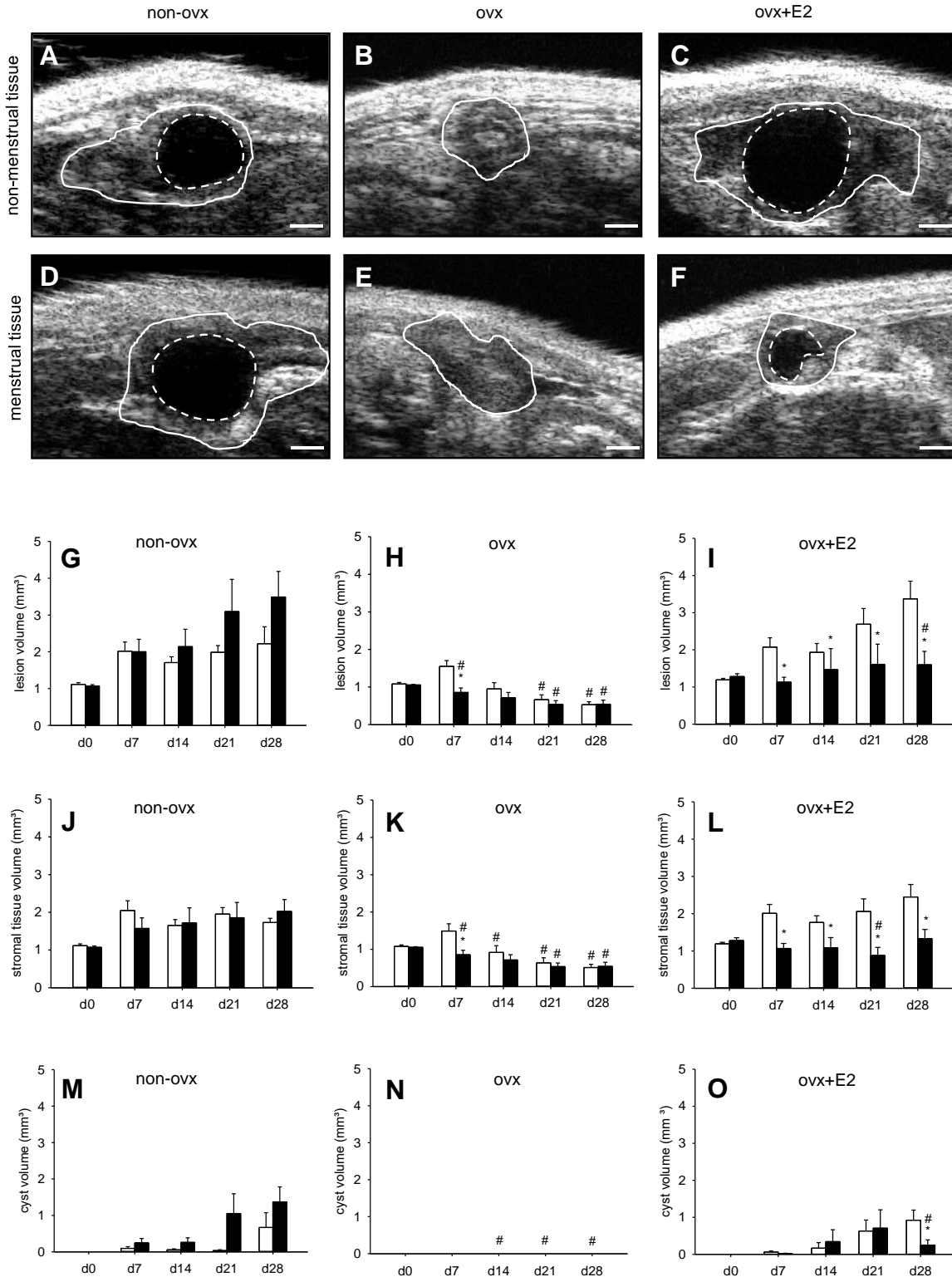


Figure 12: Analysis of endometriotic lesions in the intraperitoneal model of endometriosis by means of high-resolution ultrasound imaging. **A-F:** High-resolution ultrasound imaging of endometriotic lesions (solid line = lesion borders; broken line = cysts) on day 28 after transplantation of non-menstrual (A-C) and menstrual (D-F) uterine tissue fragments into the peritoneal cavity of non-ovx, ovx and ovx+E2 mice. Scale bars: A-F = 500 μ m. **G-O:** Lesion volume (mm³) (G-I), stromal tissue volume (mm³) (J-L) and cyst volume (mm³) (M-O) of endometriotic lesions originating from non-menstrual (white bars) and menstrual (black bars) uterine tissue fragments in the peritoneal cavity of non-ovx (n = 10), ovx (n = 10) and ovx+E2 (n = 10) mice, as assessed by high-resolution ultrasound imaging. Mean \pm SEM. *P < 0.05 vs. non-menstrual tissue fragments; #P < 0.05 vs. non-ovx mice (modified from Nenicu A et al., 2021).

6.1.3 Macroscopic assessment of intraperitoneal endometriotic lesions

At the last day of the experiment (day 28), the developed non-menstrual and menstrual endometriotic lesions were assessed macroscopically in situ before being harvested for histological and immunohistochemical analyses. The non-menstrual and menstrual endometriotic lesions, which had developed in the non-ovx mice, were round, polyp-like, pink and visibly contained fluid-filled cyst-like dilated endometrial glands (Figs. 13A, D). The non-menstrual and menstrual endometriotic lesions of the ovx mice were harder to identify due to their small size. They appeared in the form of granulation tissue that had developed around the suture used to fix the uterine tissue fragments to the peritoneal wall (Figs. 13B, E). The non-menstrual and menstrual endometriotic lesions of the ovx+E2 animals displayed macroscopically visible differences. In fact, the non-menstrual endometriotic lesions appeared significantly bigger in size compared to the menstrual endometriotic lesions of the ovx+E2 mice (Figs. 13C, F).

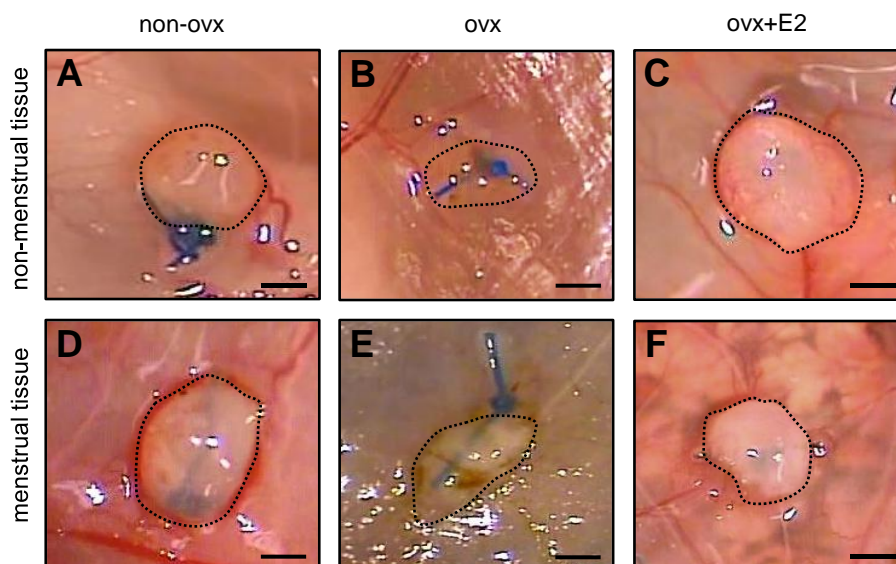


Figure 13: In situ representation of endometriotic lesions on day 28 after induction. **A-F:** Non-menstrual endometriotic lesions (A-C) of non-ovx (A), ovx (B) and ovx+E2 (C) mice. Menstrual endometriotic lesions (D-F) of non-ovx (D), ovx (E) and ovx+E2 (F) mice (dotted line = lesion border). Scale bar: 1.3 mm.

6.1.4. Engraftment of non-menstrual and menstrual uterine tissue fragments

At the end of the in vivo experiment, the developing endometriotic lesions were analyzed to determine the take rate (Figs. 14A-C). Only endometriotic lesions that contained endometrial stromal tissue and cyst-like dilated endometrial glands were included in the quantitative analysis of this thesis. It was found that in non-ovx mice, almost 90% of the non-menstrual and menstrual uterine tissue fragments had developed into typical endometriotic lesions (Figs. 14A, C). In the ovx mice, the take rate was lower than that of the non-ovx mice without significant differences between non-menstrual and menstrual uterine tissue fragments (Fig. 14C). In ovx+E2 mice, the take rate of non-menstrual uterine tissue fragments was comparable to that in non-ovx mice, while the take rate of menstrual uterine tissue fragments was significantly reduced, showing values comparable to those in the ovx animals (Fig. 14C).

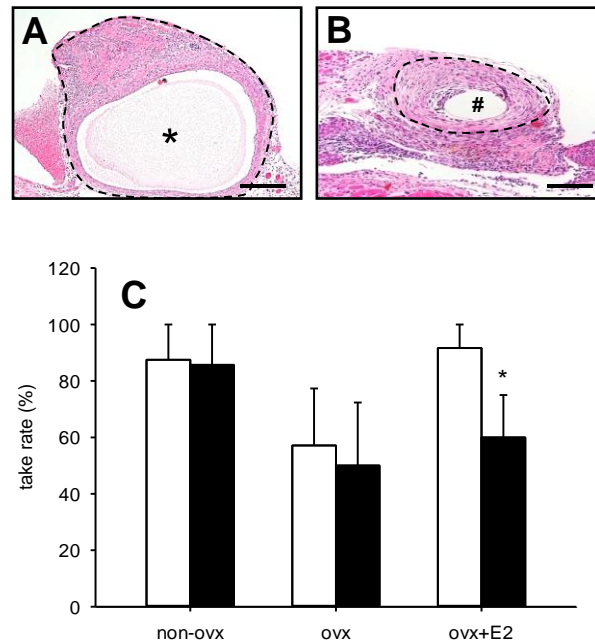


Figure 14: Histomorphological phenotypes and graphic representation of the take rate of endometriotic lesions. **A**, **B**: HE staining of the typical histomorphological phenotype of an endometriotic lesion (**A**; broken line = lesion border, asterisk = cyst-like dilated endometrial gland) and a granuloma (**B**; broken line = granuloma border, hashtag = suture material) on day 28 after transplantation of non-menstrual tissue fragments into the peritoneal cavity of non-ovx recipient mice. Scale bars: **A** = 220 μ m; **B** = 110 μ m. **C**: Take rate (%) of non-menstrual (white bars) and menstrual uterine tissue fragments (black bars) in the peritoneal cavity of non-ovx ($n = 10$), ovx ($n = 10$) and ovx+E2 ($n = 10$) mice, as assessed by histology. Mean \pm SEM. * $P < 0.05$ vs. non-menstrual tissue fragments (modified from Nenicu A et al., 2021).

6.1.5 Immunohistochemical analyses of intraperitoneal endometriotic lesions

At the end of the in vivo experiments, the vascularization of the newly developing endometriotic lesions was analyzed by means of immunohistochemistry. The microvessel density of the endometriotic lesions was assessed using CD31/GFP-double staining. For this purpose, CD31⁺/GFP⁺ as well as CD31⁺/GFP⁻ vessels were detected (Figs. 15A-F). The assessment of the microvessel density demonstrated a similar range of ~200-240 mm⁻² within endometriotic lesions originating from both menstrual and non-menstrual uterine tissue fragments in the peritoneal cavity of non-ovx mice on day 28 (Figs. 15A, D, G). In the ovx mice, both endometriotic lesion types presented with a lower microvessel density compared to endometriotic lesions of the non-ovx mice (Figs. 15B, E, G). The microvessel density of non-menstrual endometriotic lesions of the ovx+E2 mice was comparable to that of non-menstrual endometriotic lesions of the non-ovx mice (Figs. 15C, G). In contrast, menstrual endometriotic lesions within the ovx+E2 mice exhibited a significantly lower microvessel density compared to the microvessel density observed in non-menstrual endometriotic lesions of the ovx+E2 mice (Figs. 15F, G). More detailed evaluations provided insights into the origin of the vessels detected within the endometriotic lesions. CD31⁺/GFP⁺ vessels originated from the donor tissue, while CD31⁺/GFP⁻ vessels originated from the recipient tissue. This differentiation showed that menstrual endometriotic lesions of the non-ovx and ovx+E2 animals contained a significantly lower density of CD31⁺/GFP⁺ microvessels compared to that of non-menstrual endometriotic lesions of the respective animals (Figs. 15A, C, D, F, H). This indicates that menstrual endometriotic lesions contained fewer microvessels originating from the grafted GFP⁺

uterine tissue fragments and more ingrowing microvessels originating from the surrounding GFP⁺ tissue of the recipient animals.

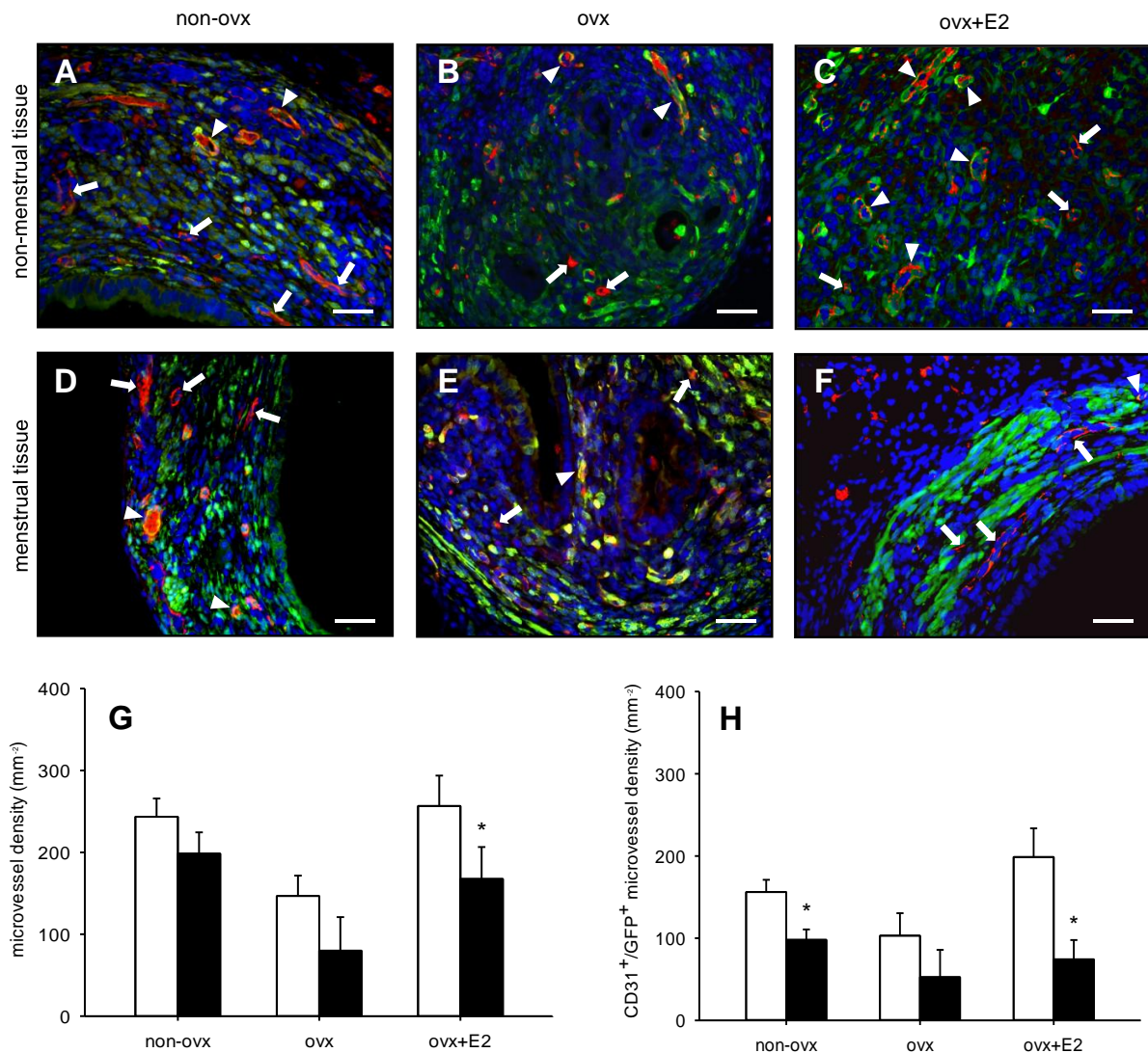


Figure 15: Histomorphology and microvessel density of endometriotic lesions, as assessed by immunofluorescence. **A-F:** Immunofluorescent detection of CD31⁺/GFP⁺ (arrows) and CD31⁺/GFP⁺ (arrowheads) microvessels within endometriotic lesions on day 28 after transplantation of non-menstrual (A-C) and menstrual (D-F) uterine tissue fragments into the peritoneal cavity of non-ovx, ovx and ovx+E2 mice. The sections were stained with antibodies against CD31 (red) and GFP (green). Cell nuclei were stained with Hoechst 33342 (blue). Scale bars: A-F = 40 μ m. **G, H:** Microvessel density (mm⁻²) (G) and CD31⁺/GFP⁺ microvessel density (mm⁻²) (H) within endometriotic lesions originating from non-menstrual (white bars) and menstrual (black bars) uterine tissue fragments in the peritoneal cavity of non-ovx (n = 5), ovx (n = 5) and ovx+E2 (n = 5) mice. Mean \pm SEM. *P < 0.05 vs. non-menstrual tissue fragments (modified from Nenicu A et al., 2021).

In addition, the fraction of proliferating Ki67⁺ glandular and stromal cells within the endometriotic lesions was analyzed. There were no significant differences in the fraction of proliferative glandular cells throughout the analyzed groups (Figs. 16A-G). In contrast, a significantly lower fraction of proliferative stromal cells was detected in menstrual endometriotic lesions of the ovx mice when compared to that in menstrual endometriotic lesions of the non-ovx mice (Figs. 16D, E, H). In addition, the fraction of

proliferating Ki67⁺ stromal cells in menstrual endometriotic lesions from the ovx+E2 mice tended to be lower when compared to non-menstrual endometriotic lesions of ovx+E2 animals (Figs. 16C, F, H).

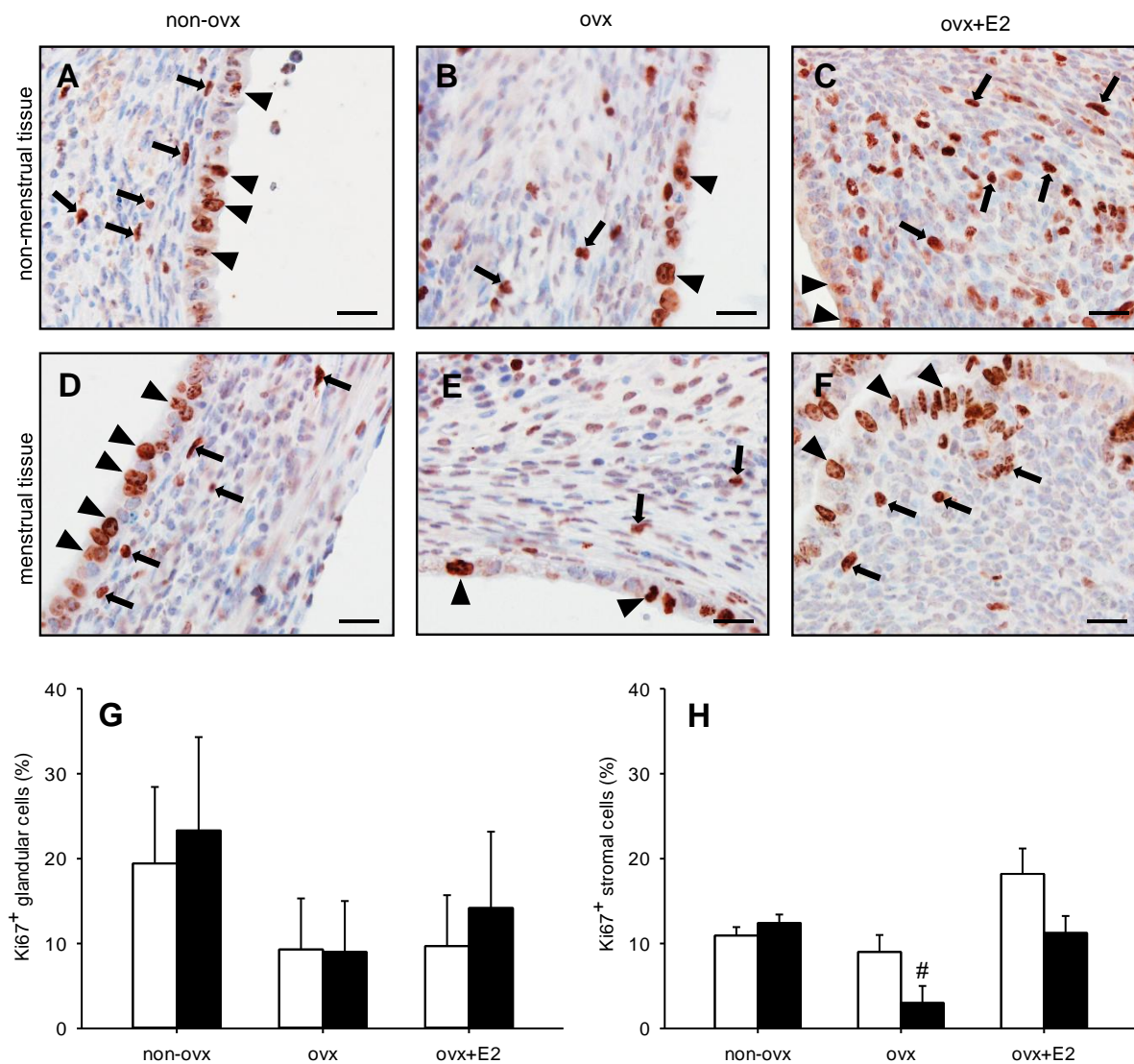


Figure 16. Cell proliferation within endometriotic lesions, as assessed by immunohistochemistry. **A-F:** Immunohistochemical detection of proliferating Ki67⁺ stromal cells (arrows) and glandular cells (arrowheads) within endometriotic lesions on day 28 after transplantation of non-menstrual (A-C) and menstrual (D-F) tissue fragments into the peritoneal cavity of non-ovx, ovx and ovx+E2 mice. The sections were stained with an antibody against Ki67 (brown). Scale bars: A-F = 20 μ m. **G, H:** Ki67⁺ glandular cells (%) (G) and Ki67⁺ stromal cells (%) (H) within endometriotic lesions originating from non-menstrual (white bars) and menstrual (black bars) tissue fragments in the peritoneal cavity of non-ovx (n = 5), ovx (n = 5) and ovx+E2 (n = 5) mice. Mean \pm SEM. [#]P < 0.05 vs. non-ovx mice (modified from Nenicu A et al., 2021).

6.2 Evaluation of the dorsal skinfold chamber model

6.2.1 Evaluation of non-menstrual and menstrual endometrial fragments

In the second part of this thesis, non-menstrual and menstrual endometrial tissue fragments were transplanted into the dorsal skinfold chambers of recipient animals. For this purpose, the animals were divided in three recipient conditions: non-ovx, ovx and ovx+E2. The endometrial tissue fragments were analyzed over a period of 14 days. Under a stereomicroscope, the endometrial tissue fragments were

detectable in the form of small tissue pieces within the observation window of the dorsal skinfold chamber (Figs. 17A-I). During the 14-day observation period, as angiogenesis started within the newly developing endometriotic lesions, minor hemorrhages became apparent within some of the endometrial tissue fragments. Finally, the endometrial tissue fragments became integrated into the recipient tissue of the dorsal skinfold chamber, resulting in the disappearance of their clearly visible borders (Figs. 17C, F, I).

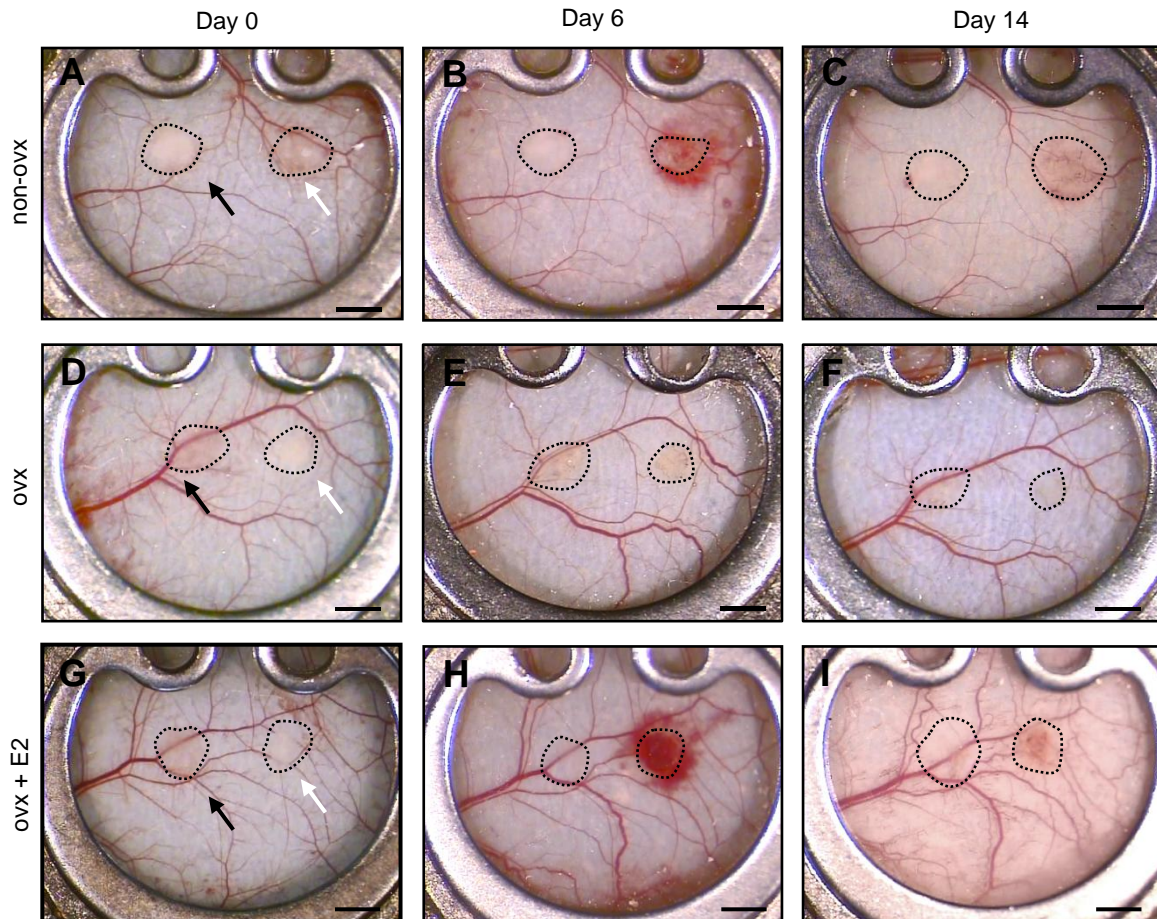


Figure 17: Stereomicroscopic imaging of newly developing endometriotic lesions within the dorsal skinfold chamber. **A-I:** Dorsal skinfold chambers of recipient animals of the non-ovx mice (A-C), ovx (D-F) and ovx+E2 mice (G-I) on day 0 (A, D, G), i.e. the day of transplantation of non-menstrual (white arrows) and menstrual endometrial tissue fragments (black arrows; dotted line = fragment borders) as well as on day 6 (B, E, H) and day 14 (C, F, I). Scale bars: 1.5 mm.

6.2.2 Early vascularization of endometriotic lesions

The analysis of the vascularization of the transplanted endometrial tissue fragments was performed by means of repeated intravital fluorescence microscopy (Fig. 18). On the day of transplantation, the endometrial tissue fragments were easily identifiable within the dorsal skinfold chamber (Figs. 18A, D, G, J, M, P), as they emitted a strong fluorescence when exposed to ultraviolet light. This fluorescence resulted from their staining with bisbenzimidazole prior to the transplantation into the dorsal skinfold chamber. This ensured a clear distinction between the stained endometrial grafts and the neighboring

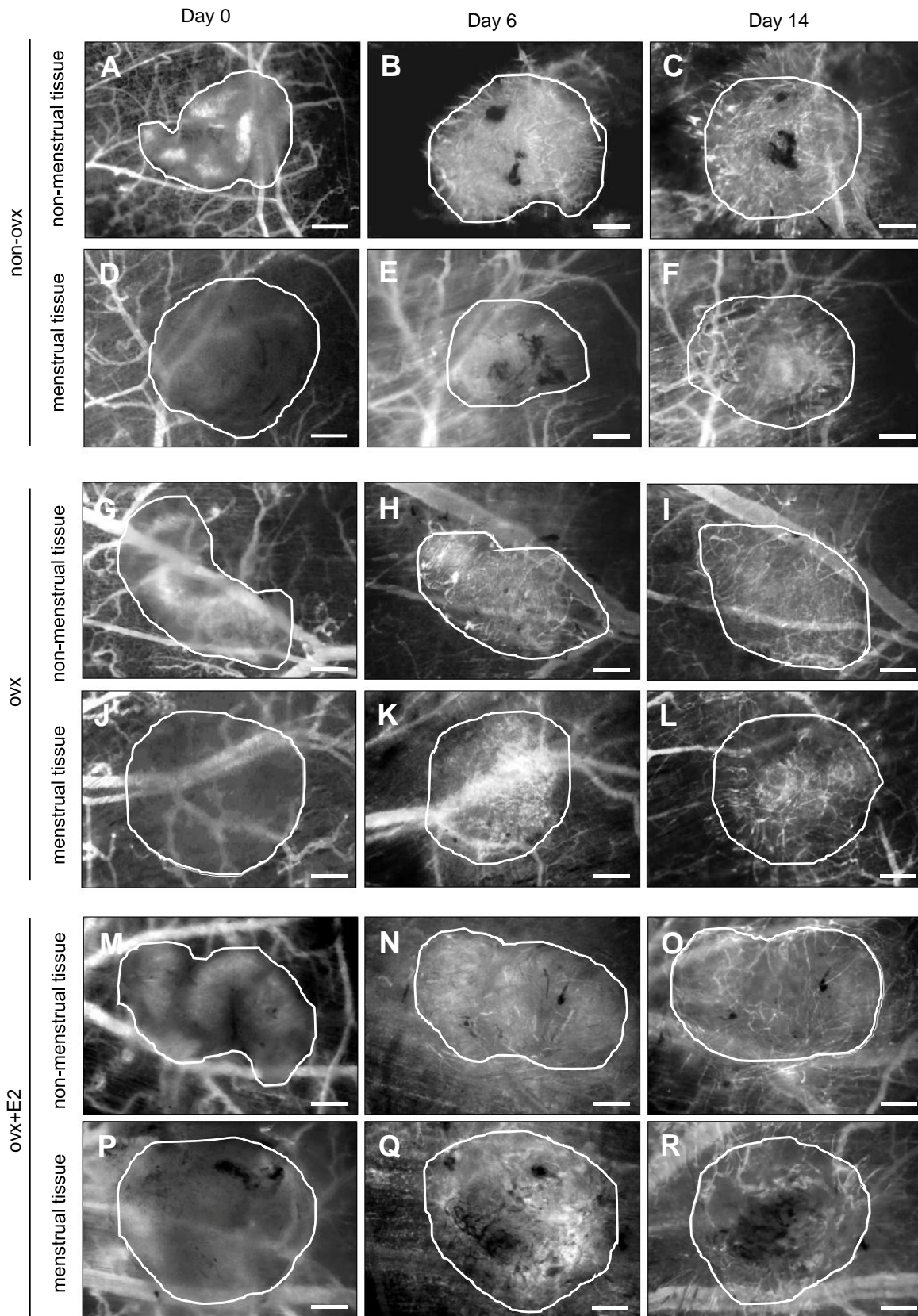


Figure 18: Imaging of newly developing endometriotic lesions in the dorsal skinfold chamber. **A-R:** Fluorescent microscopic images of endometriotic lesions. Non-menstrual (A-C; G-I; M-O) endometriotic lesions and menstrual (D-F; J-L; P-R) endometriotic lesions on day 0 (A, D, G, J, M, P), day 6 (B, E, H, K, N, Q) and day 14 (C, F, I, L, O, R) after transplantation of endometriotic tissue fragments (solid lines = lesion borders) into the dorsal skinfold chamber. The animals were assigned to a non-ovx (A-F), ovx (G-L) and ovx+E2 (M-R) recipient animals. Scale bars 220 μ m.

unstained recipient tissue. The non-menstrual endometrial tissue fragments exhibited a more compact structure (Figs. 18A, G, M) when compared to the menstrual endometrial tissue fragments, which appeared translucent and were harder to identify (Figs. 18D, J, P). On the day of transplantation into the dorsal skinfold chamber (day 0), no vascular network could be detected within the grafts. The newly developing vascular networks in both non-menstrual and menstrual endometrial tissue fragments were morphologically similar within all recipient animals (Figs. 18A-R). The newly forming vessels extended beyond the borders of the developing endometriotic lesions and interconnected with the vessels of the surrounding recipient tissue of the dorsal skinfold chamber. A noticeable difference was observed between the non-menstrual and menstrual endometriotic lesions of the non-ovx mice during the initial 6 days of observation. Notably, a complex vascular network was visible within the non-menstrual lesions on day 6 of the analysis, while only few individual vessels could be identified within the menstrual lesions (Figs. 18B, E).

The functional microvessel density, diameter and centerline RBC velocity of the microvessels within the newly developing endometriotic lesions were analyzed by means of intravital fluorescence microscopy.

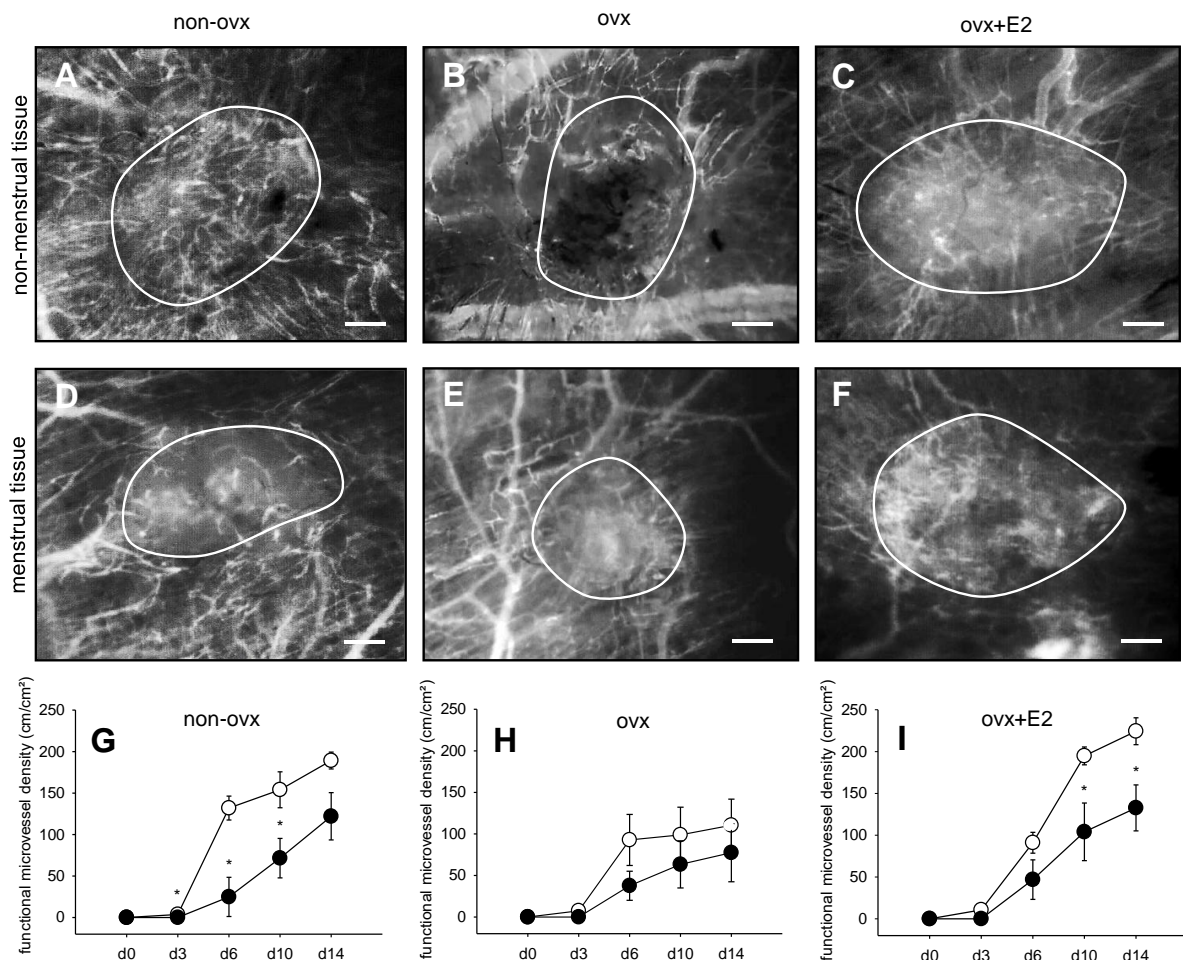


Figure 19: Functional microvessel density of newly developing endometriotic lesions within the dorsal skinfold chamber. **A-F:** Intravital fluorescence microscopy of endometriotic lesions (solid lines = lesion borders) on day 14 after transplantation of non-menstrual (A-C) and menstrual (D-F) endometrial tissue fragments into the dorsal skinfold chamber of non-ovx, ovx and ovx+E2 mice. Scale bars: A-F = 220 μ m. **G-I:** Functional microvessel density (cm/cm^2) of endometriotic lesions originating from non-menstrual (white circles) and menstrual (black circles) endometrial tissue fragments in the dorsal skinfold chamber of non-ovx ($n = 7$), ovx ($n = 7$) and ovx+E2 ($n = 7$) mice, as assessed by intravital fluorescence microscopy. Mean \pm SEM. * $P < 0.05$ vs. non-menstrual tissue fragments (modified from Nenicu A et al., 2021).

Menstrual endometriotic lesions of the non-ovx mice displayed a delayed vascularization, which was characterized by a significantly lower functional microvessel density between days 3 to 10 when compared to that of non-menstrual endometriotic lesions of the non-ovx animals (Figs. 19A, D, G). In ovx animals, there were no significant differences between non-menstrual and menstrual endometriotic lesions, as both non-menstrual and menstrual endometriotic lesions tended to exhibit a reduced vascularization when compared to that of the lesions within the non-ovx mice (Figs. 19B, E, H). In the ovx+E2 mice, non-menstrual endometriotic lesions had a functional microvessel density similar to that

Table 1. Diameter (μm) and centerline RBC velocity ($\mu\text{m/s}$) of microvessels within endometriotic lesions originating from non-menstrual and menstrual endometrial tissue fragments in dorsal skinfold chambers of non-ovx ($n = 7$), ovx ($n = 7$) and ovx+E2 ($n = 7$) mice, as assessed by intravital fluorescence microscopy (modified from Nenicu A et al., 2021).

	d3	d6	d10	d14
Diameter (μm):				
<i>non-ovx</i>				
non-menstrual tissue	20.8 \pm 1.4	13.5 \pm 0.7	11.0 \pm 0.2	10.6 \pm 0.6
menstrual tissue	-	13.3 \pm 2.0	12.4 \pm 1.9	12.5 \pm 0.9
<i>ovx</i>				
non-menstrual tissue	17.7 \pm 2.5	11.9 \pm 2.7	11.4 \pm 1.9	11.9 \pm 1.5
menstrual tissue	-	10.8 \pm 2.5	10.4 \pm 2.3	12.3 \pm 1.3
<i>ovx+E2</i>				
non-menstrual tissue	19.6 \pm 3.8	13.7 \pm 0.4	14.2 \pm 1.4 [#]	12.3 \pm 0.9
menstrual tissue	-	17.0 \pm 0.9 [*]	16.4 \pm 1.9	13.4 \pm 2.4
Centerline RBC velocity ($\mu\text{m/s}$):				
<i>non-ovx</i>				
non-menstrual tissue	166.1 \pm 40.6	265.0 \pm 59.3	355.0 \pm 51.6	453.3 \pm 58.4
menstrual tissue	-	133.3 \pm 68.1	251.7 \pm 69.3	263.3 \pm 63.0
<i>ovx</i>				
non-menstrual tissue	95.0 \pm 47.9	175.9 \pm 87.4	263.3 \pm 87.4	310.0 \pm 64.0
menstrual tissue	-	113.3 \pm 51.5	136.7 \pm 63.0	213.3 \pm 99.5
<i>ovx+E2</i>				
non-menstrual tissue	123.4 \pm 43.2	328.3 \pm 39.0	505.0 \pm 61.3	515.0 \pm 37.0
menstrual tissue	-	186.0 \pm 62.6	290.0 \pm 73.7	341.7 \pm 80.1

Mean \pm SEM. ^{*} $P < 0.05$ vs. non-menstrual tissue; [#] $P < 0.05$ vs. non-ovx mice.

observed within non-menstrual endometriotic lesions of non-ovx animals. In contrast, menstrual endometriotic lesions of the ovx+E2 mice exhibited an impaired vascularization, which was characterized by a significantly lower functional microvessel density on days 10 and 14 when compared to that of non-menstrual endometriotic lesions (Figs. 19C, F, I). The additional measurement of microhemodynamic parameters revealed no significant differences between menstrual and non-menstrual endometriotic lesions across the different recipient groups (Tab. 1). The diameter of individual microvessels progressively decreased in both non-menstrual and menstrual endometriotic lesions, while the centerline RBC velocity increased over time. Furthermore, the microvessels within menstrual endometriotic lesions showed a tendency towards lower centerline RBC velocities throughout the 14-day observation period in comparison to that within non-menstrual endometriotic lesions (Tab. 1). However, these differences were not statistically significant.

6.2.3 Histomorphology of endometriotic lesions

The endometriotic lesions within the dorsal skinfold chambers were harvested on day 14 of the experiment and further processed for immunofluorescent analysis. The GFP⁺ endometriotic lesions could be easily differentiated from the GFP⁻ surrounding recipient tissue due to the green fluorescence they emitted (Figs. 20A-F). To detect the cell nuclei within the endometriotic lesions and the donor tissue, the histological sections were additionally stained with Hoechst 33342. The analyses showed that both

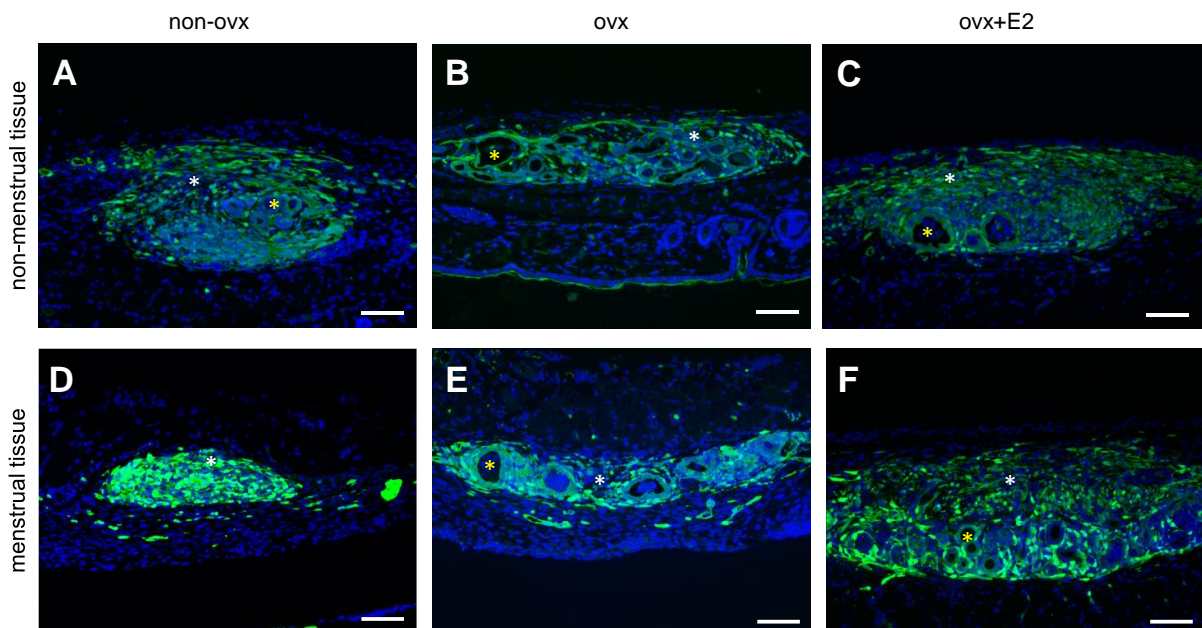


Figure 20: Histomorphology of endometriotic lesions in the dorsal skinfold chamber, as assessed by immunofluorescent staining. **A-F:** Endometriotic lesions originating from non-menstrual (A-C) and menstrual (D-F) endometrial tissue fragments in the non-ovx (A, D), ovx (B, E), oil+E2 mice (C, F) on day 14 after transplantation into the dorsal skinfold chamber. The histological sections were stained with Hoechst 33342 for the identification of the cell nuclei (blue) and antibodies against GFP to detect GFP⁺ tissue originating from C57BL/6 TgN (ACTB-eGFP) donor animals. The endometriotic lesions displayed a typical structure, consisting of stromal tissue (white asterisks) and cyst-like dilated glands (yellow asterisks). Scale bars: 110 μ m.

non-menstrual and menstrual endometriotic lesions within all recipient groups exhibited cyst-like dilated

glands surrounded by stromal tissue. This observation was in line with the characteristic morphology of the developing endometriotic lesions in the first part of this thesis.

6.3 Summary of the results

In the present thesis, the intraperitoneal mouse model of endometriosis was applied to investigate the development of non-menstrual and menstrual uterine tissue fragments into endometriotic lesions under identical, highly standardized hormonal conditions. In addition, the early vascularization of non-menstrual and menstrual endometrial tissue fragments was analyzed in the dorsal skinfold chamber model by means of intravital fluorescence microscopy. The following results were achieved:

1. Non-menstrual and menstrual uterine donor tissues exhibit a different macroscopic and histological morphology. Non-menstrual uteri showed a well-defined, compact endometrial layer containing distinct glandular and stromal tissue. In contrast, the differentiation of uterine layers within the menstrual uteri was challenging due to hyperplasia and hemorrhages. Accordingly, the menstrual donor tissue was more fragile and hemorrhagic when compared to the non-menstrual donor tissue.
2. Non-menstrual as well as menstrual donor tissue transplanted into the peritoneal cavity and the dorsal skinfold chamber of recipient animals both developed endometriotic lesions, which consisted of stromal tissue and cyst-like dilated glands,
3. Estrogen deprivation inhibited the growth of both non-menstrual and menstrual endometriotic lesions within the intraperitoneal mouse model of endometriosis. Accordingly, both non-menstrual and menstrual endometriotic lesions within the ovx mice exhibited a significantly lower lesion volume when compared to those within the non-ovx mice.
4. Estrogen substitution within the ovx-E2 animals stimulated the growth of non-menstrual endometriotic lesions but not of menstrual lesions. This was evident by the significantly smaller lesion volume of menstrual endometriotic lesions of the ovx-E2 animals when compared to that of the non-menstrual lesions of ovx-E2 animals and to the lesion volume of the menstrual endometriotic lesions of the non-ovx mice.
5. Non-menstrual and menstrual endometriotic lesions exhibited different vascularization patterns as well as different cellular proliferation rates. It was found that the intraperitoneal menstrual endometriotic lesions in ovx+E2 mice exhibited a significantly lower microvessel density when compared to non-menstrual lesions in these mice. Additionally, the menstrual uterine tissue fragments in both non-ovx and ovx+E2 mice presented with a lower number of microvessels originating from the grafted GFP⁺ tissue as well as more ingrowing microvessels from the surrounding GFP⁻ host tissue when compared to non-menstrual uterine tissue fragments. Furthermore, it was found that the menstrual endometriotic lesions within the ovx mice contained a significantly lower fraction of proliferating stromal cells when compared to that of menstrual lesions in the non-ovx mice.

6. By means of intravital fluorescence microscopy, it was shown that menstrual endometriotic lesions within the dorsal skinfold chamber model exhibit a significantly lower functional microvessel density when compared to non-menstrual endometriotic lesions in non-ovx and ovx-E2 animals. Additionally, the menstrual endometriotic lesions within all recipient groups exhibited a delay in early vascularization when compared to non-menstrual endometriotic lesions and even lacked blood-perfused microvessels on day 3.

7 Discussion

7.1 Discussion of materials and methods

7.1.1 Menstruating mouse model

Endometriosis is a common gynecological disease, which is estrogen-dependent. Despite its high prevalence, the pathogenesis of endometriosis is not yet fully understood. The implantation theory proposed by Sampson (1927) is widely accepted as the leading explanation for the development of endometriosis. According to Sampson's theory, endometrium is transported retrogradely through the fallopian tubes into the abdomen during menstruation, where it develops into endometriotic lesions. Consequently, spontaneous development of the disease can only occur in the presence of a menstrual cycle. Accordingly, endometriosis is only found in humans and non-human primates (Grümmer, 2006). Taking this into account, suitable and cost-efficient experimental models are needed for the purpose of analyzing the pathogenesis of endometriosis and developing novel therapeutic strategies. While primate models are similar to humans in terms of anatomy and hormonal cycles, the considerable expenses associated with their maintenance, intricate handling requirements and ethical considerations markedly limit their use in research (Story and Kennedy, 2004). In contrast, due to their cost-effectiveness, ease of handling and the ability to conduct genetic manipulation, rodent models continue to serve as an indispensable tool in endometriosis research. Nevertheless, rodents do not menstruate. Consequently, various techniques have been developed to induce experimental endometriosis in rodents. A common method that was also applied in this thesis is the surgical induction of endometriotic lesions by transplanting viable uterine donor tissue to ectopic sites. This method provides the ability to visualize and analyze the development of new endometriotic lesions within the abdominal cavity of the animals. It is important to note that the resulting lesions do not exactly resemble human endometriotic lesions. This discrepancy arises because the lesions in rodents originate from physiological uterine tissue, which fails to replicate the (patho)physiological tissue microenvironment during retrograde menstruation in humans.

Taking this into account, a complex protocol has been developed for the induction of menstruation in mice in order to harvest menstrual tissue (Finn and Pope, 1984; Greaves *et al.*, 2014, 2017). This protocol mimics the hormonal changes during the human menstrual cycle by priming the mice with estrogen and progesterone in order to prepare their uterus for the following decidualization, leading to endometrial bleeding. In a study conducted by Greaves *et al.* (2014), a protocol was employed involving ovariectomized mice on day 0. These mice were administered estrogen injections on days 7, 8 and 9 followed by additional injections on days 13, 14 and 15 along with progesterone delivered through an implant. On day 15, a decidualization stimulus was introduced via oil injection into one of the uterine horns. On day 19, following the removal of the progesterone implant, the uterine horns experiencing menstruation were collected after a 4-hour interval. To enhance this protocol for the purpose of the present thesis, a modified version was implemented by which the duration between ovariectomy and menstruation could be successfully reduced. Hence, the overall time period until the harvesting of the menstrual uteri in the present thesis was only 14 days. In addition, to maximize the

amount of harvestable menstrual tissue and minimize the number of donor mice required, the decidualization stimulus in the form of an oil injection was administered to both uterine horns.

It is worth noting that the withdrawal of progesterone serves as a critical final step in the induction of menstruation. In a study of Xu *et al.* (2007), two distinct types of progesterone withdrawal methods were described in the context of menstruation studies. These were referred to as physiological and pharmacological withdrawal. The physiological withdrawal involves the discontinuation of progesterone supplementation, replicating the natural decline in progesterone levels that occurs at the end of the menstrual cycle. In the context of this thesis, the equivalent of physiological progesterone withdrawal was the removal of the progesterone implant. Another method is pharmacological withdrawal, for instance, by applying progesterone receptor antagonists like mifepristone (Xu *et al.*, 2007). In order to increase the success rate in the decidualization process, both the physiological and the pharmacological methods of progesterone withdrawal were combined for the induction of menstruation in this thesis. Hence, following the removal of the progesterone implant on day 14, the mice were injected with mifepristone. This approach was highly efficient.

7.1.2 Intraperitoneal model of endometriosis

The intraperitoneal model of endometriosis, which involves the transplantation of uterine tissue fragments into the abdominal cavity of recipient animals, is a well-established approach that offers several advantages for studying endometriosis. This model was used in the first part of this thesis.

Intraperitoneal endometriotic lesions can be induced in several ways. After detachment of the endometrium from the myometrium, endometrial fragments can be suspended and injected into the abdominal cavity (Somigliana *et al.*, 1999). However, the low take rate of the tissue fragments is a major disadvantage of this method. Another possibility is the fixation of uterine tissue fragments to the peritoneal wall of the recipient animals (Grümmer *et al.*, 2001), as performed in the present thesis. Consequently, their engraftment and development into endometriotic lesions is facilitated. This approach also enables non-invasive imaging of the lesions by means of repeated high-resolution ultrasound, which ensures minimal burden on the animals while enabling the analysis of the lesions over a long period of time (Körbel *et al.*, 2010). This imaging technique has previously been successfully used to analyze the effects of different therapeutic compounds on the vascularization and growth of endometriotic lesions (Nenicu *et al.*, 2014; Rudzitis-Auth *et al.*, 2012, 2013, 2022). To better determine the localization and size of endometriotic lesions, Hirata *et al.* (2005) transplanted for the first time GFP⁺ tissue into wild-type mice. This method was also applied in the present thesis. For this purpose, transgenic C57BL/6-TgN (ACTB-eGFP) 10sb/J mice were chosen as donor animals, as they express GFP in all their body cells except erythrocytes and hair. Accordingly, the GFP⁺ donor tissue, including GFP⁺ microvessels, could be easily differentiated from the recipient tissue at any time point.

Various types of donor tissue can be used for the experimental induction of endometriosis. In heterologous mouse models, human tissue (Bruner *et al.*, 1997; Grümmer *et al.*, 2001) or endometrial tissue derived from human menstrual blood (Eggermont *et al.*, 2005) is transplanted into the abdominal cavity of immunodeficient mice. This approach enables the study of developing endometriosis within the rodent models without the risk of immunological rejection of the human tissue. Furthermore, heterologous rodent models offer a suitable platform for investigating the effects of therapeutic

compounds on human endometriosis tissue. However, the absence of an immune system in the animals is a major limitation, because it is not possible to study the immunological interactions between the ectopic tissue and the transplantation site. To overcome this limitation, researchers also use homologous mouse models. In these models, two approaches are commonly employed. In the autologous approach, uterine tissue is transplanted onto an ectopic site of the same animal. This allows for the examination of immunological interactions within an individual animal. The second approach is the syngeneic transplantation of uterine tissue from a donor animal into a genetically identical recipient animal. This approach also provides valuable insights into the immunopathogenesis of endometriosis and contributes to a better understanding of the inflammatory nature of the disease.

In the current thesis, the syngeneic approach was chosen for the induction of endometriosis. This selection was made to avoid the risk of rejection associated with using uterine tissue from another species. Additionally, the recipient animals in this study were immunocompetent, which allowed for the exposure of newly developing endometriotic lesions to the functional immune system of the recipient mouse and enabled the complex immunological interaction that occurs between ectopic tissue and the transplantation site. These conditions mimicked well the pathophysiological conditions during the formation of endometriotic lesions.

The use of syngeneic mouse models offers several further advantages. They allow for the analyses of a large number of genetically identical animals over an extended period, providing robust and consistent data. Moreover, syngeneic models are cost-effective in terms of animal housing. However, it is important to note that the surgical induction and suturing of the uterine tissue may introduce artificial inflammation, which has been previously shown to impact the development and angiogenic activity of endometriotic lesions (Becker *et al.*, 2006).

7.1.3 Dorsal skinfold chamber model

Although the intraperitoneal model of endometriosis has been previously used for the evaluation of anti-angiogenic substances in the treatment of endometriosis, it bears the disadvantage that the vascularization of endometriotic lesions cannot be repeatedly visualized *in vivo* in a non-invasive manner. Therefore, the dorsal skinfold chamber model was used in the second part of this thesis (Laschke and Menger, 2007).

The dorsal skinfold chamber model was first introduced in the field of endometriosis research by Laschke *et al.* (2005). For the preparation of the chamber, the dorsal skin of the mouse is sandwiched between two metal frames that contain an observation window in the center. As the chamber frames are made of titanium, they are light and do not disturb the normal behavior of the animals. The cutis and subcutis, as well as the two layers of retractor muscle of the skinfold within the observation window are surgically removed, allowing for direct transplantation of endometrial fragments onto the underlying striated panniculus carnosus muscle. Following this step, the chamber window is covered with a cover glass, which is secured in place with a snap ring (Laschke *et al.*, 2011). The cover glass and the snap ring create a sealed chamber protecting the transplanted tissue while enabling continuous visual access for analysis.

The dorsal skinfold chamber model is a valuable tool for investigating the microcirculation and vascularization of grafts in a controlled manner. The grafts within the chamber can be analyzed for a

period of 2 to 3 weeks by means of high-resolution multi-fluorescence microscopy and subsequent computer-assisted offline analyses. The time limitation is attributed to the loss of elasticity in the dorsal skinfold of the mice, which leads to the tilting of the chamber after some time, which can affect the blood perfusion of the chamber tissue (Laschke and Menger, 2007). Therefore, in the present thesis, the animals were only observed for a period of 14 days, which still provided the opportunity to analyze the early vascularization of newly developing endometriotic lesions (Laschke *et al.*, 2005; Laschke and Menger, 2007). The subsequent offline analyses enabled the assessment of different parameters, such as the functional microvessel density as well as the diameter and centerline RBC velocity of individual microvessels. The repeated analysis of these parameters contributed to the reduction of the number of animals required for the thesis by maximizing the data obtained from a single animal according to the 3R principle.

7.1.4 Experimental protocol of the study

In this thesis, the first direct comparison between endometriotic lesions derived from non-menstrual and menstrual rodent uterine tissue was conducted. This comparison was carried out under identical experimental conditions by transplanting both non-menstrual and menstrual uterine tissue fragments into the same recipient animals.

As endometriosis is recognized as an estrogen-dependent condition, previous investigations primarily focused on the targeting of estrogen production. Consequently, the evaluation of the development and hormonal responsiveness of non-menstrual and menstrual endometriotic lesions was of considerable interest in this thesis. For this purpose, three recipient hormonal states (recipient animal groups) were studied. The non-ovx recipient group consisted of animals with an active estrous cycle. It depicted the common syngeneic mouse model of endometriosis, providing the opportunity to directly compare the differences in the development of non-menstrual uterine tissue fragments and menstrual uterine tissue fragments under the influence of a physiological mouse cycle. The ovx (ovariectomized) recipient animals were studied in order to simulate hormonal deprivation conditions. The ovx+E2 recipient animals were ovariectomized and subjected to repeated estrogen injections, thus simulating a continuous high-dose estrogen environment.

7.2 Discussion of the results

In the present thesis, both menstrual and non-menstrual uterine donor tissue was used for the induction of endometriosis in the peritoneal cavity and the dorsal skinfold chamber. Upon removal from the donor animals, the uteri were first macroscopically and histologically examined. The visible macroscopic and histological differences observed between the non-menstrual and menstrual uteri reflected the different hormonal conditions of the donor animals. The non-menstrual uteri displayed a typical size and compact endometrium with small, round glands, as shown by HE staining (Greaves *et al.*, 2014). In contrast, the menstrual uteri appeared macroscopically enlarged, dark red in color and exhibited a hemorrhagic lumen, which indicated a successful menstruation (Xu *et al.*, 2007). Only the uteri that presented macroscopically visible signs of menstruation were used for the preparation of menstrual uterine tissue fragments. Histologically, the menstrual uteri exhibited an expanded and hemorrhagic endometrial layer.

In line with these findings, the uterine tissue fragments used for transplantation into the recipient mice also exhibited clear differences. The non-menstrual fragments had a compact structure and an intact tissue integrity, making them amenable to suturing and easy to handle. In contrast, the menstrual fragments consisted of a visibly looser tissue with hemorrhagic regions. This made it challenging to suture them to the peritoneal wall and to cut endometrial fragments for the transplantation into the dorsal skinfold chambers.

After transplantation into the peritoneal cavity of non-ovx recipient mice, both menstrual and non-menstrual uterine tissue fragments developed into endometriotic lesions consisting of endometrial stromal tissue and cyst-like dilated endometrial glands. There were no significant differences in the take rate, growth, microvessel density and cell proliferation between non-menstrual and menstrual endometriotic lesions within this recipient group. Although the overall microvessel density of non-menstrual and menstrual endometriotic lesions within the non-ovx mice presented no significant differences, the CD31⁺/GFP⁺ microvessel density of menstrual endometriotic lesions was significantly lower when compared to that of non-menstrual endometriotic lesions. This indicated that fewer newly developing vessels originated from the engrafted menstrual uterine tissue fragments. Hence, most of the detected vessels grew into the menstrual endometriotic lesions from the surrounding recipient tissue. This might be due to the fragile and hemorrhagic structure of the menstrual fragments, which disrupted the original vascular network within the tissue.

In contrast to the non-ovx animals, the ovx animals exhibited a markedly suppressed growth of both non-menstrual and menstrual endometriotic lesions, as observed by high-resolution ultrasound imaging. Both non-menstrual and menstrual endometriotic lesions had a significantly lower lesion volume and stromal tissue volume when compared to those of non-ovx animals. These findings can be attributed to the estrogen-dependent nature of endometriosis (Klemmt and Starzinski-Powitz, 2017). In fact, the ovariectomy of the recipient animals resulted in a complete hormonal deprivation, which suppressed the endometriotic lesion growth within these animals. The suppressive effect of ovariectomy was completely reversed in non-menstrual lesions by means of estrogen supplementation in the ovx+E2 mice. In contrast, menstrual endometriotic lesions in the ovx+E2 mice exhibited a significantly lower take rate than that of non-menstrual lesions as well as a significantly lower lesion volume. This surprising finding may be explained by differences in the expression levels of ER- α and ER- β within the non-menstrual and menstrual uterine tissue. Greaves *et al.* (2014) found in both human and mouse non-menstrual endometrium a high expression of ER- α and low expression of ER- β . In contrast, endometriotic lesions originating from menstrual uterine tissue presented with an increased ER- β expression and much lower ER- α expression, suggesting an altered ER- α and ER- β ratio. Further studies have demonstrated that ER- β influences the transcriptional activity of ER- α (Hall and McDonnell, 1999; Chantalat *et al.*, 2020). Additionally, it is well known that the stimulation of ER- α primarily regulates cell proliferation in newly forming endometriotic lesions (Matsuzaki *et al.*, 2001). It has been suggested that the principal and regulatory effects of estrogen might be mainly mediated through ER- α rather than ER- β (Matsuzaki *et al.*, 2001). Hence, it is suggested that the relative expression levels of the two ER isoforms play a crucial role in determining cellular sensitivity to both estrogens and anti-estrogens (Hall and McDonnell, 1999; Matsuzaki *et al.*, 2001).

In the second part of this thesis, the dorsal skinfold chamber model was used. It was shown that the development of microvascular networks within endometriotic lesions originating from menstrual endometrium seems to undergo a different vascularization mode when compared to the lesions originating from non-menstrual fragments. Notably, menstrual endometriotic lesions exhibited a delayed vascularization when compared to non-menstrual lesions. The delay in vascularization was characterized by a significantly lower functional microvessel density and blood perfusion throughout the 14-day observation period. This finding may be attributed to the natural regression of vessels that occurs within the endometrium during menstruation (Smith, 2001). Therefore, grafted menstrual endometrial tissue primarily becomes vascularized through the ingrowth of blood vessels from the surrounding host tissue via the slow process of angiogenesis. In contrast, non-menstrual endometrial tissue still contains intact, functional microvessels, which can quickly become blood-perfused by forming interconnections with the host microvasculature through inosculation (Laschke and Menger, 2018). The significantly higher fraction of CD31+/GFP+ microvessels within non-menstrual endometriotic lesions compared to menstrual endometriotic lesions in the intraperitoneal mouse model of endometriosis clearly supports this view.

Taken together, these findings show that both grafted non-menstrual and menstrual uterine tissue fragments successfully develop into endometriotic lesions with typical histomorphological characteristics. This suggests that they are both suitable for studying the basic engraftment and early development of endometriotic lesions in normal cycling mice. Given the difference in estrogen sensitivity between the non-menstrual and menstrual tissue, it can be recommended that experimental studies focusing on estrogen-mediated effects should be primarily conducted with menstrual tissue. On the other hand, the transplantation of non-menstrual endometrium offers advantages, such as an easier implementation and a comparable take rate, growth, microvessel density and cell proliferation rate of the resulting lesions when compared to menstrual lesions in cycling mice. Therefore, depending on the specific research question, both approaches may be justified.

7.3 Conclusion

In summary, this is the first study directly comparing endometriotic lesions originating from murine menstrual and non-menstrual uterine tissue fragments under identical experimental conditions. The analyses in both the intraperitoneal endometriosis model and the dorsal skinfold chamber model revealed numerous similarities between the two types of endometriotic lesions, particularly when considering non-ovx mice and ovx mice. These similarities encompass various aspects, such as morphological characteristics, growth patterns, vascularization and hormonal responsiveness. However, non-menstrual and menstrual endometriotic lesions exhibit distinct differences in growth and vascularization, specifically in ovx mice under exogenous estrogen stimulation. This may be due to the fact that, unlike endometriotic lesions originating from murine non-menstrual tissue, the ER expression profile of endometriotic lesions originating from murine menstrual tissue is similar to that in human lesions (Greaves *et al.*, 2014). However, it should be considered that exogenous estrogen stimulation does not mimic the fluctuating estrogen levels in cycling mice and may even result in supraphysiological high hormone levels. The induction of endometriosis through the transplantation of non-menstrual tissue

is much easier and the take rate, microvessel density, growth and cell proliferation of the resulting endometriotic lesions are not substantially different from those of menstrual endometriotic lesions in cycling mice. Therefore, both methods may be justified depending on the experimental setting and research question being addressed. Overall, using a combination of different experimental models may be the most suitable approach for studying the pathophysiology and drug sensitivity of a multifaceted disease like endometriosis in preclinical settings.

8. References

1. **Acar T, Acar N, Celik SC, Ekinci N, Tarcan E, Capkinoglu E.** Endometriosis within the sigmoid colon/extragenital endometriosis. *Turkish J Surg* 2015; 31:250-252.
2. **Allen C, Hopewell S, Prentice A.** Non-steroidal anti-inflammatory drugs for pain in women with endometriosis. *Cochrane Database Syst Rev* 2005; 4:CD004753.
3. **Allen E.** The oestrous cycle in the mouse. *Am J Anat* 1922; 30:297-371.
4. **Alwadhi S, Kohli S, Chaudhary B, Gehlot K.** Thoracic endometriosis - a rare cause of haemoptysis. *J Clin Diagnostic Res* 2016; 10:TD01-TD02.
5. **Bacci M, Capobianco A, Monno A, Cottone L, Di Puppo F, Camisa B, Mariani M, Brignole C, Ponzoni M, Ferrari S, Panina-Bordignon P, Manfredi AA, Rovere-Querini P.** Macrophages are alternatively activated in patients with endometriosis and required for growth and vascularization of lesions in a mouse model of disease. *Am J Pathol* 2009; 175:547-556.
6. **Becker CM, Wright RD, Satchi-Fainaro R, Funakoshi T, Folkman J, Kung AL, D'Amato RJ.** A novel noninvasive model of endometriosis for monitoring the efficacy of antiangiogenic therapy. *Am J Pathol* 2006; 168:2074-2084.
7. **Bedaiwy MA, Allaire C, Yong P, Alfaraj S.** Medical management of endometriosis in patients with chronic pelvic pain. *Semin Reprod Med* 2017; 35:38-53.
8. **Bellofiore N, Rana S, Dickinson H, Temple-Smith P, Evans J.** Characterization of human-like menstruation in the spiny mouse: Comparative studies with the human and induced mouse model. *Hum Reprod* 2018; 33:1715-1726.
9. **Bergqvist A, D'Hooghe T.** Mini symposium on pathogenesis of endometriosis and treatment of endometriosis-associated subfertility. Introduction: The endometriosis enigma. *Hum Reprod Update* 2002; 8:79-83.
10. **Berkley KJ, Rapkin AJ, Papka RE.** The pains of endometriosis. *Science* 2005; 308:1587-1589.
11. **Bertens APMG, Helmond FA, Hein PR.** Endometriosis in rhesus monkeys. *Lab Anim* 1982; 16:281-284.
12. **Brasted M, White CA, Kennedy TG, Salamonsen LA.** Mimicking the events of menstruation in the murine uterus. *Biol Reprod* 2003; 69:1273-1280.

13. **Bronson FH, Dagg CP, Snell GD.** Reproduction In: Biology of the laboratory mouse. *Dover Publications* New York, USA 1966.
14. **Brown J, Crawford TJ, Allen C, Hopewell S, Prentice A.** Nonsteroidal anti-inflammatory drugs for pain in women with endometriosis. *Cochrane Database Syst Rev* 2017; 1:CD004753.
15. **Bruner KL, Matrisian LM, Rodgers WH, Gorstein F, Osteen KG.** Suppression of matrix metalloproteinases inhibits establishment of ectopic lesions by human endometrium in nude mice. *J Clin Invest* 1997; 99:2851-2857.
16. **Bulun SE, Yilmaz BD, Sison C, Miyazaki K, Bernardi L, Liu S, Kohlmeier A, Yin P, Milad M, Wei J.** Endometriosis. *Endocr Rev* 2019; 40:1048-1079.
17. **Burney RO, Giudice LC.** Pathogenesis and pathophysiology of endometriosis. *Fertil Steril* 2012; 98:511-519.
18. **Burns KA, Pearson AM, Slack JL, Por ED, Scribner AN, Eti NA, Burney RO.** Endometriosis in the mouse: Challenges and progress toward a 'best fit' murine model. *Front Physiol* 2022; 12:806574.
19. **Byers SL, Wiles M V, Dunn SL, Taft RA.** Mouse estrous cycle identification tool and images. *PLoS One* 2012; 7:e35538.
20. **Chaffin CL, Vandevort CA.** Follicle growth, ovulation and luteal formation in primates and rodents: A comparative perspective. *Exp Biol Med (Maywood)* 2013; 238:539-548.
21. **Chang HY, Sneddon JB, Alizadeh AA, Sood R, West RB, Montgomery K, Chi JT, Van De Rijn M, Botstein D, Brown PO.** Gene expression signature of fibroblast serum response predicts human cancer progression: Similarities between tumors and wounds. *PLoS Biol* 2004; 2:206-214.
22. **Chantalat E, Valera MC, Vaysse C, Noirrit E, Rusidze M, Weyl A, Vergriete K, Buscail E, Lluet P, Fontaine C, Arnal JF, Lenfant F.** Estrogen receptors and endometriosis. *Int J Mol Sci* 2020; 21:1-17.
23. **Cohen PE, Milligan SR.** Silastic implants for delivery of oestradiol to mice. *J Reprod Fertil* 1993; 99:219-223.

24. **Cousins FL, Murray A, Esnal A, Gibson DA, Critchley HOD, Saunders PTK.** Evidence from a mouse model that epithelial cell migration and mesenchymal-epithelial transition contribute to rapid restoration of uterine tissue integrity during menstruation. *PLoS One* 2014; 9:1-12.
25. **Culley L, Law C, Hudson N, Denny E, Mitchell H, Baumgarten M, Raine-Fenning N.** The social and psychological impact of endometriosis on women's lives: A critical narrative review. *Hum Reprod Update* 2013; 19:625-639.
26. **Cummings AM, Metcalf JL.** Induction of endometriosis in mice: A new model sensitive to estrogen. *Reprod Toxicol* 1995; 9:233-238.
27. **Debus G, Schuhmacher I.** Endometriose. In: *Duale Reihe Gynäkologie und Geburtshilfe. Georg Thieme Verlag Stuttgart, Deutschland* 2013; 4:298-303.
28. **D'Hooghe TM, Bambra CS, Suleman MA, Dunselman GA, Evers HL, Koninckx PR.** Development of a model of retrograde menstruation in baboons (*Papio anubis*). *Fertil Steril* 1994; 62:635-638.
29. **D'Hooghe TM, Bambra CS, Raeymaekers BM, De Jonge I, Lauweryns JM, Koninckx PR.** Intrapelvic injection of menstrual endometrium causes endometriosis in baboons (*Papio cynocephalus* and *Papio anubis*). *Am J Obstet Gynecol* 1995; 173:125-134.
30. **D'Hooghe TM, Bambra CS, De Jonge I, Lauweryns JM, Koninckx PR.** The prevalence of spontaneous endometriosis in the baboon (*Papio anubis*, *Papio cynocephalus*) increases with the duration of captivity. *Acta Obstet Gynecol Scand* 1996; 75:98-101.
31. **D'Hooghe TM, Bambra CS, Raeymaekers BM, Koninckx PR.** Development of spontaneous endometriosis in baboons. *Obstet Gynecol* 1996; 88:462-466.
32. **D'Hooghe TM, Debrock S.** Endometriosis, retrograde menstruation and peritoneal inflammation in women and in baboons. *Hum Reprod Update* 2002; 8:84-88.
33. **Dmowski WP, Radwanska E.** Current concepts on pathology, histogenesis and etiology of endometriosis. *Acta Obstet Gynecol Scand Suppl* 1984; 123:29-33.
34. **Dogan E, Saygili U, Posaci C, Tuna B, Caliskan S, Altunyurt S, Saatli B.** Regression of endometrial explants in rats treated with the cyclooxygenase-2 inhibitor rofecoxib. *Fertil Steril* 2004; 82 Suppl 3:1115-1120.
35. **Eggermont J, Donnez J, Casanas-Roux F, Scholtes H, Van Langendonck A.** Time course of pelvic endometriotic lesion revascularization in a nude mouse model. *Fertil Steril* 2005; 84:492-499.

36. **Einspanier A, Lieder K, Brüns A, Husen B, Thole H, Simon C.** Induction of endometriosis in the marmoset monkey (*Callithrix jacchus*). *Mol Hum Reprod* 2006; 12:291-299.
37. **Emera D, Romero R, Wagner G.** The evolution of menstruation: A new model for genetic assimilation: Explaining molecular origins of maternal responses to fetal invasiveness. *BioEssays* 2012; 34:26-35.
38. **Eskenazi B, Warner ML.** Epidemiology of endometriosis. *Obstet Gynecol Clin North Am* 1997; 24:235-258.
39. **Evans J, Kaitu'u-Lino T, Salamonsen LA.** Extracellular matrix dynamics in scar-free endometrial repair: Perspectives from mouse in vivo and human in vitro studies. *Biol Reprod* 2011; 85:511-523.
40. **Evans S, Moalem-Taylor G, Tracey DJ.** Pain and endometriosis. *Pain* 2007; 132:22-25.
41. **Fazleabas AT, Brudney A, Gurates B, Chai D, Bulun S.** A modified baboon model for endometriosis. *Ann N Y Acad Sci* 2002; 955:308-317.
42. **Feng D, Welker S, Körbel C, Rudzitis-Auth J, Menger MD, Montenarh M, Laschke MW.** Protein kinase CK2 is a regulator of angiogenesis in endometriotic lesions. *Angiogenesis* 2012; 15:243-252.
43. **Ferrero H, Buigues A, Martínez J, Simón C, Pellicer A, Gómez R.** A novel homologous model for noninvasive monitoring of endometriosis progression. *Biol Reprod* 2017; 96:302-312.
44. **Finn CA, Pope M.** Vascular and cellular changes in the decidualized endometrium of the ovariectomized mouse following cessation of hormone treatment: A possible model for menstruation. *J Endocrinol* 1984; 100:295-300.
45. **Galle PC.** Clinical presentation and diagnosis of endometriosis. *Obstet Gynecol Clin North Am* 1989; 16:29-42.
46. **Giannarini G, Scott CA, Moro U, Grossetti B, Pomara G, Selli C.** Cystic endometriosis of the epididymis. *Urology* 2006; 68:10-12.
47. **Giudice LC, Kao LC.** Endometriosis. *Lancet* 2004; 364:1789-1799.
48. **Giudice LC.** Clinical practice: Endometriosis. *N Engl J Med* 2010; 362:2389-2398.

49. **Greaves E, Cousins FL, Murray A, Esnal-Zufiaurre A, Fassbender A, Horne AW, Saunders PTK.** A novel mouse model of endometriosis mimics human phenotype and reveals insights into the inflammatory contribution of shed endometrium. *Am J Pathol* 2014; 184:1930-1939.
50. **Greaves E, Critchley HOD, Horne AW, Saunders PTK.** Relevant human tissue resources and laboratory models for use in endometriosis research. *Acta Obstet Gynecol Scand* 2017; 96:644-658.
51. **Groothuis PG, Nap AW, Winterhager E, Grümmer R.** Vascular development in endometriosis. *Angiogenesis* 2005; 8:147-156.
52. **Grümmer R, Schwarzer F, Bainczyk K, Hess-Stumpff H, Regidor PA, Schindler AE, Winterhager E.** Peritoneal endometriosis: Validation of an in-vivo model. *Hum Reprod* 2001; 16:1736-1743.
53. **Grümmer R.** Animal models in endometriosis research. *Hum Reprod Update* 2006; 12:641-649.
54. **Hadfield R, Mardon H, Barlow D, Kennedy S.** Delay in the diagnosis of endometriosis: A survey of women from the USA and the UK. *Hum Reprod* 1996; 11:878-880.
55. **Hall JM, McDonnell DP.** The estrogen receptor beta-isoform (ERbeta) of the human estrogen receptor modulates ERalpha transcriptional activity and is a key regulator of the cellular response to estrogens and antiestrogens. *Endocrinology* 1999; 140:5566-5578.
56. **Harada T.** Pathological Aspect and Pathogenesis of Endometriosis. In: *Endometriosis: Pathogenesis and treatment. Springer Verlag Tokyo, Japan* 2014; 9-18.
57. **Healy DL, Rogers PA, Hii L, Wingfield M.** Angiogenesis: A new theory for endometriosis. *Hum Reprod Update* 1998; 4:736-740.
58. **Hirata T, Osuga Y, Yoshino O, Hirota Y, Harada M, Morimoto C, Koga K, Yano T, Tsutsumi O, Taketani Y.** Development of an experimental model of endometriosis using mice that ubiquitously express green fluorescent protein. *Hum Reprod* 2005; 20:2092-2096.
59. **Hull ML, Prentice A, Wang DY, Butt RP, Phillips SC, Smith SK, Charnock-Jones DS.** Nimesulide, a COX-2 inhibitor, does not reduce lesion size or number in a nude mouse model of endometriosis. *Hum Reprod* 2005; 20:350-358.
60. **Intaglietta M, Tompkins WR, Richardson DR.** Velocity measurements in the microvasculature of the cat omentum by online method. *Microvasc Res* 1970; 2:462-473.

61. **Jabbour HN, Kelly RW, Fraser HM, Critchley HOD.** Endocrine regulation of menstruation. *Endocr Rev* 2006; 27:17-46.
62. **Johnson NP, Hummelshoj L, Adamson GD, Keckstein J, Taylor HS, Abrao MS, Bush D, Kiesel L, Tamimi R, Sharpe-Timms KL, Rombauts L, Giudice LC.** World endometriosis society consensus on the classification of endometriosis. *Hum Reprod* 2017; 32:315-324.
63. **Kaitu'u-Lino TJ, Morison NB, Salamonsen LA.** Estrogen is not essential for full endometrial restoration after breakdown: Lessons from a mouse model. *Endocrinology* 2007; 148:5105-5111.
64. **Kalaitzopoulos DR, Samartzis N, Kolovos GN, Mareti E, Samartzis EP, Eberhard M, Dinas K, Daniilidis A.** Treatment of endometriosis: A review with comparison of 8 guidelines. *BMC Womens Health* 2021; 21:1-9.
65. **Kennedy S, Mardon H, Barlow D.** Familial endometriosis. *J Assist Reprod Genet* 1995; 12:32-34.
66. **Kennedy S, Bergqvist A, Chapron C, D'Hooghe T, Dunselman G, Greb R, Hummelshoj L, Prentice A, Saridogan E.** ESHRE guideline for the diagnosis and treatment of endometriosis. *Hum Reprod* 2005; 20:2698-2704.
67. **Kiani K, Rudzitis-Auth J, Scheuer C, Movahedin M, Sadati Lamardi SN, Malekafzali Ardakani H, Becker V, Moini A, Aflatoonian R, Ostad SN, Menger MD 2, Laschke MW.** Calligonum comosum (Escanbil) extract exerts anti-angiogenic, anti-proliferative and anti-inflammatory effects on endometriotic lesions. *J Ethnopharmacol* 2019; 239:111918.
68. **Kitawaki J, Kado N, Ishihara H, Koshiba H, Kitaoka Y, Honjo H.** Endometriosis: The pathophysiology as an estrogen-dependent disease. *J Steroid Biochem Mol Biol* 2002; 83:149-155.
69. **Klemmt P, Starzinski-Powitz A.** Molecular and cellular pathogenesis of endometriosis. *Curr Womens Heal Rev* 2017; 13:1-11.
70. **Kyama CM, Overbergh L, Debrock S, Valckx D, Vander Perre S, Meuleman C, Mihalyi A, Mwenda JM, Mathieu C, D'Hooghe TM.** Increased peritoneal and endometrial gene expression of biologically relevant cytokines and growth factors during the menstrual phase in women with endometriosis. *Fertil Steril* 2006; 85:1667-1675.
71. **Körbel C, Menger MD, Laschke MW.** Size and spatial orientation of uterine tissue transplants on the peritoneum crucially determine the growth and cyst formation of endometriosis-like lesions in mice. *Hum Reprod* 2010; 25:2551-2558.

72. **Laschke MW, Elitzsch A, Vollmar B, Menger MD.** In vivo analysis of angiogenesis in endometriosis-like lesions by intravital fluorescence microscopy. *Fertil Steril* 2005; 84:1199-1209.
73. **Laschke MW, Elitzsch A, Scheuer C, Holstein JH, Vollmar B, Menger MD.** Rapamycin induces regression of endometriotic lesions by inhibiting neovascularization and cell proliferation. *Br J Pharmacol* 2006; 149:137-144.
74. **Laschke MW, Menger MD.** In vitro and in vivo approaches to study angiogenesis in the pathophysiology and therapy of endometriosis. *Hum Reprod Update* 2007; 13:331-342.
75. **Laschke MW, Körbel C, Rudzitis-Auth J, Gashaw I, Reinhardt M, Hauff P, Zollner TM, Menger MD.** High-resolution ultrasound imaging: A novel technique for the noninvasive in vivo analysis of endometriotic lesion and cyst formation in small animal models. *Am J Pathol* 2010; 176:585-593.
76. **Laschke MW, Vollmar B, Menger MD.** The dorsal skinfold chamber: Window into the dynamic interaction of biomaterials with their surrounding host tissue. *Eur Cells Mater* 2011; 22:147-167.
77. **Laschke MW, Menger MD.** Basic mechanisms of vascularization in endometriosis and their clinical implications. *Hum Reprod Update* 2018; 24:207-224.
78. **Lebovic DI, Mueller MD, Taylor RN.** Immunobiology of endometriosis. *Fertil Steril* 2001; 38:38-50.
79. **Lee SY, Koo YJ, Lee DH.** Classification of endometriosis. *Yeungnam Univ J Med* 2021; 38:10-18.
80. **Longo LD.** Classic pages in obstetrics and gynecology. Aberrant portions of the Mullerian duct found in an ovary: William Wood Russell Johns Hopkins hospital bulletin, vol. 10, pp. 8-10, 1899. *Am J Obstet Gynecol* 1979; 134:225-226.
81. **MacKenzie WF, Casey HW.** Animal model of human disease. Endometriosis. Animal model: Endometriosis in rhesus monkeys. *Am J Pathol* 1975; 80:341-344.
82. **Magon N.** Gonadotropin releasing hormone agonists: Expanding vistas. *Indian J Endocrinol Metab* 2011; 15:261-267.
83. **Marks J.** Evolutionary tempo and phylogenetic inference based on primate karyotypes. *Cytogenet Cell Genet* 1982; 34:261-264.

84. **Matsuura K, Ohtake H, Katabuchi H, Okamura H.** Coelomic metaplasia theory. *Gynecol Obstet Invest* 1999; 47:18-22.
85. **Matsuzaki S, Murakami T, Uehara S.** Expression of estrogen receptor alpha and beta in peritoneal and ovarian endometriosis. *Fertil Steril* 2001; 75:1198-1205.
86. **Mattos RM de, Machado DE, Perini JA, Alessandra-Perini J, Meireles da Costa N de O, Wiekowski AF da R de O, Cabral KMDS, Takiya CM, Carvalho RS, Nasciutti LE.** Galectin-3 plays an important role in endometriosis development and is a target to endometriosis treatment. *Mol Cell Endocrinol* 2019; 486:1-10.
87. **McLaren J, Prentice A, Charnock-Jones DS, Smith SK.** Vascular endothelial growth factor (VEGF) concentrations are elevated in peritoneal fluid of women with endometriosis. *Hum Reprod* 1996; 11:220-223.
88. **McLaren J.** Vascular endothelial growth factor and endometriotic angiogenesis. *Hum Reprod Update* 2000; 6:45-55.
89. **Menning A, Walter A, Rudolph M, Gashaw I, Fritzemeier KH, Roese L.** Granulocytes and vascularization regulate uterine bleeding and tissue remodeling in a mouse menstruation model. *PLoS One* 2012; 7:e41800.
90. **Merrill JA.** Spontaneous endometriosis in the Kenya baboon (*Papio doguera*). *Am J Obstet Gynecol* 1968; 101:569-570.
91. **Miller BH, Takahashi JS.** Central circadian control of female reproductive function. *Front Endocrinol (Lausanne)* 2014; 4:195.
92. **Mok-Lin EY, Wolfberg A, Hollinquist H, Laufer MR.** Endometriosis in a patient with Mayer-Rokitansky-Küster-Hauser syndrome and complete uterine agenesis: Evidence to support the theory of coelomic metaplasia. *J Pediatr Adolesc Gynecol* 2010; 23:e35-e37.
93. **Momoeda M, Taketani Y, Terakawa N, Hoshiai H, Tanaka K, Tsutsumi O, Osuga Y, Maruyama M, Harada T, Obata K, Hayashi K.** Is endometriosis really associated with pain? *Gynecol Obstet Invest* 2002; 54:18-23.
94. **Nap AW, Groothuis PG, Demir AY, Maas JW, Dunselman GA, de Goeij AF, Evers JL.** Tissue integrity is essential for ectopic implantation of human endometrium in the chicken chorioallantoic membrane. *Hum Reprod* 2003; 18:30-34.

95. **Nap AW, Griffioen AW, Dunselman GA, Bouma-Ter Steege JC, Thijssen VL, Evers JL, Groothuis PG.** Antiangiogenesis therapy for endometriosis. *J Clin Endocrinol Metab* 2004; 89:1089-1095.
96. **Nenicu A, Körbel C, Gu Y, Menger MD, Laschke MW.** Combined blockade of angiotensin II type 1 receptor and activation of peroxisome proliferator-activated receptor- γ by telmisartan effectively inhibits vascularization and growth of murine endometriosis-like lesions. *Hum Reprod* 2014; 29:1011-1024.
97. **Nenicu A, Yordanova K, Gu Y, Menger MD, Laschke MW.** Differences in growth and vascularization of ectopic menstrual and non-menstrual endometrial tissue in mouse models of endometriosis. *Hum Reprod* 2021; 36:2202-2214.
98. **Nisolle M, Casanas-Roux F, Anaf V, Mine JM, Donnez J.** Morphometric study of the stromal vascularization in peritoneal endometriosis. *Fertil Steril* 1993; 59:681-684.
99. **Nnoaham KE, Hummelshoj L, Webster P, d'Hooghe T, de Cicco Nardone F, de Cicco Nardone C, Jenkinson C, Kennedy SH, Zondervan KT.** Impact of endometriosis on quality of life and work productivity: A multicenter study across ten countries. *Fertil Steril* 2011; 96:366-373.
100. **Oral E, Arici A, Olive DL, Huszar G.** Peritoneal fluid from women with moderate or severe endometriosis inhibits sperm motility: The role of seminal fluid components. *Fertil Steril* 1996; 66:787-792.
101. **Osuga Y, Seki Y, Tanimoto M, Kusumoto T, Kudou K, Terakawa N.** Relugolix, an oral gonadotropin-releasing hormone (GnRH) receptor antagonist, in women with endometriosis-associated pain: Phase 2 safety and efficacy 24-week results. *BMC Womens Health* 2021; 21:1-8.
102. **Parkening TA, Collins TJ, Smith ER.** Plasma and pituitary concentrations of luteinizing hormone, follicle-stimulating hormone and prolactin in aged, ovariectomized CD-1 and C57BL/6 mice. *Exp Gerontol* 1982a; 17:437-443.
103. **Parkening TA, Collins TJ, Smith ER.** Plasma and pituitary concentrations of LH, FSH and prolactin in aging C57BL/6 mice at various times of the estrous cycle. *Neurobiol Aging* 1982b; 3:31-35.
104. **Pellicer A, Navarro J, Bosch E, Garrido N, Garcia-Velasco J a, Remohí J, Simón C.** Endometrial quality in infertile women with endometriosis. *Ann N Y Acad Sci* 2001; 943:122-130.

105. **Peterse D, De Clercq K, Goossens C, Binda MM, Dorien FO, Saunders P, Vriens J, Fassbender A, D'Hooghe TM.** Optimization of endometrial decidualization in the menstruating mouse model for preclinical endometriosis research. *Reprod Sci* 2018; 25:1577-1588.
106. **Petruškevičiūtė E, Bužinskienė D.** Acute diffuse peritonitis due to spontaneous rupture of an infected endometrioma: A case report. *Acta Med Lit* 2021; 28:360-366.
107. **Plant TM.** A comparison of the neuroendocrine mechanisms underlying the initiation of the preovulatory LH surge in the human, old world monkey and rodent. *Front Neuroendocrinol* 2012; 33:160-168.
108. **Potente M, Gerhardt H, Carmeliet P.** Basic and therapeutic aspects of angiogenesis. *Cell* 2011; 146:873-887.
109. **Practice Committee of the American Society for Reproductive Medicine.** Treatment of pelvic pain associated with endometriosis: A committee opinion. *Fertil Steril* 2014; 101:927-935.
110. **Rakhila H, Girard K, Leboeuf M, Lemyre M, Akoum A.** Macrophage migration inhibitory factor is involved in ectopic endometrial tissue growth and peritoneal-endometrial tissue interaction in vivo: A plausible link to endometriosis development. *PLoS One* 2014; 9:e110434.
111. **Revised American Society for Reproductive Medicine classification of endometriosis: 1996.** *Fertil Steril* 1997; 67:817-821.
112. **Rice VM.** Conventional medical therapies for endometriosis. *Ann N Y Acad Sci* 2002; 955:343-352.
113. **Rock JA, Prendergast RA, Bobbie D, Green WR, Parmley TH, Dubin NH.** Intraocular endometrium in the rabbit as a model for endometriosis. *Fertil Steril* 1993; 59:232-235.
114. **Rolla E.** Endometriosis: Advances and controversies in classification, pathogenesis, diagnosis, and treatment. *F1000Res* 2019; 8:F1000.
115. **Rudolph M, Döcke WD, Müller A, Menning A, Röse L, Zollner TM, Gashaw I.** Induction of overt menstruation in intact mice. *PLoS One* 2012; 7:e32922.
116. **Rudzitis-Auth J, Körbel C, Scheuer C, Menger MD, Laschke MW.** Xanthohumol inhibits growth and vascularization of developing endometriotic lesions. *Hum Reprod* 2012; 27:1735-1744.
117. **Rudzitis-Auth J, Menger MD, Laschke MW.** Resveratrol is a potent inhibitor of vascularization and cell proliferation in experimental endometriosis. *Hum Reprod* 2013; 28:1339-1347.

118. **Rudzitis-Auth J, Nenicu A, Nickels RM, Menger MD, Laschke MW.** Estrogen stimulates homing of endothelial progenitor cells to endometriotic lesions. *Am J Pathol* 2016; 186:2129-2142.
119. **Rudzitis-Auth J, Becker M, Scheuer C, Menger MD, Laschke MW.** Indole-3-carbinol inhibits the growth of endometriotic lesions by suppression of microvascular network formation. *Nutrients* 2022; 14:4940.
120. **Russell W.** Aberrant portions of the Müllerian duct found in an ovary: Ovarian cysts of Müllerian origin. *Bull John Hopkins Hosp* 1899; 10:8-10.
121. **Sampson JA.** Metastatic or embolic endometriosis, due to the menstrual dissemination of endometrial tissue into the venous circulation. *Am J Pathol* 1927; 3:93-110.
122. **Schleedoorn MJ, Nelen WLDM, Dunselman GAJ, Vermeulen N.** Selection of key recommendations for the management of women with endometriosis by an international panel of patients and professionals. *Hum Reprod* 2016; 31:1208-1218.
123. **Simpson JL, Elias S, Malinak LR, Buttram VCJ.** Heritable aspects of endometriosis. I. Genetic studies. *Am J Obstet Gynecol* 1980; 137:327-331.
124. **Smith SK.** Regulation of angiogenesis in the endometrium. *Trends Endocrinol Metab* 2001; 12:147-151.
125. **Smolarz B, Szyłło K, Romanowicz H.** Endometriosis: Epidemiology, classification, pathogenesis, treatment and genetics (Review of literature). *Int J Mol Sc.* 2021; 22:10554.
126. **Soares SR, Martinez-Varea A, Hidalgo-Mora JJ, Pellicer A.** Pharmacologic therapies in endometriosis: A systematic review. *Fertil Steril* 2012; 98:529-555.
127. **Somigliana E, Viganò P, Rossi G, Carinelli S, Vignali M, Panina-Bordignon P.** Endometrial ability to implant in ectopic sites can be prevented by interleukin-12 in a murine model of endometriosis. *Hum Reprod* 1999; 14:2944-2950.
128. **Sotnikova NY, Antsiferova YS, Posiseeva L V, Shishkov DN, Posiseev D V, Filippova ES.** Mechanisms regulating invasiveness and growth of endometriosis lesions in rat experimental model and in humans. *Fertil Steril* 2010; 93:2701-2705.
129. **Steinleitner A, Lambert H, Suarez M, Serpa N, Robin B, Cantor B.** Periovarian calcium channel blockade enhances reproductive performance in an animal model for endometriosis-associated subfertility. *Am J Obstet Gynecol* 1991; 164:949-952.
130. **Story L, Kennedy S.** Animal studies in endometriosis: A review. *ILAR J* 2004; 45:132-138.

131. **Suginami H.** A reappraisal of the coelomic metaplasia theory by reviewing, endometriosis occurring in unusual sites and instances. *Am J Obstet Gynecol* 1991; 165:214-218.
132. **Surrey ES.** Add-back therapy and gonadotropin-releasing hormone agonists in the treatment of patients with endometriosis: Can a consensus be reached? *Fertil Steril* 1999; 71:420-424.
133. **Tambo TOM, Fedorcsak P.** Endometriosis-associated infertility: Aspects of pathophysiological mechanisms and treatment options. *Acta Obstet Gynecol Scand* 2017; 96:659-667.
134. **Te Linde RW, Scott RB.** Experimental endometriosis. *Am J Obstet Gynecol* 1950; 60:1147-1173.
135. **Teschner A, Hinrichsen M.** Gynäkologische Endokrinologie. In: Duale Reihe Gynäkologie. Georg Thieme Verlag Stuttgart, Deutschland 2013; 4:87-102.
136. **Tirado-González I, Barrientos G, Tariverdian N, Arck PC, García MG, Klapp BF, Blois SM.** Endometriosis research: Animal models for the study of a complex disease. *J Reprod Immunol* 2010; 86:141-147.
137. **Tomac J, Cekinová D, Arapović J.** Biology of the corpus luteum. *Period Biol* 2011; 113:43-49.
138. **Valle RF, Sciarra JJ.** Endometriosis: Treatment strategies. *Ann N Y Acad Sci* 2003; 997:229-239.
139. **Ver Z.** Menstruationszyklus: Sexualentwicklung und Reproduktionsphysiologie. In: Duale Reihe Physiologie. Georg Thieme Verlag Stuttgart, Deutschland 2013; 4:422-425.
140. **Vernon MW, Wilson EA.** Studies on the surgical induction of endometriosis in the rat. *Fertil Steril* 1985; 44:684-694.
141. **Whitten WK.** Occurrence of anoestrus in mice caged in groups. *J Endocrinol* 1959; 18:102-107.
142. **Wilkosz S, Pullen N, De-Giorgio-Miller A, Ireland G, Herrick S.** Cellular exchange in an endometriosis-adhesion model using GFP transgenic mice. *Gynecol Obstet Invest* 2011; 72:90-97.
143. **Xu XB, He B, Wang JD.** Menstrual-like changes in mice are provoked through the pharmacologic withdrawal of progesterone using mifepristone following induction of decidualization. *Hum Reprod* 2007; 22:3184-3191.
144. **Zamah NM, Dodson MG, Stephens LC, Buttram VCJ, Besch PK, Kaufman RH.** Transplantation of normal and ectopic human endometrial tissue into athymic nude mice. *Am J Obstet Gynecol* 1984; 149:591-597.

9. Acknowledgements

This thesis would not have been possible without the support and work of many people. Therefore, I would like to take this opportunity to thank everyone, who supported and accompanied me. Many thanks to:

Prof. Dr. Michael D. Menger for the opportunity to perform a thesis at the Institute for Clinical and Experimental Surgery at Saarland University. Prof. Dr. Matthias W. Laschke for the constant support and motivation in all phases of the work. Dr. Anca Nenicu for starting and keeping this project alive, allowing me to be a part of it, teaching and supporting me through all steps. Janine Becker and Ruth M. Nickels for the technical assistance in the histological and immunohistochemical analyses. In addition, I thank Dr. Erin Greaves, University of Edinburgh, for the helpful discussion about the mouse menstruation protocol. Finally, I thank to all animal keepers for their technical assistance in the animal facilities.

For data protection reasons, the curriculum vitae is not included in the electronic version of the dissertation.

10. Publications

Original article resulting from this thesis

1. Nenicu A, **Yordanova K**, Gu Y, Menger MD, Laschke MW. Differences in growth and vascularization of ectopic menstrual and non-menstrual endometrial tissue in mouse models of endometriosis. *Hum Reprod* 2021; 36:2202-2214.

Other original articles

1. Christofyllakis K, Pföhler C, Bewarder M, Müller CSL, Thurner L, Rixecker T, Vogt T, Stilgenbauer S, **Yordanova K**, Kaddu-Mulindwa D. Adjuvant therapy of high-risk (Stages IIC-IV) malignant melanoma in the post interferon-alpha era: A systematic review and meta-analysis. *Front Oncol* 2021; 10:637161.
2. Müller C, Vogt T, **Yordanova K**. Dermatologische Impfpraxis - Herausforderungen im klinischen Alltag. *Aktuelle Derm* 2020; 46:434-448.
3. **Yordanova K**, Stilgenbauer S, Bohle RM, Lesan V, Thurner L, Kaddu-Mulindwa D, Bittenbring JT, Scharberger M, Aßmann G, Bewarder M. Spontaneous regression of a plasmablastic lymphoma with MYC rearrangement. *Br J Haematol* 2019; 186:e203-e207.
4. **Yordanova K**, Pföhler C, Schweitzer LF, Bourg C, Adam L, Vogt T. Etanercept leads to a rapid recovery of a Dabrafenib-/Trametinib-associated toxic epidermal necrolysis-like severe skin reaction. *Ski Heal Dis* 2022; 3:e185.

Congress contributions

1. **Yordanova K**, Schweitzer LF, Cathérine B, Adam L, Vogt Th, Pföhler C. Effektives und schnelles Ansprechen einer durch BRAF- und MEK-Inhibitoren induzierten toxischen epidermalen Nekrolyse (TEN) mittels einmaliger Gabe von Etanercept. 31. Deutscher Hautkrebskongress der Arbeitsgemeinschaft Dermatologische Onkologie (ADO), online 2021.
2. **Yordanova K**, Adam L, Albrecht L, Vogt Th, Pföhler C. Zeitversetztes Auftreten von akuter immunvermittelter Leberschädigung und interstitieller Nephritis bei einem Patienten mit malignem Melanom nach einmaliger Pembrolizumabgabe. 32. Deutscher Hautkrebskongress der Arbeitsgemeinschaft Dermatologische Onkologie (ADO), Hannover 2022.

3. **Yordanova K.** Erfolgreiche Therapie eines großflächigen, ulzerierenden Basalzellkarzinoms mit Sonidegib. Hautkrebs Update, online 2022.
4. **Yordanova K,** Adam L, Preiß M-M, Albrecht L, Gevaerd C, Vogt Th, Pföhler C. Auftreten einer kryptogen organisierenden Pneumonie (COP) mit konsequentem Spannungspneumothorax bei einem Patienten mit malignem Melanom unter Kombinationsimmuntherapie mit Ipilimumab und Nivolumab. 33. Deutscher Hautkrebskongress der Arbeitsgemeinschaft Dermatologische Onkologie (ADO), Hamburg 2023.

Date of Doctoral Defense: April 22, 2025

Dean: Prof. Dr. med. dent. M. Hannig

Reviewers:

Prof. Dr. Matthias Werner Laschke

Prof. Dr. Erich Solomayer